Dominik Rabl, BSc

Enzyme Based Optical Sensors in Microfluidics

MASTER'S THESIS

to achieve the university degree of

Master of Science (MSc)

Master's degree programme: Chemistry

submitted to

Graz University of Technology

Supervisor
Mayr, Torsten, Assoc.Prof. Dipl.-Chem. Dr.rer.nat.

Institute of Analytical Chemistry and Food Chemistry

Graz, May, 2019

"In the beginning there was nothing, which exploded."
Terry Pratchett, Lords and Ladies

Abstract

The aim of this thesis was to integrate optical glucose sensors in microfluidic chips for the use at physiological conditions. In the sensors the enzyme glucose oxidase (GOx) was implemented. This enzyme catalyses the reaction of glucose and oxygen (O_2) to gluconolactone and hydrogen peroxide H_2O_2. O_2 is a luminescence-quencher for many luminophores, such as the here used O_2-dye. Glucose concentrations can be determined by measuring the O_2-consumption of the sensor.

The final sensors consisted of 2 layers containing a bottom layer acting as the sensitive layer, consisting of sensor-particles (polystyrene-particles stained with the oxygen indicator) as well as GOx embedded in a D_7-Matrix. This sensor layer was coated with a polyHEMA diffusion barrier to prevent from leaching of GOx out of the sensor layer.

These layers were spotted into the channels of microfluidic chips using a ink-jet printer (microdispenser). In the microdispenser a drop of liquid (sensor cocktail, etc.) was pressed through a nozzel with the help of a piezoelectric tapped. Microfluidic chips with a volume of 10 µl, 100 µl as well as single channel chips were used. A syringe pump was used to pump the glucose solutions through the chips and the microfluidic chips were embedded in a heating block to control the temperature.

The sensors were characterized employing different glucose concentrations (1-10 mM, at physiological conditions), flow rates and temperatures (25 and 37°C).

The measurements at 25°C delivered satisfying results. Additionally, the influence of the sensor thickness on the sensor response was investigated (several layers of sensor cocktail were spotted on top of each other to achieve a variation in the sensor layer thickness). At 37°C the problem of GOx-leaching was observed. Subsequently, to prevent from leaching, the sensor spots were covered with a polyHEMA diffusion barrier. After adjusting the thickness of the sensor layer and the thickness of the diffusion barrier reasonable measurements without detecting noticeable leaching effects could be obtained. Another approach to prevent from leaching was to swap GOx with GOx-CLEA. However, nonetheless, at least a thin layer of polyHEMA diffusion barrier was needed to prevent from leaching effects.

Kurzfassung

Das Hauptziel dieser Arbeit war es optische Glukose Sensoren in mikrofluidischen Chips zu integrieren, welche bei physiologischen Bedingungen verwendet werden können. In den Sensoren ist das Enzym Glukose Oxidase (GOx) eingebaut. Dieses enzym katalysiert die Reaktion von Sauerstoff (O_2) mit Glukose zu Glukonolacton und Wasserstoffperoxid (H_2O_2). O_2 ist ein Lumineszenzquencher für viele verschiedene Luminophore, sowie auch für den hier verwendeten O_2-Farbstoff. Die Glukose-Konzentration kann durch das messen des O_2-Verbrauchs des Sensors bestimmt werden.
Die finalen Sensoren bestanden aus 2 Schichten, die untere Schicht ist die empfindliche Schicht, sie besteht aus Sensorpartikeln (Polystyrene-Partikel mit Sauerstoff Indikator gefärbt) und GOx in einer D_7-Hydrogel Matrix. Diese Sensorschicht wurde mit einer polyHEMA Diffusionsbarriere überzogen um das auswaschen der GOx aus der Sensorschicht zu verhindern.
Die einzelnen Schichten wurden mit Hilfe eines Ink-Jet Printers (Mikrodispenser) in die Kanäle des Mikrofluidik-Chips aufgebracht. Bei dem Mikrodispenser wird ein Flüssigkeitstropfen (Sensor Cocktail, etc.) mit Hilfe eines piezoelktrischen Stößels durch eine Düse gepresst. Mikrofluidische Chips mit einem Volumen von 10 µl, 100 µl sowohl als auch ein 1 Kanal Chip wurden verwendet. Eine Spritzenpumpe wurde verwendet um die Glukose-Lösungen durch die mikrofluidischen Chips zu pumpen, welche sich in einem Heizblock befanden um die Temperatur zu regeln.
Die Sensoren wurden bei verschiedenen Glukose-Konzentrationen (0-10 mM Glukose; bei physiologischen Bedingungen), Flussraten und Temperaturen (25 und 37°C) charakterisiert.
Die Messungen bei 25°C erzielten gute Ergebnisse. Zusätzlich wurde der Einfluss der Sensor Dicke wurde untersucht (es wurden mehrere Schichten an Sensor Cocktail übereinander gespottet um die Schichtdicke zu variieren). Bei 37°C wurde das Problem des Herauswaschens der GOx beobachtet. Daher, um das Problem des Auswaschens zu lösen, wurden die Sensor Spots mit einer polyHEMA-Diffusionsbarriere überzogen. Nach einstellen der Dicke der Sensor-Schicht als auch der Schichtdicke der Diffusionsbarriere wurden gute Ergebnisse erzielt ohne dass ein Auswaschen der GOx beobachtet wurde. Eine andere Lösungsansatz um das Auswaschen des Enzyms in den Griff zu bekommen war es die GOx durch GOx-CLEA zu ersetzen. Jedoch wurde auch hier schnell klar dass zumindest eine dünne polyHEMA-Schicht notwendig war.

EIDESSTATTLICHE ERKLÄRUNG

Ich erkläre an Eides statt, dass ich die vorliegende Arbeit selbstständig verfasst, andere als die angegebenen Quellen/Hilfsmittel nicht benutzt, und die den benutzten Quellen wörtlich und inhaltlich entnommenen Stellen als solche kenntlich gemacht habe. Das in TUGRAZonline hochgeladene Textdokument ist mit der vorliegenden Masterarbeit identisch.

AFFIDAVIT

I declare that I have authored this thesis independently, that I have not used other than the declared sources/resources, and that I have explicitly indicated all material which has been quoted either literally or by content from the sources used. The text document uploaded to TUGRAZonline is identical to the present master‘s thesis.

Datum/Date	Unterschrift/Signature

Danksagung

Als erstes möchte ich mich bei Torsten bedanken, dafür dass ich die Arbeit bei dir machen durfte, für deinen großartigen Input und dafür dass ich jederzeit und so unkompliziert mit dir reden konnte.

Desweiteren möchte ich der ganzen ACFC-Crew für die geile Zeit danken, für das gemeinsame Mittagessen, die entspannten Kaffeepausen, das lustige gelegentliche Kochen abends und für die unterhaltsamen Aktivitäten nach der Arbeitszeit. Besonders hervorheben möchte ich hier Fips, Berni, Christoph und Peter welche stets bereit waren bei meinen (oft dummen) Problemen während der Arbeit zu helfen. An dieser Stelle möchte ich auch noch Josef erwähnen, danke dafür dass ich meine Projektlabor bei dir machen durfte und dass du mich in diese super Arbeitsgruppe gebracht hast.

Nicht vergessen möchte ich an dieser Stelle all jene welche mir in den letzten Jahren meine Zeit in Graz versüßt haben und mich ertragen haben. Ein großer Dank geht an den VSC-Graz, der Verein der mir die Passion für Volleyball wiedergegeben hat. Michi, Gudrun, Elke und Eli für die lustigen (und oft absurden) DnD-Spieleabende. Sowie David und Kosmas mit welchen ich schon so manch interessantes Abenteuer erlebt habe.

Last but not least möchte ich meiner tollen Familie Danken bei der ich weis dass ich immer willkommen bin. Danke Mama und Papa dafür dass ihr mir mein Studium ermöglicht habt und für eure Geduld mit mir. Danke Chris, Lene, Roli und Berni, die besten Geschwister welche man haben kann und mit denen es nie fad wird.

Dominik Rabl Bsc Graz, May, 2019

Contents

1 Introduction

Glucose is the main energy source for most living organisms, making it the most abundant carbohydrate, making glucose an very important analyte in different areas such as biotechnology, food chemistry, biochemistry and various other fields. One of the most important tasks is the measurement of glucose in blood, approximately 40% of all blood tests are related to glucose measurements [1]. The drive for this work was to develop a glucose sensor system that can be applied to monitor the glucose concentration during cell-cultivation in microfluidic devices.

There are several techniques for measuring glucose. These methods can be based on the recognition of glucose by certain (co-)enzymes, which leads to a change in the absorption/luminescence behaviour; measurements of consumption or formation of metabolites caused by enzymes (most used GOx); boronic acid as a molecular receptor for saccharides (binding of boronic acid changes the optical properties) or competitive binding of glucose and a labelled carbohydrate to concanavalin A (ConA) [1]. The principle of the glucose sensors constructed for this thesis is based on the consumption or formation of metabolites, specific the consumption of O_2. Subsequently, enzyme based sensors can be further divided into electrochemical sensors and optical sensors. Compared to mostly used electrochemical glucose sensors, the big advantage of optical sensors is that there is no need of a reference electrode and the possibility of positioning the readout device on an external position. Therefore this system is very suitable for implementation in microfluidic systems.

The glucose sensors investigated in this thesis consisted of a two layer layout, a first layer containing of an O_2-sensitive dye and glucose oxidase (GOx) embedded in a hydrogel matrix as well as a second layer applied on top acting as a diffusion barrier to prevent leaching effects of GOx.

In this setup glucose and O_2 were metabolized to gluconolactone and H_2O_2 catalysed by GOx as enzyme. Oxygen acted as a quencher molecule for a luminescent dye and so the glucose concentration could be determined by the change of the measured O_2 concentration.

To implement the glucose sensor in the microfluidic chips a microdispenser (inkjet printer) was used to print the glucose sensor cocktail directly into the channel of the microfluidic chamber. The microdispenser allowed precise positioning and control over the size of the sensor spots. Additionally oxygen sensors were implemented into the microfluidic chips

to measure the total oxygen change of the sample over time.
A main part of the work was to solve the issue of GOx leaching and to investigate the flow rate dependency, channel height, thickness of the sensor spot and of the diffusion barrier and to get the sensors working at 25 and 37°C.

2 Theoretical Background

2.1 Luminescence

If photons hit any objects, different interactions like transmission, light scattering and absorption can occur. Absorption of photons lead to excitation of an electron of the object, subsequently leading to varying results.

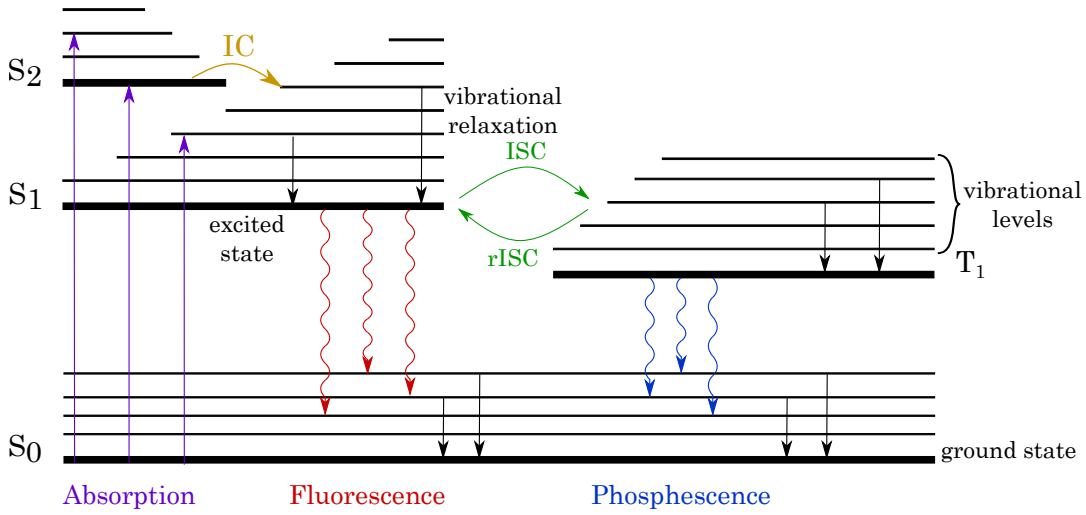

Figure 2.1: Jablonski diagram

Figure 2.1 shows the Jablonski diagram. It depicts the absorption of a photon leading to the excitation of an electron from the ground state (S_0) to the first and second electronic states (S_1 and S_2) and their respective vibrational levels (displayed as the thin lines). Internal conversion (IC) can occur; here an electron jumps from an higher electronic state to a high vibrational level of a lower electronic state (shown as the yellow arrow), this transition doesn't lead to the emission of light and it takes around 10^{-12} s or less. When the direct relaxation from the excited state to the ground state results in the emission of a photon, it is called fluorescence, this takes around 10^{-8} s.
A (quantumchemical forbidden) transition of the S_1 state to the triplet state (T_1) is called intersystem crossing (ISC, green arrows in the figure), from here the state can return to S_1 and then relax to the S_0 by emitting light (called delayed fluorescence). The electron can also go direct from the T_1 state to the S_0 state by emitting light (which is

technically also forbidden due to spin conversion), this is called phosphorescence. The lifetime of phosphorescence can last from µs to several hours.

2.1.1 Luminescence Lifetime

Luminescence lifetime is the average time a molecule stays in the excited state before emitting light and occurs withn a range of nanoseconds. Phosphorescence lifetimes tend to be longer and can last up to hours. Phosphorescence heavily depends on the molecule and its surrounding. Γ is the emissive rate of a fluorophore, k_{nr} is the non radiative decay to the ground state S_0, with this two constants the quantum yield Q of a luminophore can be calculated. For optical sensors high quantum yields are desired, because higher quantum yields lead to higher emission intensities.

$$Q = \frac{\Gamma}{\Gamma + k_{nr}} \tag{2.1}$$

Q	...	quantum yield
Γ	...	emissive rate of fluorophore
k_{nr}	...	rate of nonradiative decay to S_0

The luminescence lifetime τ can also be calculated using Γ and k_nr:

$$\tau = \frac{1}{\Gamma + k_{nr}} \tag{2.2}$$

τ	...	luminescence lifetime

The lifetime of τ depends on chemical and physical parameters, such as the structure of the luminophore, temperature, matrix in which the luminophore is embedded and quenching materials.

2.1.2 Luminescence Quenching

Luminescence quenching is the reduction of emission by interaction of a luminophore with a quencher molecule. There are 2 quenching mechanisms, static and dynamic quenching.

Static quenching

During the process of static quenching, a quencher-luminophore complex (QL) is formed. The lifetime of the luminescence isn't affected, only the emission intensity gets decreased.

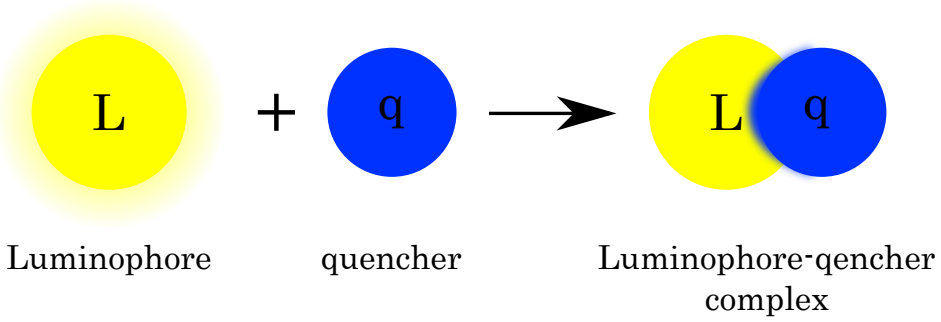

Figure 2.2: Static quenching mechanism

Optical sensors using this effect measure the analyte concentration through observation of the luminescence intensity. The analyte in this case is the quencher, the higher the concentration of the analyte, the lower the luminescence intensity.

Dynamic quenching

In dynamic quenching, an energy transfer happens when the excited luminophore collides with a quencher molecule, no luminophore quencher complex is formed. As a result of dynamic quenching, not only the luminescence intensity decreases with the increase of quencher concentration, but also the lifetime.

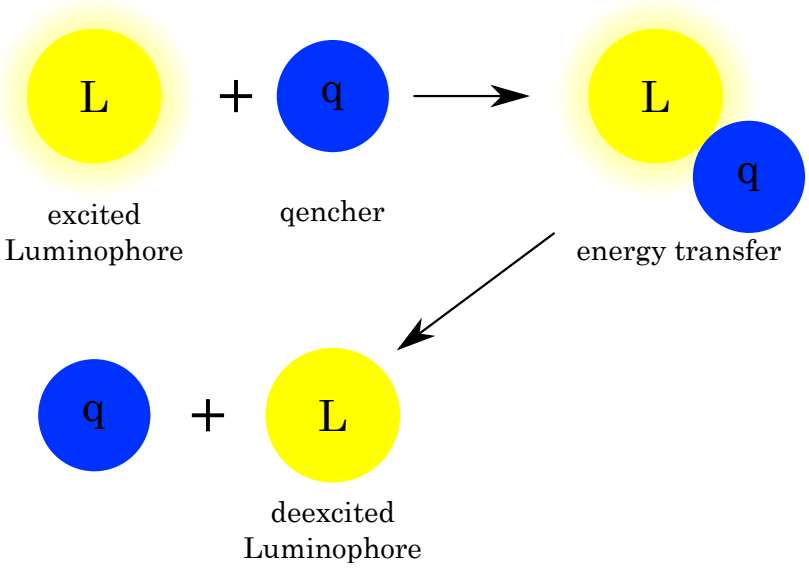

Figure 2.3: Dynamic quenching mechanism

The decrease in luminescence intensity and lifetime can be described with the Stern-Volmer equation:

$$\frac{I_0}{I} = \frac{\tau_0}{\tau} = 1 + k_Q \tau_0 [Q] = 1 + K_{SV}[Q] \tag{2.3}$$

I_0	...	intensity of the luminescence without quencher
I	...	intensity of the luminescence at given quencher concentration
τ_0	...	luminescence lifetime without quencher
τ	...	luminescence lifetime at given quencher concentration
k_Q	...	bimolecular quenching constant
[Q]	...	concentration of quencher
K_{SV}	...	Stern-Volmer constant

2.2 Enzyme-based sensors

Enzyme-based sensors detect the products (or reactants) of an enzymatic reaction. The change in concentration of the analyte can be measured using electrochemical or optical methods. For optical measurements changes in absorption, reflectance or emission are detected. Enzymes have benefits like being very selective, working at a (near-)neutral pH and have relative short reaction times [2].

2.2.1 Enzyme

Enzymes are macromolecular biological catalysts lowering the activation energy of reactions, leading to an increased reaction rate. During this process the enzyme is not metabolized.
Enzyme names often derive from the substrate or the reaction + the ending "-ase". Furthermore the International Union of Biochemistry and Molecular Biology have developed the EC (Enzyme Commission) numbers for nomenclature for enzymes. The nomenclature consists of four numbers. The first number classifies the type of reaction that gets catalyzed. Top-level Classifications:

EC 1	**Oxidoreductases:**	catalyze oxidation/reduction reactions
EC 2	**Tranferases:**	transfers a functional group
EC 3	**Hydrolases:**	catalyze the hydrolysis of various bonds
EC 4	**Lyases:**	cleaves bonds by other means than hydrolysis or oxidation often a double bond or ring-structure is formed
EC 5	**Isomerases**	catalyze isomerization changes within a molecule
EC 6	**Ligases**	join molecules with covalent bonds

The remaining 4 numbers of the EC nomeclature are subdivided in substrate, product and reaction mechanism.

The selectivity of enzymes can be described with the "lock and key" model by Emil Fischer in 1894 [3]. The reactive site of the enzyme is shaped that the substrate can fit exactly into it.

2.2.2 Enzyme-based glucose sensors

Glucose biosensors are the most investigated type of biosensors. The majority of glucose biosensors are based on the reaction of glucose with glucose oxidase (GOx), which reacts in the following way:

$$\beta - \mathrm{D} - \mathrm{Glucose} + \mathrm{O_2} \xrightarrow{\mathrm{GOx}} \mathrm{D} - \mathrm{Glucono} - \delta - \mathrm{lactone} + \mathrm{H_2O_2}$$
$$\mathrm{D} - \mathrm{Glucono} - \delta - \mathrm{lactone} + \mathrm{H_2O} \longrightarrow \mathrm{D} - \mathrm{Gluconate} + \mathrm{H^+}$$

As the reaction shows, GOx converts D-glucose and O_2 to D-Gluconolactone and H_2O_2, the D-gluconolactone further reacts to D-gluconic acid. So the concentration of glucose correlates with the consumption of O_2, the production of H_2O_2 and with the pH-change due to the formation of D-gluconic acid [2].
The measurement of glucose separates into 2 big types of glucose sensors, electrochemical and optical glucose sensors.

2.2.3 Electrochemical enzyme-based sensors

Electrochemical biosensors are the most widely used biosensors and have been studied since the 1960s, they can be impedimetric, potentiometric or amperometric [4].

- Amperometric biosensors

For amperometric biosensors the working electrode is either made out of a noble metal or a screen-printed layer covered with a biorecognition component. When a potential is applied, conversion of the electroactive species, which is generated in the enzyme layer, occurs at the electrode leading to a current that can be measured [4].

- Impedimetric Biosensors

Impedimetric biosensors have two electrodes with alternating voltage, the applied voltage amplitude can range from a few mV to 100 mV. The change in impedance or its components resistance is measured afterwards. Enzymatically produced ions lead to a significant increase of impedance [4].

- Potentiometric Biosensors

Ion-selective electrodes (ISE) and ion-sensitive field effect transistors (ISFET) are used for potentiometric biosensors, a biorecognition element is immobilized on the outer surface or captured inside of a membrane. An example for a potentiometric biosensor is glucose oxidase (GOx) immobilized on a pH-electrode, the glucose does only have a minimal influence on the pH of the working medium, but the gluconate, which is produced by the enzymatic reaction of β-*D*-glucose with GOx, causes an acidification of the working medium [4].

Electrochemical glucose sensors

Electrochemical glucose sensors get further divided into 2 sensing methods: Into nonenzymatic electrochemical glucose sensors and into enzyme-based electrochemical glucose sensors [5].

- Nonenzymatical electrochemical sensors

Nonenzymatical electrochemical sensors work with direct oxidation of glucose using noble metals like Pt and Au and their composites as the electrodes. This method has 3 major problems:
The first problem is that the sensitivity is restricted by the sluggish kinetics of glucose electro-oxidation [5]. The second problem is the intermediates of glucose often get irreversibly adsorbed to the electrodes, which leads to a reduction of activity of the electrodes [5]. The third problem is the poor selectivity of the nonenzymatic glucose sensors, since some other sugars and other interferer substances can get oxidized in the potential range of the glucose oxidation [6].

- Enzymatic electrochemical sensors

There are 3 generations of enzymatical glucose sensors.
For the **first generation** of enzymatic glucose sensors a thin layer of GOx was immobilized on the electrode. The anodic oxidation of H_2O_2 is measured, an positive aspect of the the anodic oxidation is that O_2 is formed and thus the oxygen gets recycled [7].
In the **second generation** of enzymatic glucose sensor a mediator (Med_{ox}) substitutes O_2. This is done due to the fact that most times the glucose concentration is much higher than the O_2-concentration. The mediator is either a solution-state mediator that can diffuse into and out of the active site of the enzyme [8], or it can be an mediator that is attached directly to the enzyme [9]. Also an redox-conduction polymer can be used, which can shuttle its electrons from and to the active site of the enzyme .
The **third generation** of enzymatic glucose sensor is the ideal biosensing model, this generation doesn't need any mediators and it works via direct electron communication

between the redox-active cofactor of the enzyme and the electrode surface. To electrically wire the redox enzymes with electrodes is a very complicated procedure which hinder a practical wide use [5].

2.2.4 Enzyme-based optical sensors

The description of enzyme-based optical sensors is taken from the review of Borisov and Wolfbeis. [2].

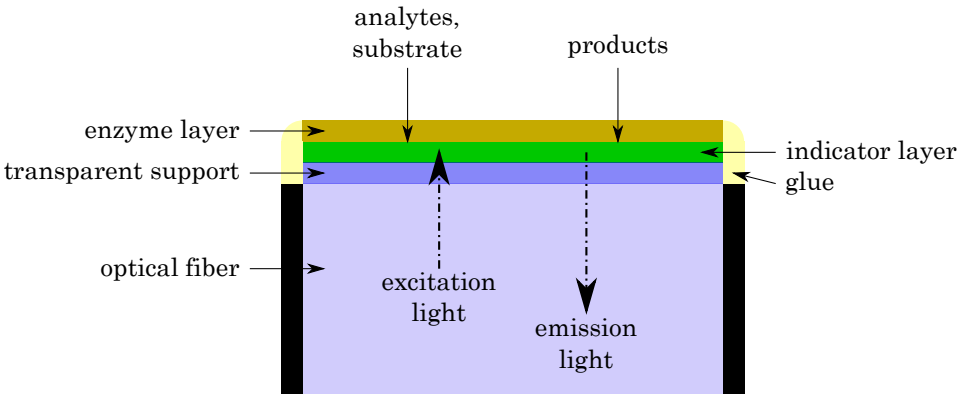

Figure 2.4: Scheme of a typical enzyme-based optical sensor

Figure 2.4 shows the setup of a typical enzyme-based optical sensor. On top of an transparent support layer is the indicator layer and on top of the indicator layer is an enzyme layer. The indicator layer consists of the indicator dye, which is usually either directly dissolved in the polymer matrix, or covalently bond or adsorbed on the surface of microbeads, which then are embedded in a polymer matrix. The enzyme in the enzyme layer is either covalently bond on the surface of a membrane or entrapped in a polymer (usually sol-gels, hydrogels, Lagnmuir-Blodgett films, etc.). Leaching can be prevented by cross-linking the enzyme with bovine serum via glutaraldehyde as a linker.
The analyte diffuses into the enzyme layer, there it gets converted by the enzyme. The indicator dye is either sensitive for one of the products, or on of the co-reactants.

Enzyme-based optical glucose sensors

The transducers pH, O_2 and H_2O_2 are the most interesting for enzyme-based optical glucose and enzyme-based electrochemical glucose sensors.
When pH transduction is used, the starting pH and the puffer capacity control the the shape and relative signal change. Additionally the enzymatic activity is influenced by pH.

Glucose sensors measuring H_2O_2 have the nice perk that there is virtually no background, but optical continuous sensors for H_2O_2 are very rare. Because of this most optical glucose sensors are based on O_2 measurements. The first optical glucose senors, based on the dynamic quenching of certain indicator dyes in the presence of O_2, were most likely first described by the group of Lübbers [10].
The layout of glucose sensors can vary and are described in a review by Steiner et al. [1] and can be separated into planar-, fiber fluorescent optic sensors and sensors based on micro- and nanoparticles.

- Planar optical glucose sensors

In this sensor layout, the GOx is immobilized on or in a polymer (hydrogels or polyacrylamide are most commonly used). The indicator dye is immobilized in either the same layer or a second polymer layer. A glucose sensor of this kind was already reported in 1988, there decacylene was used as the indicator dye, the dye was immobilized in a silicone layer and on top of this was a nylon membrane with GOx immobilized on it [1]. A more resent example for a glucose sensor where the indicator dye and the GOx were entrapped in the same layer was made by Zach et al, the GOx and Pt-TTTBPtBu-PS-DVB microspheres were together entrapped in a hydrogel-matrix [11]. This kind of sensors can easily be cut out and integrated in microfluidic devices as an example.

- Fiber optical glucose sensors

This kind of sensor has pretty much the same layout as the planar optical glucose sensor, but on a smaller scale. As the name suggests, the glucose sensor here is placed on the tip of an optical fiber. Such a sensor for instance was made by Moreno-Bondi et al, they absorbed Ru(bpy) on silica gel, incorporated in a silicone matrix and put it on top of an optical fiber, GOx was immobilized by linking it with glutardialdehyde to the surface [12].

- Glucose sensors based on micro- and nanoparticles

As the name suggests, for this type of sensor the indicator dye and the GOx is immobilized in micro- or nanoparticles. An example for this kind of sensors was made by Rossi et al., they covalently bond GOx on magnetite-based nanoparticles, allowing to trap the nanoparticles on a specific position, or to separate the nanoparticles after the measurement from the analyte sample using a magnet. The easy separation step makes the particles reusable [13].

2.3 Microfluidic systems

2.3.1 Microfluidic System Definition

The characteristics of a microfluidic system are very well described by Professor George Whitesides [14]:
What is microfluidics? It is the science and technology of systems that process or manipulate small (10^{-9} to 10^{-18} litres) amounts of fluids, using channels with dimensions of tens to hundreds of micrometres.
[...]
A microfluidic system must have a series of generic components: a method of introducing reagents and samples (probably as fluids, although ideally with the option to use powders); methods for moving these fluids around on the chip, and for combining and mixing them; and various other devices (such as detectors for most microanalytical work, and components for purification of products for systems used in synthesis).
[...]

Microfluidic systems have a wide range of applications which are very well described in a review by Chiu et al. [15]:
[...]
Contemporary assessments of microfluidics often propose fields that are best set to benefit from the technique. These include genetic analysis, capillary electrophoresis, DNA amplification, clinical chemistry, cell-based assays and cellular analysis, single-cell analysis, proteomics, point-of-care (PoC) diagnostics, drug discovery, and small-molecule and nanomaterial synthesis.
[...]

2.3.2 Advantages of Microfluidic Systems in bioprocessing

Microfluidic systems have a lot of benefits when compared with conventional batch reactors, these benefits are very well described in the review of Wohlgemuth et al. [16].

High surface-to-volume ratio

Due to the high surface-to-volume and thus short diffusion paths mass and heat transfer are dramatically increased when compared to conventional platforms, the rapid heat transfer enables fast cooling and heating which allows good control over the temperature and makes it very attractive for highly exothermic reactions [17]. The high surface to

volume ratio makes it advantageous for catalytic reaction on the inner surfaces of the channel, immobilized biocatalysts and packed-bed microreactors offer a high catalyst load.

Better spatial and temporal control

Reaction time can easily controlled through the flow rate of the reagents [18] or the channel length [19]. The reaction time control is especially useful for short-lived reactive species, the reactive species can be generated and transported to the next site of the reaction before decomposition starts.

Continuous processing at smaller scales

Continuous operations have benefits in reduced costs, equipment size, energy consumption, solvent utilization and waste. Highly automated production plants with control loops allow the maintenance of high product quality. Biocatlytic reactions that are continuously operated, especially for reactions at phase boundaries, have shown to be superior when compared to batch reactors [20–22]

Product removal/product isolation

Good integrated product removal is possible because of the high volume-to-surface ratio of microfluidic devices and using two-liquid flow [23] or membranes [24]. The in situ extraction of inhibitory products is especially useful to overcome thermodynamic limitations of the reaction and to enhance the product purity. It also helps to prevent catalyst poisoning by removing undesired by-products from the reaction-zone.

Improved transport in multi-phasic systems

Microfluidic devices do have a better control of the fluid flow, short diffusion paths and high interfacial areas. This is advantageous for enzymatic reactions with poorly water-soluble compounds, to increase the biocatalyst stability and/or to increase the yield by in situ extraction of thermodynamically limited reactions [23].

2.3.3 Microbioreactors - MBR

Microbioreactors (MBRs) are microfluidic devices used as screening tools for bacterial and cell culturing systems. There are two big main applications for MBRs, firstly being high throughput applications to screen bacterial cell cultures and optimizing the growth and production of the culture in planktonic suspensions and secondly being investigating

the inter- and intracellular processes of mammalian or human cells. The challange for the microfluidic device lies here in simulating the in vivo conditions for the cell cultures. [25]

Advantages of Microbioreactors

Microbioreactors have several advantages towards macro scale bioreactors. The first advantage is the fast mass transfer, caused by the high surface to volume ratio and smaller distances. MBRs allow a precise control over different process parameters such as: temperature, pH, substrate concentrations, metabolic concentrations, etc. [26]
Additionally, microfluidic systems do show a better performance in mimicking *in vivo* conditions when compared with conventional macroscale cell culturing methods. The size of the microchannels/microchambers correspond very well with the *in vivo* cellular microniches. The precise set-up of co-cultures allows the modelling of more accurate organotypic cultures. By changing the fluid flow the shear stress can be adjusted to *in vivo* conditions, which individual cell types are experiencing. Last but not least the design of high throughput microfluidic systems show promise. [27]

2.4 Sensor Printing Methods

There are several established printing techniques to apply a layer of polymer cocktail on a substrate. The most utilized printing methods are inkjet printing, aerosol jet printing, spin coating, knife coating and microdispensing. Knife coating and microdispensing have been the chosen printing techniques for this work.

2.4.1 Knife coating

Knife coating, also called doctor blading, is a printing technique that allows the formation of films with a well-defined thickness. A sharp blade (scraper) is placed at a fixed distance from the substrate surface (usually 10-500µm). The coating cocktail is placed in front of the scraper, the scraper is then moved linearly across the substrate, leaving behind a wet film. Ideally the thickness of the wet film is half the gap between the scraper and the substrate, but it may vary due to surface energy of the substrate, surface tension and viscosity of the cocktail. [28]

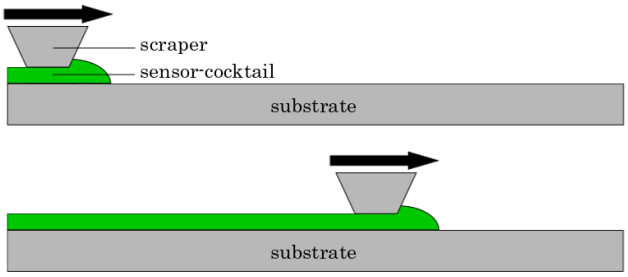

Figure 2.5: Principle of knife coating

Knife coating has almost 100% material usage and can be integrated in roll-to-roll processes with high throughput production [29]. This makes it an interesting coating technique, especially for solar cells.

2.4.2 Microdispensing

Microdispensing is a variant of inkjet printing. The microdispenser works using a piezo-electrically guided tappet, that dispenses cocktail droplets through a nozzle.

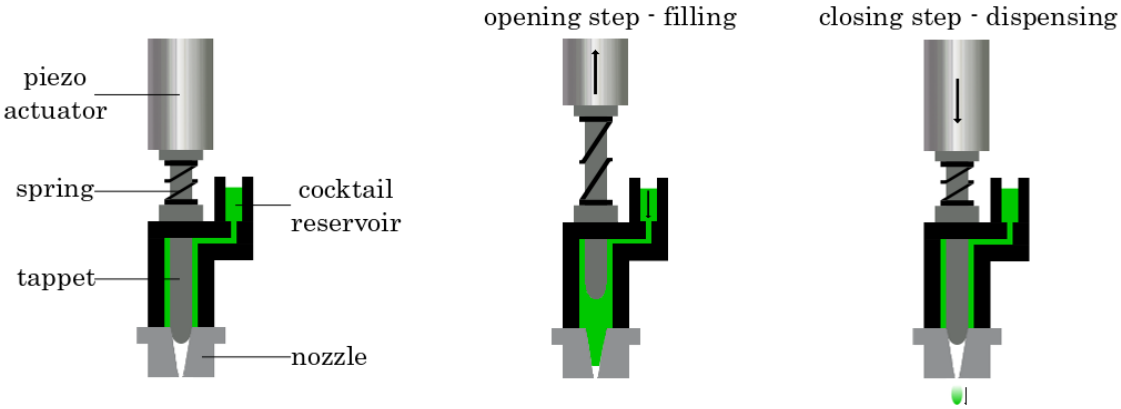

Figure 2.6: Microdispensing process

Four parameters determine a dispensing step: **tappet lift, rising time, open time** and **falling time.**
First the piezo actuator pulls the tappet up, so the cocktail can fill the space formed. During this procedure the cocktail reservoir is under pressure. The tappet lift determines the distance the tappet gets pulled up and the rising time determines how fast the tappet gets pulled up. During the subsequent the open time the tapped stays open. For dispensing the piezo actuator pushes the tappet down, which causes the cocktail to

be pressed through a nozzle. The size of the nozzle can be changed. The falling time describes how fast the tappet is pushed down by the piezo actuator.

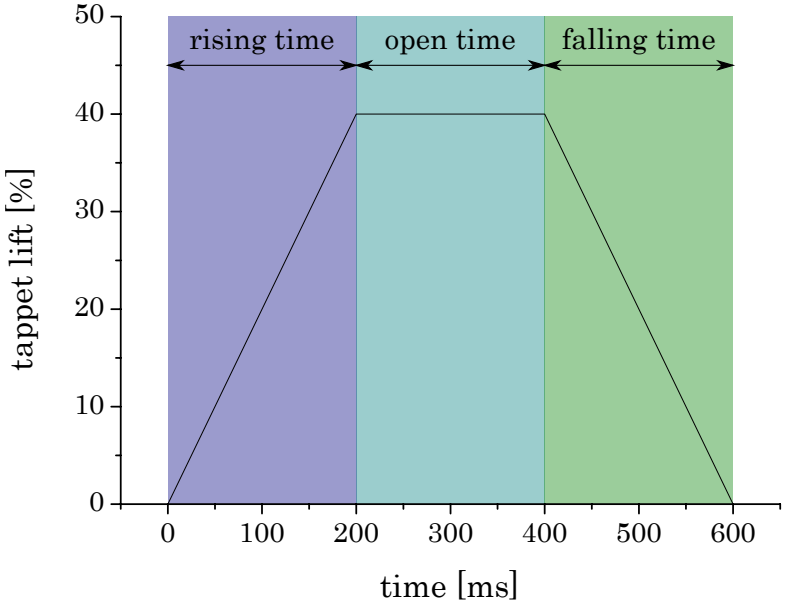

Figure 2.7: Tappet lift - microdispensing steps

Figure 2.7 shows the procedure of the dispensing. At first the tapped lift rises 40 % in 200 ms, then it stays open for another 200 ms and the cocktail gets dispensed in the end with a falling time of 200 ms.
Oxygen and pH sensors have already been printed using the microdispenser. Oxygen sensors consisted of O_2 dye, silicone (E4), polystyrene dissolved in a mixture of chloroform and toluene. The pH sensors consisted of pH dye, D4 hydrogel, Egyptian blue and THF. [30]

3 Materials and Methods

3.1 Devices

Table 3.1: Printer parts

Manufacturer	Device	Description
VERMES	MDC 3200+	microdispensing control unit
VERMES	MDV 3200A-HS-UF	microdispenser
Benezan Electronics	Triple Beast	CNC microstep driver
Isert-Electronic	axis Motor	step motor for single axis movement

Table 3.2: Devices for measurements

Manufacturer	Device	Description
Pyrosciene	FireStingO2	phase fluorimeter with fibre
Tecan	Cavro-XLP-Pump	12 way pump
neoLab	neoBlock-Heizer Mono 1	heating block

3.2 Chemicals

Table 3.3: List of chemicals

Solvent	Supplier	CAS-Number
Ethanol	TCI	109-99-9
D_7 Hydrogel	AdvanSource	67-66-3
Polyhydroxyethylemthacrylate	Polyscience	95-50-1
D(+)-Glucose-Monohydrate	Carl Roth GmbH	108-88-3
Glucose Oxidase	Sigma-Aldrich	68-12-2
Sodiumdihydrogenphosphate waterfree	Carl Roth GmbH	60-29-7
Disodiumhydrogenphosphate waterfree	Carl Roth GmbH	127-19-5
Sodiumchloride	VWR chemicals	75-09-2
PtTPTBPF in 1% PS	synthesised in house	

4 Experimental

4.1 Cocktail Preperation

4.1.1 D_7 Stock Solution

750 mg of D_7 have been dissolved in 4,25 ml of a mixture of EtOH and H_2O (9:1 v:v) using an ultrasonic bath, the resulting stock cocktail had 15 wt% D_7. Until further use the cocktail was kept on a stirring plate to prevent precipitation/aggregation of the hydrogel.

4.1.2 Sensor Cocktails

Glucose Oxidase Cocktail

Glucose Oxidase was aggregated according to Zach et al. [11]:
7,5 mg GOx was dissolved in 150 µl H_2O in an Eppendorf tube and precipitated afterwards with 500 µl EtOH. After the precipitation the mixture was centrifuged at 4000 rotations per minute for 5 minutes. Roughly 450 µl of the supernatant liquid was removed with the help of a piston operated pipette.
To make the stock-solution the aggregated GOx was given into 670 mg of D_7 cocktail, 72,3 mg of O_2-particles were added with the help of a 100 µl mixture of EtOH and H_2O (9:1 v:v).
The stock-solution was diluted with a mixture of EtOH and H_2O (9:1, v:v). The diluting ratio was varied through from Chip to Chip, but the best handling was achieved when 380 mg of the Stock Solution was diluted with 370 mg EtOH and H_2O mixture (9:1, v:v).

Table 4.1: Sensor cocktail compositions

	O_2-particles [mg/g]	**GOx** [mg/g]	**D_7 Cocktail** [mg/g]	**EtOH : H_2O** (9:1, v:v) [mg/g]
Chip 1	64,5	19,6	915,9	-
Chip 2	64,5	19,6	915,9	-
Chip 3	3,7	1,12	52,68	942,5
Chip 4	3,7	1,12	52,68	942,5
Chip 5	3,7	1,12	52,68	942,5
Chip 6	37,0	4,11	410,7	548,3
Chip 7	37,0	4,11	410,7	548,3
Chip 8	43,9	4,50	405,8	545,8
Chip 9	43,9	4,50	405,8	545,8
Chip 10	43,9	4,50	405,8	545,8
Chip 11	43,9	4,47	410,3	541,3
Chip 12	58,7	6,29	545,8	389,2
Chip 13	38,1	3,91	353,3	604,7
Chip 14	25,5	2,62	236,5	735,3
Chip 15	42,3	4,47	395,5	557,8
Chip 16	43,0	4,62	401,1	551,3
Chip 17	43,0	4,62	401,1	551,3
Chip 18	43,0	4,62	401,1	551,3
Chip 19	43,0	4,62	401,1	551,3
Chip 20	42,7	4,41	400,3	552,6
Chip 21	42,7	4,41	400,3	552,6
Chip 22	42,7	4,41	400,3	552,6
Chip 23	43,1	4,45	403,3	549,2
Chip 24	42,9	4,57	399,9	552,6

Glucose Oxidase-CLEA Cocktail

For the preperation of the sensor cocktails containing GOx-CLEA's 32,4 mg O_2-particles, 3,39 mg GOx-CLEA, 292,0 mg D_7 cocktail and 418,2 mg EtOH:H_2O (9:1) were mixed and further homogenised with the use of an ultrasonic sonifier. The ultrasonic sonifier was operated under ice cooling with an amplitude of 25 %, a pulse time of 1 second, pause between two pulse was 10 second and the total time of the pulse was 60 seconds.

Table 4.2: Ultrasonic sonifier settings

Amplitude	25 %
Pulse Time	1 [s]
Pause Time	10 [s]
Total Time	60 [s]

4.1.3 Oxygen Sensor Cocktail

For the preparation of the oxygen sensor cocktails different mixtures were tried, but the best sensor spots were made with a mixture of 36,6 mg O_2-Particles, 330,6 mg D_7 cocktail and 412,8 mg of an EtOH and H_2O solution (9:1 v:v)

Table 4.3: Oxygen sensor cocktail compositions

	O_2-particles [mg/g]	**D_7 Cocktail** [mg/g]	**EtOH : H_2O** (9:1, v:v) [mg/g]
Chip 8	48,2	411,6	540,2
Chip 9	48,2	411,6	540,2
Chip 10	48,2	411,6	540,2
Chip 11	48,4	407,1	544,4
Chip 12	63,8	545,4	390,7
Chip 13	48,4	407,1	544,4
Chip 14	48,4	407,1	544,4
Chip 15	47,0	423,8	529,2
Chip 16	47,0	427,6	525,4
Chip 17	47,0	427,6	525,4
Chip 18	47,0	427,6	525,4
Chip 19	47,0	427,6	525,4
Chip 20	47,4	419,6	533,0
Chip 21	47,4	419,6	533,0
Chip 22	47,4	419,6	533,0
Chip 23	47,4	419,6	533,0
Chip 24	47,4	421,9	531,0
Chip 27	44,5	419,8	535,7
Chip 28	44,5	419,8	535,7

4.1.4 Diffusion Barrier Cocktails

Two different diffusion barriers were used. For Chips 1-10 a D_7 diffusion barrier was used. The first diffusion barrier (D_7) caused a dissolution of the top layer and subsequently permeability for GOx at higher temperature. Therefore a polyHEMA diffusion barrier was used for chips 18-28.

D_7 Diffusion Barrier

For the knife coated sensors a 15 wt% D_7 Cocktail was used (for preperation of this Cocktail see 4.1.1 D_7 Stock Solution on page 17).
The diffusion barrier for the chips 3-5 was a 5 wt% D_7 cocktail, achieved through dilution

of 199,7 mg stock cocktail with 350,0 mg of a mixture of EtOH/H_2O (9:1 v/v).
In the chips 6 and 7 a 6 wt% diffusion barrier was used, it was made by adding 457,3 mg of a EtOH/H_2O mixture (9:1 v:v) to 304,9 mg of the D_7-stock solution.
The diffusion barrier in chips 8-10 was a 12 wt% D_7 cocktail, for this 921 mg of the D_7-stock solution was diluted with 226,9 mg of a mixture consisting of EtOH and H_2O (9:1 v:v).

PolyHEMA Diffusion Barrier

The diffusion barrier was a 10 wt% polyHEMA cocktail made by dissolving 75 mg of polyHEMA in 675 mg of a H_2O/EtOH mixture (80:20 v:v).
Due to the high water-content of this cocktail it didn't dissolve the sensor spots when the diffusion barrier was spotted on top of it via microdispensing.

4.2 Knife-Coated Sensor Spots

The sensors in chips 1 and 2 were knife-coated sensor spots. The fabrication and content of the cocktails used are described in 4.1.2 Glucose Oxidase Cocktail and 4.1.4 D_7 Diffusion Barrier.
50 µl of the sensor cocktail were pipetted on a approx. 5-6 cm straight line on a mylar support and was spread immediately afterwards with a 1 mil knife. After the sensor cocktail had dried, 230 µl of the D_7 cocktail (15 wt%) was spread on top of it with 40 µm spacer and a 3 mil knife.
For Chip 1 a piece of 2 mm x 8 mm was cut out and glued into a 10 µl rhombic Chip made out of PMMA using a solution of PS dissolved in a little bit of DCM. The Chip was closed afterwards using double-sided adhesive tape and a PMMA-slide.
For Chip 2 a circle with a diameter of 2 mm was cut out of the sensor-foil and was also glued into a 10 µl rhombic Chip made out of PMMA using PS dissolved in DCM. The Chip was closed using double-sided adhesive tape and a PMMA-slide.

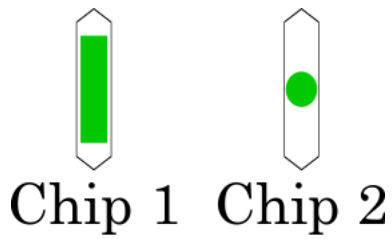

Figure 4.1: Sensor spots in chip 1 and 2

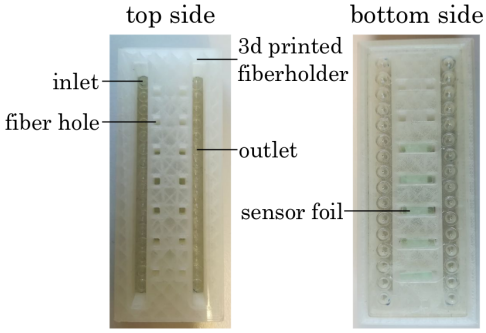

Figure 4.2: Chip 1

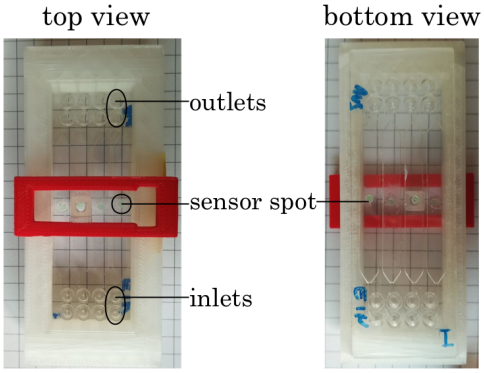

Figure 4.3: Chip 2

4.3 Microdispensed Sensor Spots

The preparation and composition for the cocktails used are described in 4.1 Cocktail Preperation

Chips 3-5

For Chips 3-5 the sensor cocktail was spotted on a PMMA-slide using the microdispenser. The sensor cocktail was spotted at first with the same settings for all chips. Afterwards a D_7 diffusion barrier was spotted on top of the sensor spots with different settings for the microdispenser. The slide was afterwards glued together with a 10 µl rhombic PMMA-chip. The sensor spots were located in the centre of the channel.

Chips 6-7

Chips 6 and 7 were prepared equally to chips 3-5 and the sensor cocktail was spotted on a PMMA-slide using the microdispenser. The sensor spots were spotted, so the spots are, after the slide was glued together with a 10 µl rhombic PMMA-chip, in the centre of the channels. The sensor cocktail was spotted first and with the same settings for all chips. Afterwards a D_7 diffusion barrier was spotted on top of the sensor spots, but with different amounts of layers. Different thicknesses of diffusion barriers were used (channel 1-3 - 2 layers; channel 4 and 5 - 1 layer; channel 6 and 7 - no diffusion barrier)

Chips 8-10

Chips 8-10 were 100 µl rhombic Chips. Oxygen sensors were spotted at the front side and at the end side of the Channel, 4 glucose sensors, 6,5 mm apart, were placed between the 2 oxygen sots. The glucose sensor spots were coated with a D_7 diffusion barrier. The

glucose sensors of the various channels were coated with different numbers of layers of D_7 diffusion barrier (channel 1 - 3 layers; channel 2 - 2 layers; channel 3 - 1 layer; channel 4 - no diffusion barrier).

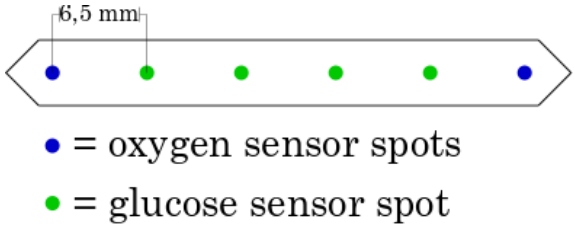

Figure 4.4: Spotalignment 0.1 ml chips

Figure 4.4 shows the alignment in which the sensors have been spotted into the channels.

Chips 11-12

Both chips 11 and 12 were 100 µl rhombic chips with the same sensor spot alignment as in chips 8-10. The sensors were printed on top of the PMMA-slide an were assembled with a 100 µl rhombic chip using double-sided adhesive tape.
For chip 11 the glucose sensor cocktail and the oxygen cocktail contained 6 wt% D_7, whereas in in chip 12 the cocktails contained 8 wt% D_7. The ratio between D_7, GOx and O_2-Particles was kept the same. For the exact composition of the Cocktails see table 4.3 Oxygen sensor cocktail compositions on page 19. The glucose sensors of chips 11 and 12 did not contain a diffusion barrier.

Chips 13-14

Similar to chips 11 and 12, both chips chips 13 and 14 were 100 µl rhombic Chips with the same sensor spot alignment as in the chips 8-10. The sensors were printed directly into the channels and were assembled with a PMMA-slide using double-sided adhesive tape.
For chip 13 the glucose cocktail and the oxygen cocktail contained 6 wt% D_7, in chip 14 the cocktails contained 4 wt% D_7. The ratio between D_7, GOx and O_2-Particles was kept the same. For the exact composition of the Cocktails see table 4.3 Oxygen sensor cocktail compositions on page 19. The glucose sensors did not contain a diffusion barrier.

Chip 15

Chip 15 was a 100 µl rhombic Chip with the same sensor spot alignment as in chips 8-10. The sensors were printed inside the channels and were assembled with a TOPAS-slide using double-sided adhesive tape.

A different spot thickness of the glucose sensors of the various channels was used by spotting layers on top of each other (channel 1 - 4 layers; channel 2 - 3 layers; channel 3 - 2 layers; channel 4 - 1 layer). The glucose sensors were not coated with a diffusion barrier.

Chips 16-17

Chips 16 and 17 were 100 µl rhombic Chips with the same sensor spot alignment as in chips 8-10. The sensors were printed inside the channels and were assembled with a TOPAS-slide using double-sided adhesive tape.
A different spot thickness of the glucose sensors of the various channels was used by spotting layers on top of each other (channel 1 - 4 layers; channel 2 - 3 layers; channel 3 - 2 layers; channel 4 - 1 layer). The glucose sensors were not coated with a diffusion barrier.

Chips 18-19

Chips 18 and 19 were 100 µl rhombic Chips with same sensor spot alignment as in the chips 8-10. The sensors were printed inside the channels and were assembled with a TOPAS-slide using double-sided adhesive tape.
A different spot thickness of the glucose sensors of the various channels was used by spotting layers on top of each other (channel 1 - 4 layers; channel 2 - 3 layers; channel 3 - 2 layers; channel 4 - 1 layer). Various diameters of glucose sensors were used by changing the settings of the microdispenser (chip 18 had smaller diameter for the sensor spots and chip 19 had a bigger diameter for the sensor spots). The glucose spots were coated with a polyHEMA diffusion barrier.

Chips 20-22

Chips 20 - 22 were 100 µl rhombic Chips with the same sensor spot alignment as in chips 8-10. The sensors were printed inside the channels and were assembled with a TOPAS-slide using double-sided adhesive tape.
A different spot thickness of the glucose sensors was used by spotting layers on top of each other (chip 20 - 4 layers; chip 21 - 8 layers; chip 22 - 12 layers). The glucose spots were coated with a polyHEMA diffusion barrier. The thickness of the polyHEMA barrier varied within the different channels (channel 1 - 12 layers; channel 2 - 9 layers; channel 3 - 6 layers; channel 4 - 3 layers of polyHEMA). .

Chip 23

Chip 23 was a 100 µl rhombic Chip with the same sensor spot alignment as in chips 8-10. The sensors were printed inside the channels and were assembled with a TOPAS-slide using double-sided adhesive tape.
A different spot thickness of the glucose sensors of the various channels was used by spotting layers on top of each other (channel 1 and 2 - 8 layers; channel 3 and 4 – 12 layers). The glucose sensors were coated with 4 layers of polyHEMA diffusion barrier.

Chip 24

Chip 24 was a single channel chip with a height of 100 µm (250 µm after assembly, due to the double sided adhesive tape), a diameter of 2,5 mm and a length of 58.5 mm. 10 Sensors (5 mm apart) have been printed in the channel with oxygen sensors at the first and last spot, respectively. The residual 8 spots in-between contained glucose sensors coated with a polyHEMA diffusion barrier. The thickness of the sensors was 2 layers for the oxygen sensors and 12 layers for the glucose sensors. The thickness of the diffusion barrier of the glucose sensor was 4 layers.

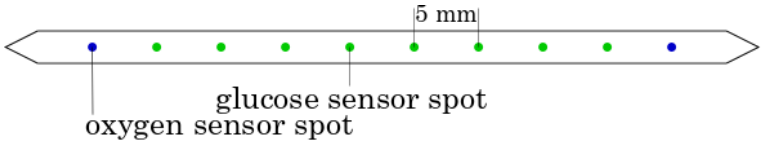

Figure 4.5: Spotalignment single-channel chip

Chip 27

Chip 27 was a 100 µl rhombic Chip with the same sensor spot alignment as in chips 8-10. For the glucose sensors a GOx-CLEA Cocktail has been used. The sensors were printed inside the channels and were assembled with a TOPAS-slide using double-sided adhesive tape.
A different spot thickness of the glucose sensors of the various channels was used by spotting layers on top of each other (channel 1 - 12 layers; channel 2 – 9 layers; channel 3 – 6 layers; channel 4 – 3 layers). The glucose sensors had no diffusion barrier.

Chip 28

Chip 28 was a single channel chip with the same spot arrangement as in chip 24. The thickness of the sensors was 3 layers for the oxygen sensors, 12 layers for the glucose sensors of channel 1 and 2 and 9 layers for the glucose sensors of channel 3 and 4. The

thickness of the diffusion barrier was 2 layers in channel 1 and 3 as well as 1 layer in channel 2 and 4.

4.4 Puffer and Sample Solution Preperation

4.4.1 Puffer Solution

A puffer solution containing 10 mM Na_2HPO_4 and 130 mM NaCl at pH=7,00 was prepared.
For the puffer-solution 0,8889 g NaH_2PO_4 and 3,7936 g NaCl were dissolved in 450 ml deionized water, pH-value was brought to ph=7,01 by using NaOH and HCl. Afterwards the solution was filled up to a total of 500 ml.

4.4.2 Glucose Solution

For the glucose solution a 100 mM stock solution was prepared by dissolving 0,9908 g D-Glucose-Monohydrate in 50 ml puffer solution.
10; 8; 6; 4; 2 and 1 mM glucose solution were made by pipetting a certain amount of stock solution into 50 ml test-tubes and filling them up to 50 ml with puffer.
The solutions were prepared at least 1 day before the measurements, so the α- and β-form of the glucose had reached equilibrium before the measurements.

Table 4.4: Glucose solution

c Glucose [mol/l]	**Stock solution [ml]**	**Total volume[ml]**
10	5,00	50
8	4,00	50
6	3,00	50
4	2,00	50
2	1,00	50
1	0,50	50

4.5 Experimantal Set-Up and Measurement Settings

4.5.1 Knife-Coated sensors

Chip 1

Chip 1 was a 10 µl rhombic Chip made out of PMMA. A 2x8 mm sensor-foil was glued into the channel. One of the inlets and one of the outlets of the microfluidic chamber were closed with a Mini Luer Plug.
A fibre-holder was 3d-printed containing holes for the optical fibres (see Figure 4.5.1 Chip

1)
Glucose solutions with concentrations of 2, 4, 6, 8 and 10 mM were pumped through the inlet with flow rates of 0,2 and 1 µl/s.
The O_2-content was measured using a FirestingO2 (4 Channels), the optical fibres were kept in place using a 3d printed fibre-holder. The modulation frequency was 4 kHz. The measurements were performed at room-temperature.

Chip 2

Chip 2 was a 10 µl rhombic Chip made out of PMMA. A circleshaped piece of sensor-foil with a diameter of 2 mm was glued into the channel. One of the inlets and one of the outlets of the microfluidic chamber were closed with a Mini Luer Plug.
The O_2-content was measured using a FirestingO2 (4 Channels), the optical fibres were placed on top of the sensor spots with the help of a 3d-printed fibre-holder. All measurements were made at room-temperature.
2 mM Glucose solution was measured at flow rates of 0,2; 0,4; 0,6; 0,8 and 1 µl/s. Additionally 2; 4; 6; 8 and 10 mM glucose solutions were measured at flow rates of 0,2 and 0,6 µl/s.

4.5.2 Microdispensed Sensors

Chip 3-5

Chips 3-5 were 10 µl rhombic chips made out of PMMA. The sensor spots were inkjet printed into the channel using a microdispenser. The sensor spots were coated with a D_7 diffusion barrier. The D_7 diffusion barrier was spotted with different microdispenser settings (see table 10.2 Microdispenser Settings for Chips 3-5 on page 74).
0; 2; 4; 6; 8 and 10 mM glucose solutions were pumped through the chip at a flow rate of 0,2 µl/s. The O_2-content was measured using a FirestingO2 (4 Channel), the optical fibres were kept on top of the sensor spots using a 3d-printed fibre-holder.

Chip 6-7

Chips 6-7 were 10 µl rhombic chips out of PMMA. The sensor spots were inkjet printed into the channel using a microdispenser. The sensor spots were coated with a D_7 diffusion barrier. The D_7 diffusion barrier was spotted with a different amount of layers in the channels. Channel 1-3 had 2 layers, channel 4 and 5 had 1 layer and channel 6 and 7 had no diffusion barrier. (For the settings of the microdispenser see table 10.3 Microdispenser Settings for Chips 6 and 7 on page 74)
Measurements with glucose concentrations of 0; 1; 2; 4; 6; 8 and 10 mM was performed at flow rates of 0,2 µl/s. Also the leaching of the GOx out of glucose sensor spots was

tested. Therefore this 6 mM Glucose was permanently pumped for 1000 min through the chamber. All measurements were made at room-temperature.

Chip 8-10

Chips 8-10 were 100 µl rhombic chips out of PMMA. Each chamber contained 6 sensor spots with oxygen sensors at the first and the last spot, respectively. The residual 4 spots in-between contained glucose sensors. All sensor spots were spotted on the PMMA-slide and not direct into the chamber of the chip. The glucose sensor spots were coated with a D_7 diffusion barrier. (For the settings of the microdispenser see table 10.4 Microdispenser settings for chips 8 - 10 on page 75)
Measurements with glucose concentrations of 0; 1; 2; 4; 6; 8 and 10 mM were performed at flow rates of 0,5; 1,0; 1,5; 2,0 and 5,0 µl/s. Measurements at all flow rates have been done at 25°C, additional to this measurements at a flow rate of 0,5 µl/s were done at 37°C using a water bath.

Chip 11-12

Chips 11 and 12 were 100 µl rhombic chips out of PMMA. The sensor spot arrangement was equal to chips 8-10. The glucose sensor spots were not coated with a diffusion barrier. (For the settings of the microdispenser see table 10.5 Microdispenser settings for chips 11 and 12 on page 75).
Measurements with glucose concentrations of 0; 1; 2; 4; 6; 8 and 10 mM were performed at flow rates of 0,5; 1,0; 1,5; 2,0 and 5,0 µl/s. All measurements were done at room temperature.

Chip 13-14

Chips 13 and 14 were 100 µl rhombic chips out of PMMA. The sensor spot arrangement was equal to chips 8-10. The glucose sensor spots were not coated with a diffusion barrier. The ratio between D_7, oxygen sensor particles and GOx were the same in both chips, but the dilution factor was different (chip 11 had 6 wt% total D_7, chip 12 had 4 wt% total D_7).(For the settings of the microdispenser see table 10.6 Microdispenser settings for chips 13 and 14 on page 75).
Measurements with glucose concentrations of 0; 1; 2; 4; 6; 8 and 10 mM were performed at flow rates of 0,5; 1,0; 1,5; 2,0 and 5,0 µl/s. All measurements were done at room temperature.

Chip 15

Chip 15 was a 100 µl rhombic chips out of PMMA. Each chamber contained 6 sensor spots with oxygen sensors at the first and the last spot, respectively. The residual 4 spots in-between contained glucose sensors. The sensors were spotted direct into the channel of the chip instead of the slide side. The glucose sensors did not contain a diffusion barrier. The thickness of the glucose sensors was 4 layers in channel 1, 3 layers in channel 2, 2 layers in channel 3 and 1 layer in channel 4. (For the settings of the microdispenser see table 10.7 Microdispenser settings for chip 15 on page 76).
This time, the chip was kept on temperature with the help of a heating block, the optical fibres were placed on top of the sensor spots with the help of a 3d printed fibre-holder.

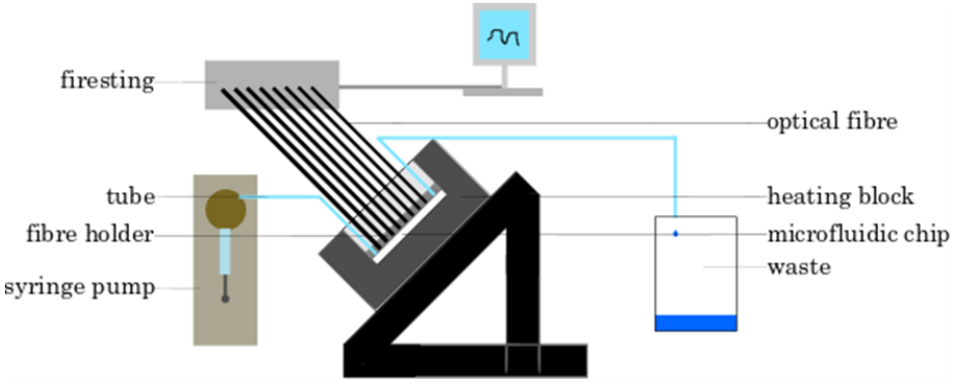

Figure 4.6: Measurement setup-of chip 15

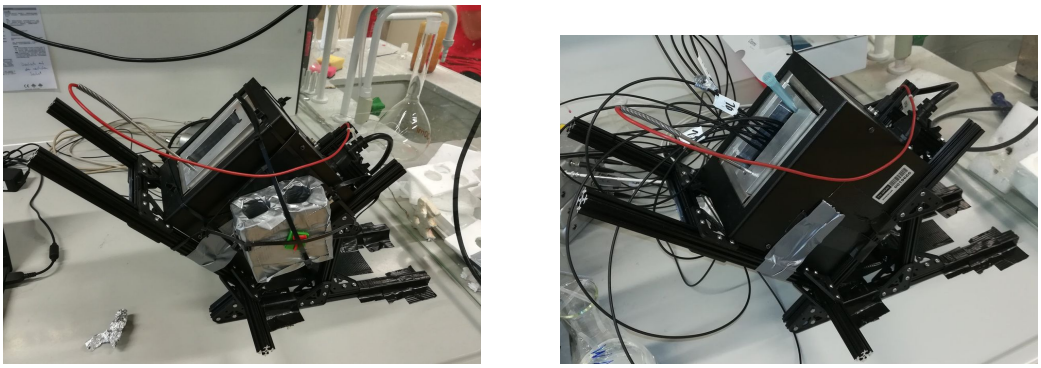

(a) without fibers connected

(b) with fibers connected

Figure 4.7: Chip in heating block - side view

Figure 4.8: Chip in heating block - top view

Measurements with glucose concentrations of 0; 1; 2; 4; 6; 8 and 10 mM were done at flow rates of 0,5; 1,0; 1,5; 2,0 and 5,0 µl/s. All measurements were done at room temperature and at 37°C.

Chips 16 and 17

Chips 16 and 17 were made similar to chip 15, with slightly different settings of the microdispenser. (For the settings of the microdispenser see table 10.8 Microdispenser settings for chips 16 and 17 on page 76).
This time the leaching of the GOx was tested by measuring 8 mM Glucose at a flow rate of 0,5 µl/s 10 times at 37°C.

Chips 18 and 19

The chips 18 and 19 had the same spot-arrangement and measurement set-up as chip 15. This time the glucose sensors were coated with a polyHEMA diffusion barrier (10 wt% polyHEMA dissolved in a mixture of $H_2O$and EtOH (80:20, v:v)). The thickness of the glucose sensors was 4 layers in channel 1, 3 layers in channel 2, 2 layers in channel 3 and 1 layer in channel 4. Chip 19 had slightly bigger glucose sensor spots due to different settings for the microdispenser. (For the settings of the microdispenser see table 10.9 Microdispenser settings for chips 18 and 19 on page 77).
Leaching tests were performed by measuring 8 mM glucose solution at 37°C for a period of 15 hours.

Chips 20-22

Chips 20, 21 and 22 had the same spot-arrangement and measurement set-up as chip 15. This time the glucose sensors were coated with a polyHEMA diffusion barrier (10 wt% polyHEMA dissolved in a mixture of $H_2O$and EtOH (80:20, v:v)). Chip 20 had 4 layers of glucose sensor, Chip 21 8 layers and Chip 22 12 layers. The thickness of the polyHEMA diffusion barrier was 12 layers in channel 1, 9 layers in channel 2, 6 layers in channel 3 and 3 layers in channel 4. (For the settings of the microdispenser see table 10.10 Microdispenser settings for chips 20 - 22 on page 77.
Leaching tests were performed by measuring 8 mM glucose solution at 37°C for a period of 15 hours.

Chip 23

Chip 23 had the same spot-arrangement and measurement set-up as chip 15. This time the glucose sensors were coated with a polyHEMA diffusion barrier (10 wt% polyHEMA dissolved in a mixture of $H_2O$and EtOH (80:20, v:v)). The thickness of the glucose sensors was 12 layers in channel 1 and 2, 8 layers in channel 3 and 4. (For the settings of the microdispenser see table 10.11 Microdispenser settings for chip 23 on page 78.
Leaching tests were performed by measuring 8 mM glucose solution at 37°C for a peiod of 4 hours. Measurements with glucose concentrations of 0; 1; 2; 4; 6; 8 and 10 mM were done at flow rates of 0,5; 1,0; 1,5; 2,0 and 5,0 µl/s at a temperature of 37°C.

Chip 24

Chip 24 was a single channel chip containing 10 sensors. Oxygen sensors were placed at the first and last spot, respectively. The residual 8 spots in-between contained glucose sensors coated with a polyHEMA diffusion barrier (10 wt% polyHEMA dissolved in a mixture of $H_2O$and EtOH (80:20, v:v)). (For the settings of the microdispenser see table 10.12 Microdispenser settings for chip 24 on page 78).
Measurements with glucose concentrations of 0; 1; 2; 4; 6; 8 and 10 mM were performed at flow rates of 0,5; 1,0; 1,5; 2,0 and 5,0 µl/s and at a temperature of 37°C.

Chip 27

Chip 27 had the same spot-arrangement and measurement set-up as chip 15. The glucose sensor spot was made out of a GOx-CLEA cocktail (see 4.1.2 Glucose Oxidase-CLEA Cocktail). The glucose sensors did not contain a diffusion barrier. The thickness of the glucose sensors was 12 layers in channel 1, 9 layers in channel 2, 6 layers in channel 3 and 3 layers in channel 4. (For the settings of the microdispenser see table 10.13 Microdispenser settings for chip 27 on page 78).

Leaching tests were performed by measuring 6 mM glucose solution at 37°C for a period of 25 hours.

Chip 28

Chip 28 had the same spot-arrangement and measurement set-up as chip 15. The glucose sensor spots were made out of a GOx-CLEA cocktail. The glucose sensors were coated with a polyHEMA diffusion barrier. The thickness of the glucose sensors was 12 layers in channel 1 and 2 as well as 9 layers in channel 3 and 4. The thickness of the polyHEMA diffusion barrier was 2 layers in channel 1 and 3 as well as 1 layer in channel 2 and 4. (for the settings of the microdispenser see table 10.14 Microdispenser settings for chip 28 on page 79).
Leaching tests were performed by measuring 6 mM glucose solution at 37°C for a period of 25 hours. Also measurements of glucose solutions with concentrations of 0; 1; 2; 4; 6; 8 and 10 mM have been done at flow rates of 0,25; 0,5; 1,0; 1,5; 2,0 and 5,0 µl/s at a temperature of 37°C.

5 Results and Discussion

5.1 Sensor Spot Morphology

5.1.1 Oxygen Sensor Spots

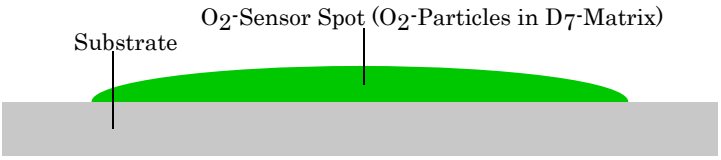

Figure 5.1: Design of the O_2-Sensor Spots

Figure 5.1 shows the design of the oxygen sensor spots, the O_2 sensor cocktail was spotted into the channels of the microfluidic chip.
The pictures and the depth measurements of the sensor spots were made with a Keyence VHX 5000 microscope. The transparency of the microfluidic chips was a major challenge for the thickness measurement of the sensor spots. Therefore, results must be considered as approximate estimation and not as exact values.

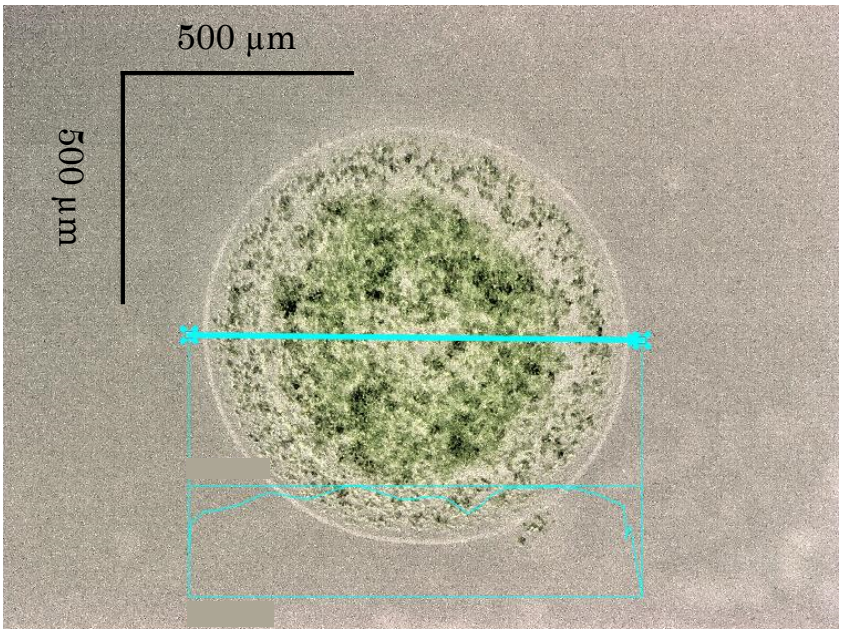

Figure 5.2: Photo of a oxygen sensor spot in Chip 24

Figure 5.2 shows the picture of an oxygen sensor spot under the microscope with a spot height of 20-30 µm. The polystyrene nanoparticles, which were stained with a green oxygen sensitive dye, can be seen as the green grain-like structure in the spot. Due to the transparency of the chip material a exact determination of the sensor spot height was not possible. Therefore it was estimated to be in the range of 20-30 µm. Oxygen sensor spots were thinner than glucose sensor spots due to fewer layers and the absence of an additional diffusion barrier.

5.1.2 Glucose Sensor Spots

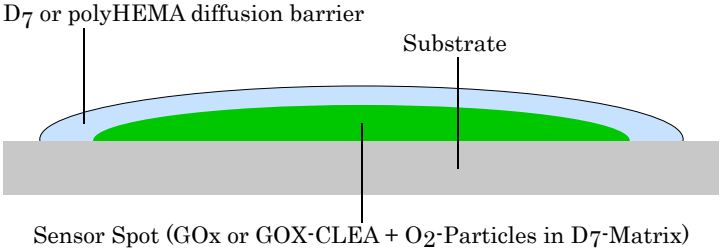

Figure 5.3: Design of the glucose sensor spots

Figure 5.3 shows the design of the glucose sensor spots. The sensor cocktail (GOX + O_2-particles + D_7-Hydrogel) was spotted on the chip. In some chips the sensor spots were coated with a D_7 or polyHEMA diffusion barrier.

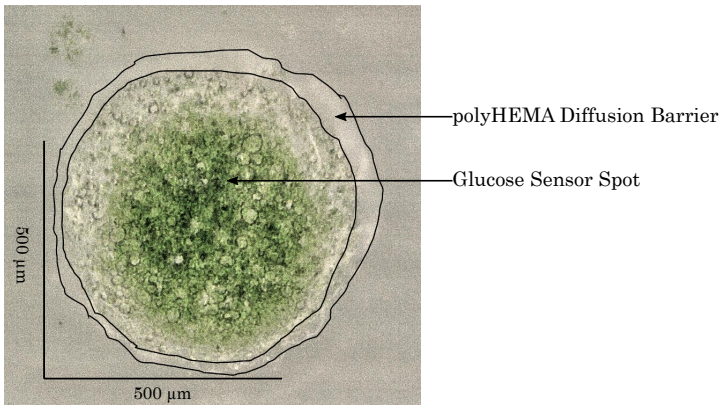

Figure 5.4: Photo of a glucose sensor spot covered with a polyHEMA diffusion barrier in chip 24

Figure 5.4 shows the picture of a ∼50 µm thick glucose sensor spot in a swollen state at room temperature (the channels were filled with puffer solution the day before photos have been taken), the clear border that can be seen is the diffusion barrier and the green center is the result of microdispensing several layers of glucose sensor cocktail on top

of each other. The visible grain like texture results from the polystyrene nanoparticles stained with a green oxygen sensitive dye.

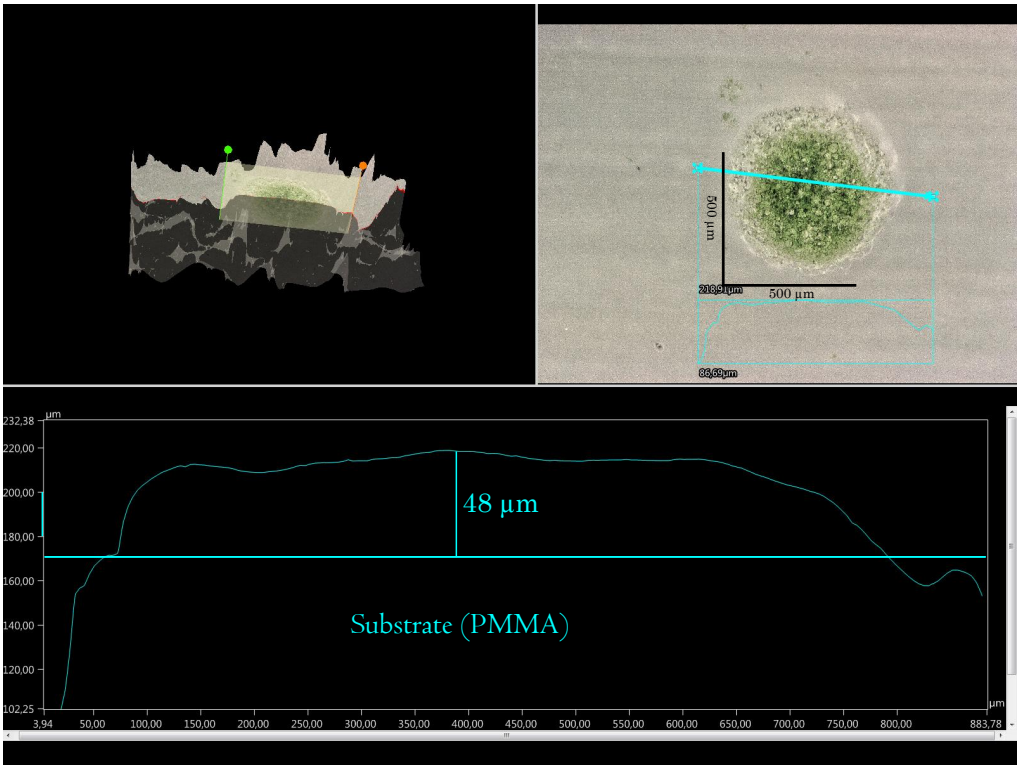

Figure 5.5: Thickness-measurement of a glucose sensor spot in chip 24

Figure 5.5 shows the result of the depth measurement with the microscope. Due to the transparency of the chip material, a exact determination of the spot thickness was not possible. Therefore, the thickness of depicted spot was estimated to be in a range of 50-60 µm. The height of the spots varied from ca. 30 to 80 µm, depending on the amount of sensor layers, the sensor cokctail composition and the diffusion barrier thickness of the spots.
A perfect alignment of the layers was not achieved every time, causing differences in thickness and surface of the glucose sensor spots resulting in a visible impact on the measurements (effect is described when it occurred).

5.2 Sensors based on Knife Coated layers

Two different chips with sensors were produced by knife coating a sensor cocktail (GOx, O_2-particles and D_7 dispersed in H_2O:EtOH=9:1 (v:v)) and a D_7 diffusion barrier on top of the sensor layer. The substrate was a mylar foil and for chip 1 a rectangle shaped sensor and for chip 2 a circular shaped sensor was glued into the microfluidic chip.

In Chip 1 Glucose concentrations of 2, 4, 6, 8 and 10 mM were measured at flow rates of 0,2 µl/s and 1,0 µl/s.

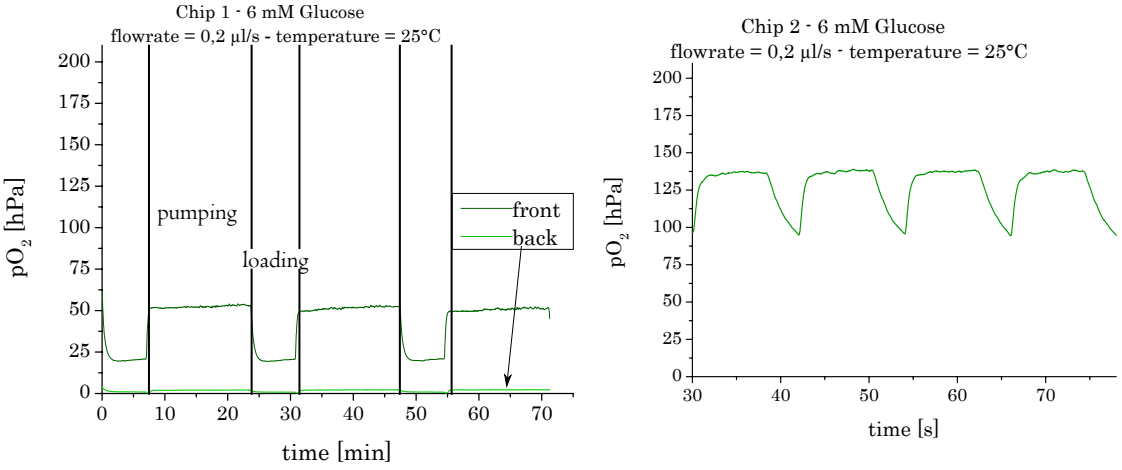

Figure 5.6: Example measurement of 6 mM glucose at a flow rate of 0,2 µl/s and 25°C in chip 1 (rectangular shaped sensor) and chip 2 (circular shape)

Figure 5.2 shows example measurements of a 6 mM glucose solution at 25°C and at a flow rate of 0,2 µl/s in chips 1 and 2.
For Chip 1 the oxygen content of the sensor was measured at the front end and at the back end of the rectangular shaped sensor. In the graph the pumping and the loading phase can be seen. During the pumping phase the glucose solution was pumped through the microfluidic chip with a flow rate of 0,2 µl/s. During the loading phase the syringe pump was filled with the glucose solution and due to the absence of flow in the microfluidic chip a drop in the oxygen contend was observed (GOx consumes the O_2). The front side of the sensor did show a nice response, however, at the back side the sensor already reached anaerobe conditions caused by the large size of the sensor stripe, which also led to a higher amount of GOx and a large consumption of oxygen.
Chip 2 had a circular shaped sensor. The oxygen content was measured in the centre of the sensor spot. The sensor spot in chip 2 was much smaller when compared with the sensor in chip 1. Chip 2 had channels with a volume of 100 µl, while chip 1 had only 10 µl channels (meaning that in chip 2 is more total O_2) possibly explaining the high oxygen content at same settings.

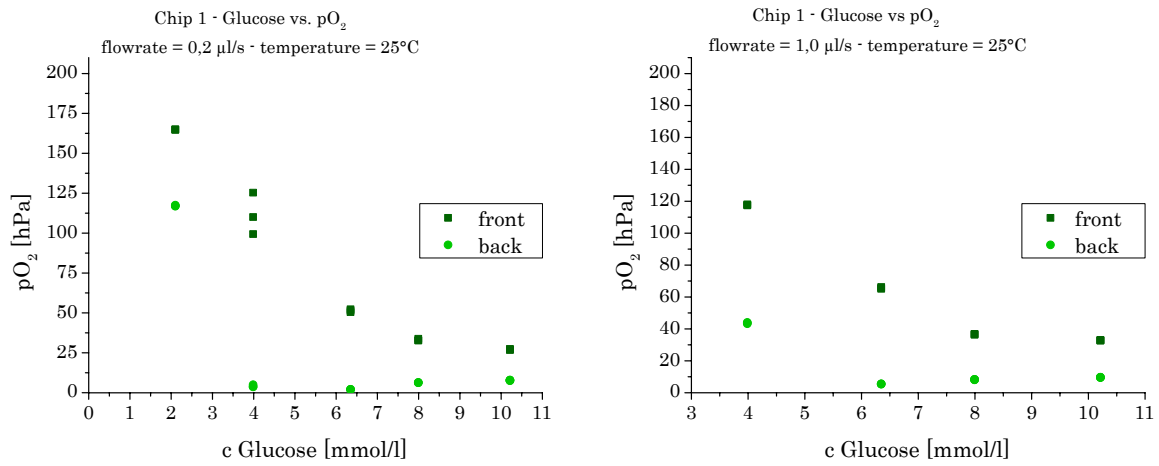

Figure 5.7: Summary of the measurements in chip 1 at flow rates of 0,2 µl/s (left) and 1,0 µl/s (right), at a temperature of 25°C. Measurements were done at the front and back end of the sensor, each glucose concentration was measured 3 times.

Figure 5.7 shows the measured oxygen content of the sensor-stripe in chip 1 at different glucose concentrations. The left graph shows the results at a flow rate of 0,2 µl/s and the right graph shows the results at a flow rate of 1,0 µl/s. The optical fibres were placed at the front end (darker green) and at the back end (brighter green) of the sensor-stripe. Each glucose concentration was measured 3 times. The back end of the glucose sensors quickly became anaerobe, indicating that such big sensors are not necessary.

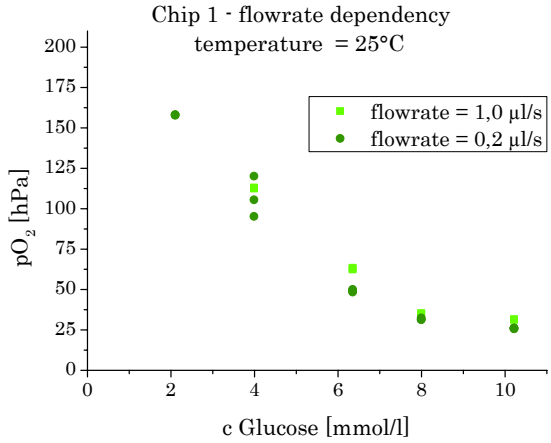

Figure 5.8: Flow rate influence in chip 1 at 1-8 mM glucose concentration and at a temperature of 25°C. Only front-end results of the sensor stripes are depicted.

Figure 5.8 shows the comparison of measurements at 2 different flow rates (0,2 and 1,0 µl/s) in chip 1 at a temperature of 25°C. Each measurement has been performed 4 times. Only the measured oxygen of the front-end side of the sensor is depicted, since the back-end side reaches anaerobe conditions at glucose concentrations higher than

4 mM. The change of flow rate from 0,2 µl/s to 1,0 µl/s seemed to have only a minor impact, the sensor consumes a little bit more O_2 at 0,2 µl/s.

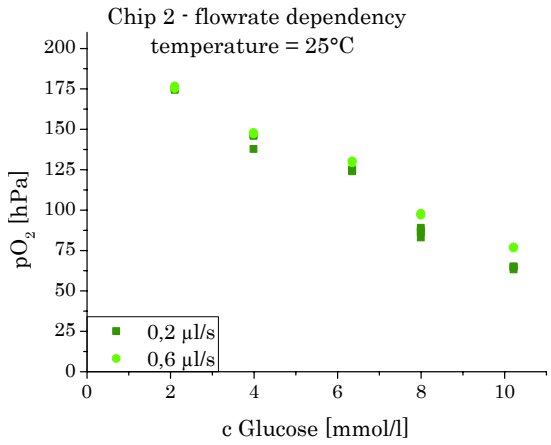

Figure 5.9: Flow rate influence in chip 2 (circular shaped sensors) at 1-8 mM glucose concentration and at a temperature of 25°C

Figure 5.9 shows the comparison of measurements at two different flow rates (0,2 and 0,6 µl/s) in chip 2 at a temperature of 25°C. The change of flow rate from 0,2 µl/s to 0,6 µl/s seemed to have only a minor impact, a small trend for lower O_2-concentrations in the sensor at the smaller flow rate was observed.
Overall the results of the sensors prepared via knife coating technique are promising, but have 2 major drawbacks.
Firstly, the big size of the sensors (e.g. circular shaped sensors in chip 2 with a diameter of 2mm) made it impossible to apply these sensors in smaller microfluidic devices. Producing smaller, reproducible sensors was not successful.
Secondly, the position of the sensors in the chips. Precise positioning of the sensors in the chips was challenging, since the sensors had to be fixed manually in the chips.
Based on these outcomes, the following sensors were made by microdispensing the sensor cocktail directly into the microfluidic chips. The microdispenser allows to make smaller sensors spots and, since the microdispenser is strapped on a CNC machine, the exact positioning of sensors spots is possible.

5.3 Sensors fabricated using microdispensing techniques

Multiple chips were prepared with sensor spots. The sensors differed in the amount of sensor layers and diffusion barrier layers, diffusion barrier material (D_7 and polyHEMA) and enzyme used (GOx and GOx-CLEA). The impact of conditions like glucose concentration, temperature, flow rate and channel dimension on the sensor spots were investigated.

5.3.1 Sensors without a Diffusion Barrier - 25°C

Glucose sensors consisting of a layer with GOx and O_2-nanoparticles were integrated in 10 and 100 µl rhombic chips. The glucose sensors varied in the amount of layers that were spotted on top of each other. Measurements were done at different glucose concentrations and different flow rates.

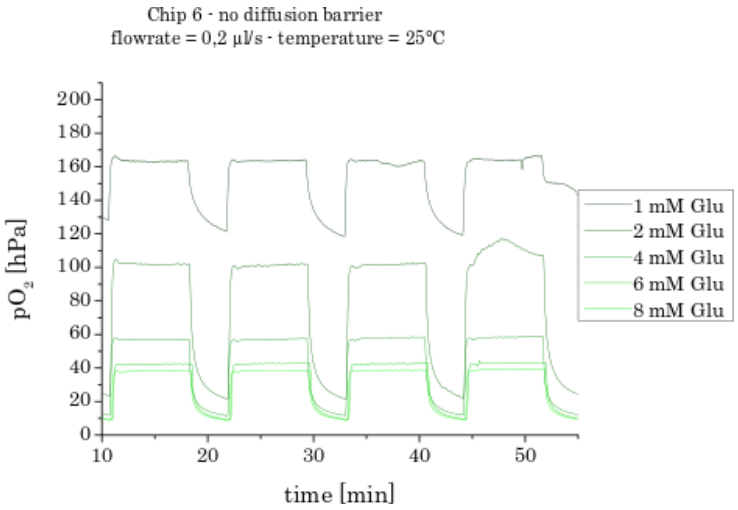

Figure 5.10: Microdispensed sensor spots exposed to 1 - 8 mM glucose at a flow rate of 0,2 µl/s and a temperature of 25°C in chip 6

Figure 5.10 shows an example measurement of the sensor spots in chip 6 (10 µl volume) exposed to glucose concentrations of 1 - 8 mM and a flow rate of 0,2 µl/s.

Influence of Spot Thickness

The thickness of the glucose sensor spots was varied by microdispensing several layers of sensor cocktail on top of each other. The influence of the sensor spot thickness was investigated.

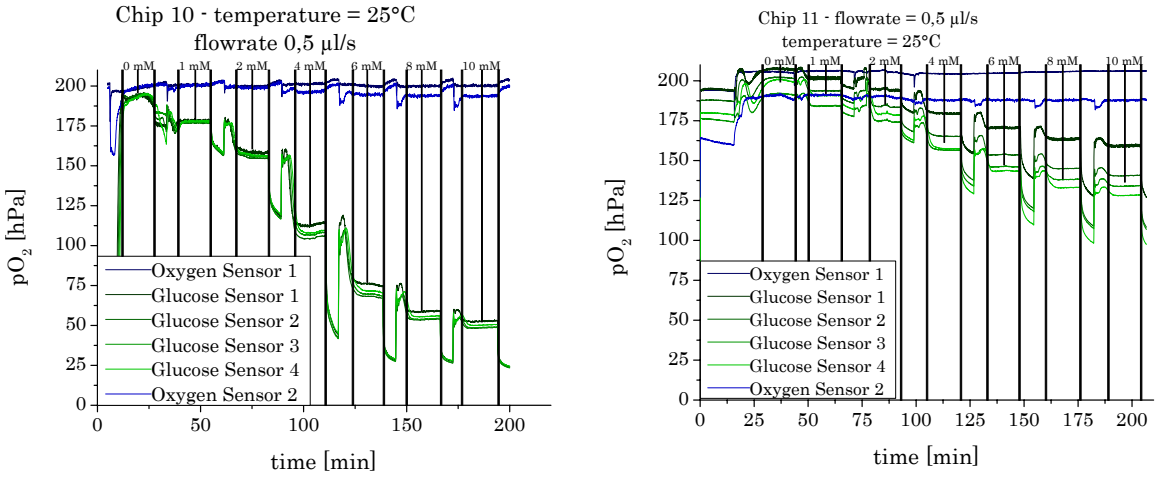

Figure 5.11: Measurement of the Glucose- and Oxygen Sensor Spots in chips 10 and 11 (volume=100 µl) at glucose concentrations of 0 - 10 mM, at a flow rate of 0,5 µl/s and at a temperature of 25°C

Figure 5.11 shows the measurements of the chips 10 and 11 at glucose concentrations from 0; 1; 2; 4; 6; 8 and 10 mM, at a flow rate of 0,5 µl/s and a temperature of 25°C. The glucose sensors in chip 10 were fabricated by pulsing 10 layers of sensor cocktail on top of each other. The glucose sensor in chip 11 was a single layer of sensor cocktail. The glucose sensor cocktail composition was the same. To further investigate this assumption another 100 µl chamber chip was prepared. In this chip the amount of layers for each glucose sensor varied from chamber to chamber.

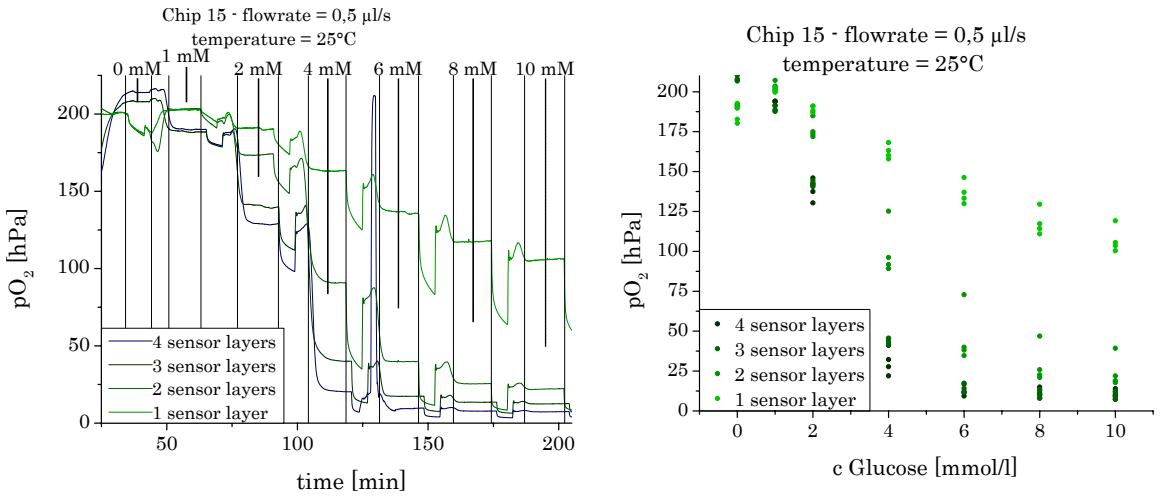

Figure 5.12: Measurement of sensors in chip 15, the sensor consisted of 1-4 layers and were measured at glucose concentrations of 0; 1; 2; 4; 6; 8 and 10 mM at a flow rate of 0,5 µl/s and a temperature of 25°C

Figure 5.12 shows the signal of the glucose sensor spots in dependence of the amount of layers spotted on top of each other. The left graph shows the progression of the

measurement, the right graph the measured oxygen mean value. The oxygen content was measured in 4 different glucose sensor spots. These graphs prove that the oxygen consumption is directly linked to spot size. This can be explained by the increase of the total GOx content of the sensor due to the increase of the spot size. Additionally, a second effect is most likely caused by the increase of the spot size. Due to additional space and therefore increased residence time of glucose within the spot, the possibility of the conversion of glucose by the GOx is increased.

Influence of the Flow Rate

An important factor to consider is the influence of the flow rate at the measurement results of the glucose sensors. To investigate this aspect we exposed the sensor spots to glucose concentrations of 0 - 10 mM at flow rates of 0,5; 1,0; 1,5; 2,0 and 5,0 µl/s.

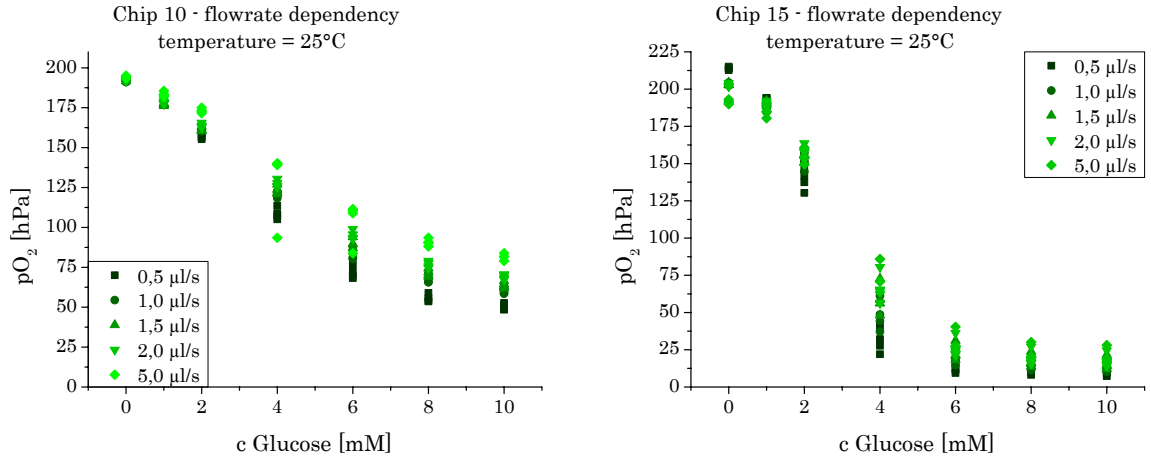

Figure 5.13: Influence of the flow rate on the measurements in the microfluidic chips 10 and 15 (volume = 100 µl), measurements were performed at 25°C and flow rates of 0,5; 1,0; 1,5; 2,0 and 5,0 µl/s

Figure 5.13 shows the measured oxygen content of 4 different glucose sensors in the chips 10 and 15 (volume=100 µl) at different glucose concentrations (0; 1; 2; 4; 6; 8 and 10 mM) and at different flow rates (0,5; 1,0; 1,5; 2,0 and 5,0 µl/s).
A small trend of higher oxygen content at higher flow rates was measured in the glucose sensor spots (especially at higher glucose concentrations). This can be explained by the affection of the diffusion of glucose and oxygen by the flow rate (higher flow rate leads to faster diffusion rates), leading to a shift of the equilibrium by decreased residence time of oxygen and glucose in the sensor spots.

Leaching of Enzyme

The leaching of the immobilized enzyme was investigated by pumping a 6 mM glucose solution through the microfluidic chip (volume=10 µl) for 16,7 h at a temperature of 25°C and a flow rate of 0,2 µl/s.

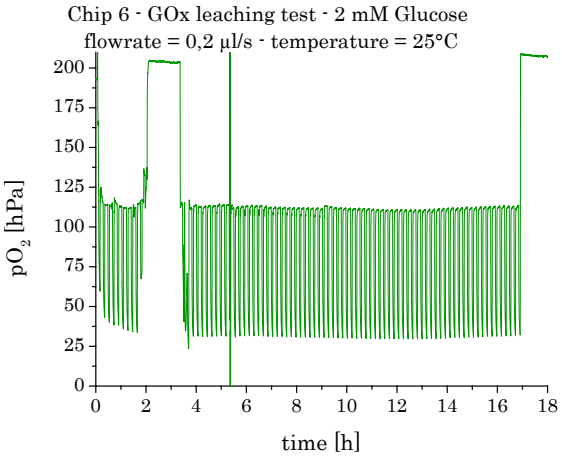

Figure 5.14: GOx leaching test of channel 6 in chip 6 (volume=10 µl) at a flow rate of 0,2 µl/s and at a temperature of 25°C

Figure 5.14 shows the course of the GOx-leaching test, 6 mM glucose solution was pumped through chip 6 (voluem=10 µl) repeatedly at a flow rate of 0,2 µl/s and a temperature of 25°C.
The graph shows slight scattering during the measurements. No trend could be observed indicating a leaching effect of the GOx at 25°C.

5.3.2 Sensors without a Diffusion Barrier - 37°C

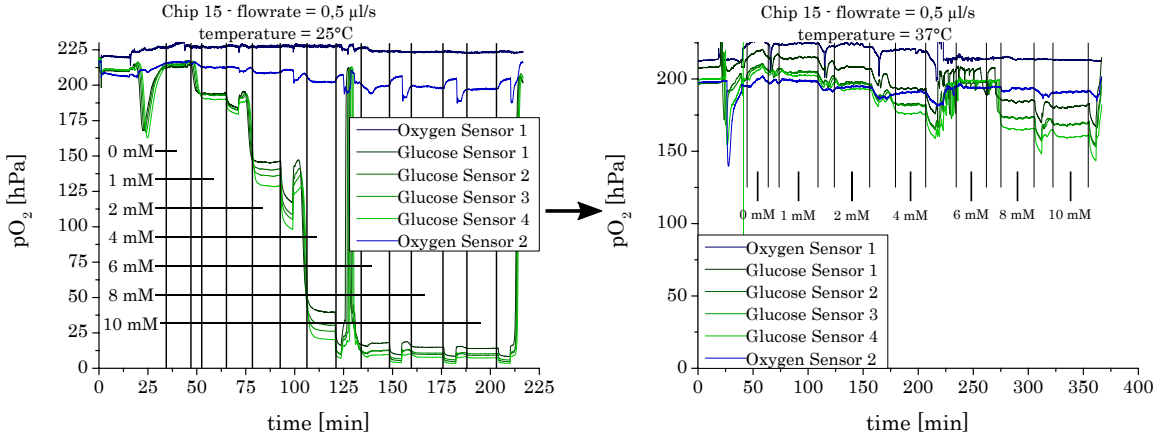

Figure 5.15: Measurements of 0; 1; 2; 4; 6; 8 and 10 mM glucose solution at 25°C (left) and 37°C (right, heated via heating block).

In figure 5.15 the change of signal in chip 15 at a temperature of 25°C and 37°C is displayed. At 25°C the glucose spots show a nice signal splitting, however, at 37°C hardly any signal splitting can be observed with the same sensors. There are 2 possible explanations for this result. Firstly, at 37°C the diffusion rate of O_2 is faster than the consumption rate of GOx. Secondly (and more plausible), at 37°C GOx leaches out of the sensors. A possible reason for leaching out is the higher water uptake of the D_7-hydrogel (35% at 25°C and 46% at 37°C [11]) and a better solubility of GOx in water at 37°C.

Leaching of Enzyme

To confirm that the GOx is leaching out of the sensor spots at 37°C, chip 16 was prepared and the channels were pumped for multiple cycles with a 8 mM glucose solution and the measured oxygen content of the glucose sensor spots were monitored.

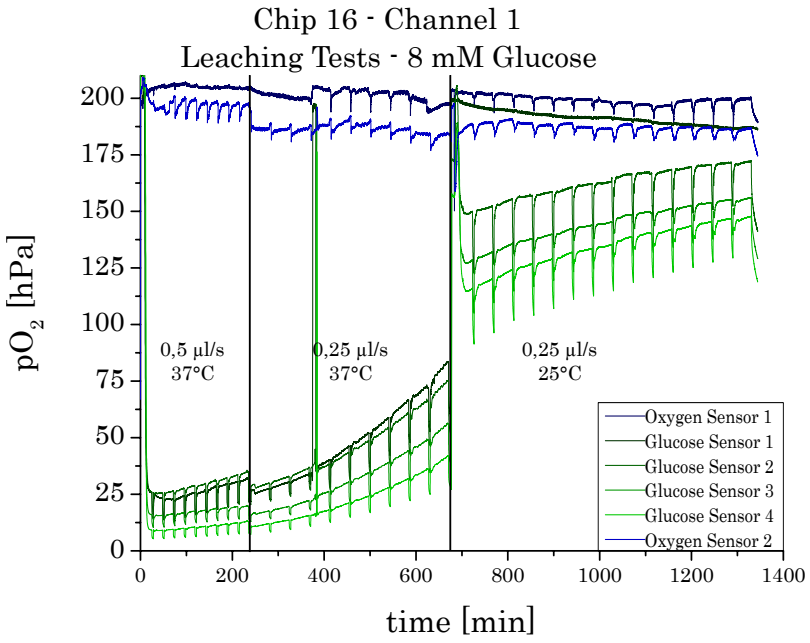

Figure 5.16: GOx leaching tests of channel 1 in chip 16 (volume=100 µl), the graph is composed of 3 different measurements. First measurement at a flow rate of 0,5 µl/s and a temperature of 37°C, second measurement at a flow rate of 0,25 µl/s and a temperature of 37°C and third measurement at a flow rate of 0,25 µl/s and a temperature of 25°C. Between each measurement the sensor spots were soaked (for several hours) in the glucose solution until the next measurement was started

Figure 5.16 shows the course of the GOx leaching test. The rising of O_2 content of the glucose sensor spots clearly indicates the leaching of the GOx out of the glucose sensor spots, as decreasing GOx content in the spots leads to decreasing O_2-consumption of the sensors.
One possibility to prevent the leaching of the GOx is to cover the glucose sensor spots with a polyHEMA diffusion barrier. Another way is the use of GOx-CLEA (GOx-Cross Linked Enzyme Aggregates) instead of normal GOx. The advantage of GOx-CLEA is a greatly reduced water solubility.

5.3.3 Sensors coated with a D_7-Diffusion Barrier - 25°C

Glucose sensors covered with a D_7-diffusion barrier were prepared. The diffusion barrier was added to alter the dynamic range of the glucose sensors to higher glucose concentrations (by limiting the glucose diffusion to the sensor) and to possibly prevent the leaching of the GOx.

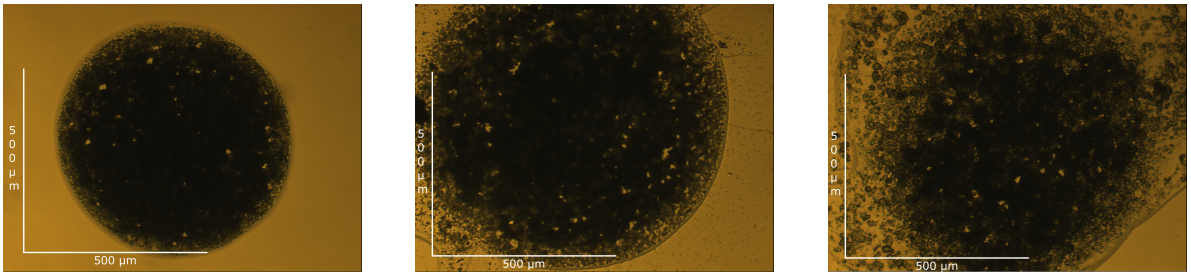

Figure 5.17: Glucose sensor spots in Chip 6, on the left side without a diffusion barrier, in the middle with 1 layer of D_7-diffusion barrier and on the right side with 2 layers of D_7-diffusion barrier

Figure 5.17 shows the glucose sensors of chip 6, one with no D_7 diffusion barrier (picture on the left side) one with one layer (picture in the center) and one with two layers (picture on the right side). The pictures show that the diffusion barrier was merging with the sensor spot. The reason of merging was D_7 as the matrix element of the glucose sensitive layer, which can be dissolved by the D_7 diffusion barrier cocktail. GOx-leaching tests were not performed at 25°C, since the sensor spots without a diffusion barrier already showed any signs of leaching at 25°C (see figure 5.14 on page 41). Based on these results further measurements at 37°C were cancelled.

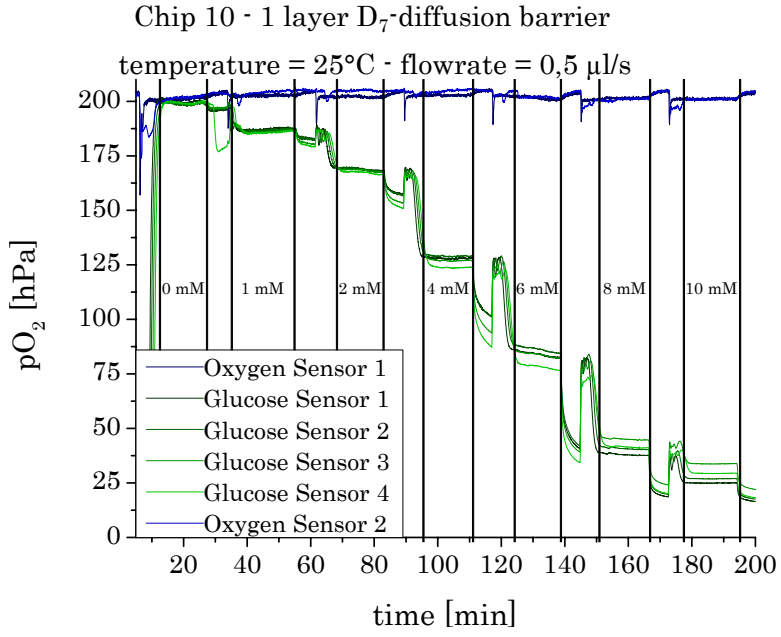

Figure 5.18: Example measurement of the sensor spots coated with 1 layer of D_7 diffusion barrier in chip 10 at a flow rate of 0,5 µl/s and a temperature of 25°C

Figure 5.18 shows an examplary measurement of sensor spots coated with 1 layer of D_7 diffusion barrier. The sensors were located in chip 10 (volume=100 µl) and were exposed to glucose concentrations of 0; 1; 2; 4; 6; 8 and 10 mM at a flow rate of 0,5 µl/s and a

temperature of 25°C.

Diffusion Barrier Thickness

The influence of the diffusion barrier was tested by comparing the measurements of 0, 1 and 2 layers of D_7 diffusion barrier deposited on top of the glucose sensitive layer.

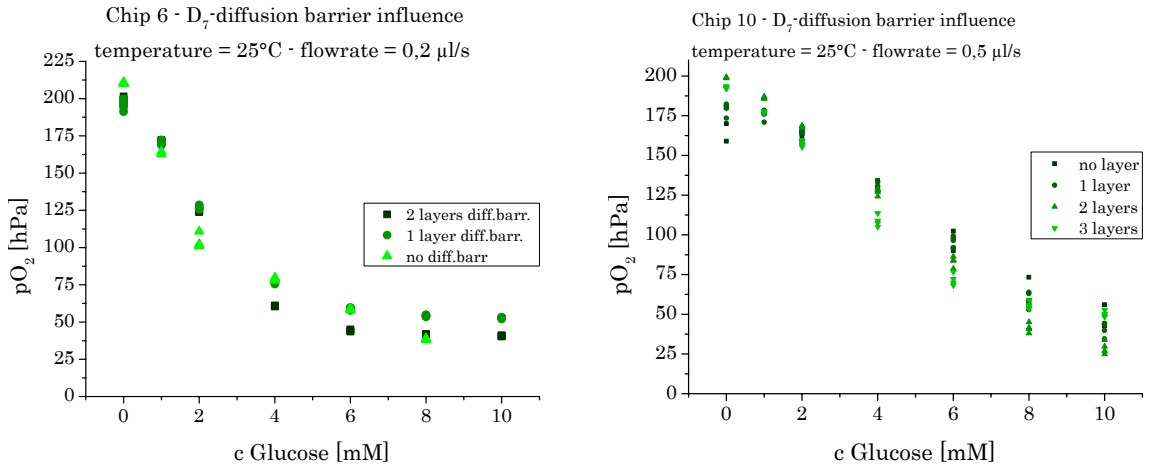

Figure 5.19: Measurements of 0; 1; 2; 4; 6; 8 and 10 mM glucose solution at a temperature of 25°C and flow rates of 0,2 µl/s (chip 6; volume=10 µl) as well as 0,5 µl/s(chip 10; volume = 100 µl) at varying numbers of D_7 diffusion barrier layers

Figure 5.19 shows the results of the glucose sensors exposed to glucose concentrations of 0; 1; 2; 4; 6; 8 and 10 mM, a temperature of 25°C and a flow rate of 0,2 µl/s for chip 6 (10 µl rhombic chip) and 0,5 µl/s for chip 10 (100 µl rhombic chip). The number of layers of D_7 diffusion barrier ranged from 0 to 2 for chip 6, and from 0 to 3 for chip 10.
The measurements did not show any distinct change in oxygen consumption related to the change in numbers of D_7 diffusion barrier layers. This outcome strengthens the results already described in figure 5.17, declaring the D_7 diffusion barrier obsolete for this kind of measurement.

Flow Rate Dependency

The flow rate dependency and the response to glucose were measured at 4 different flow rates: 0,5; 1,0; 1,5 and 2,0 µl/s.

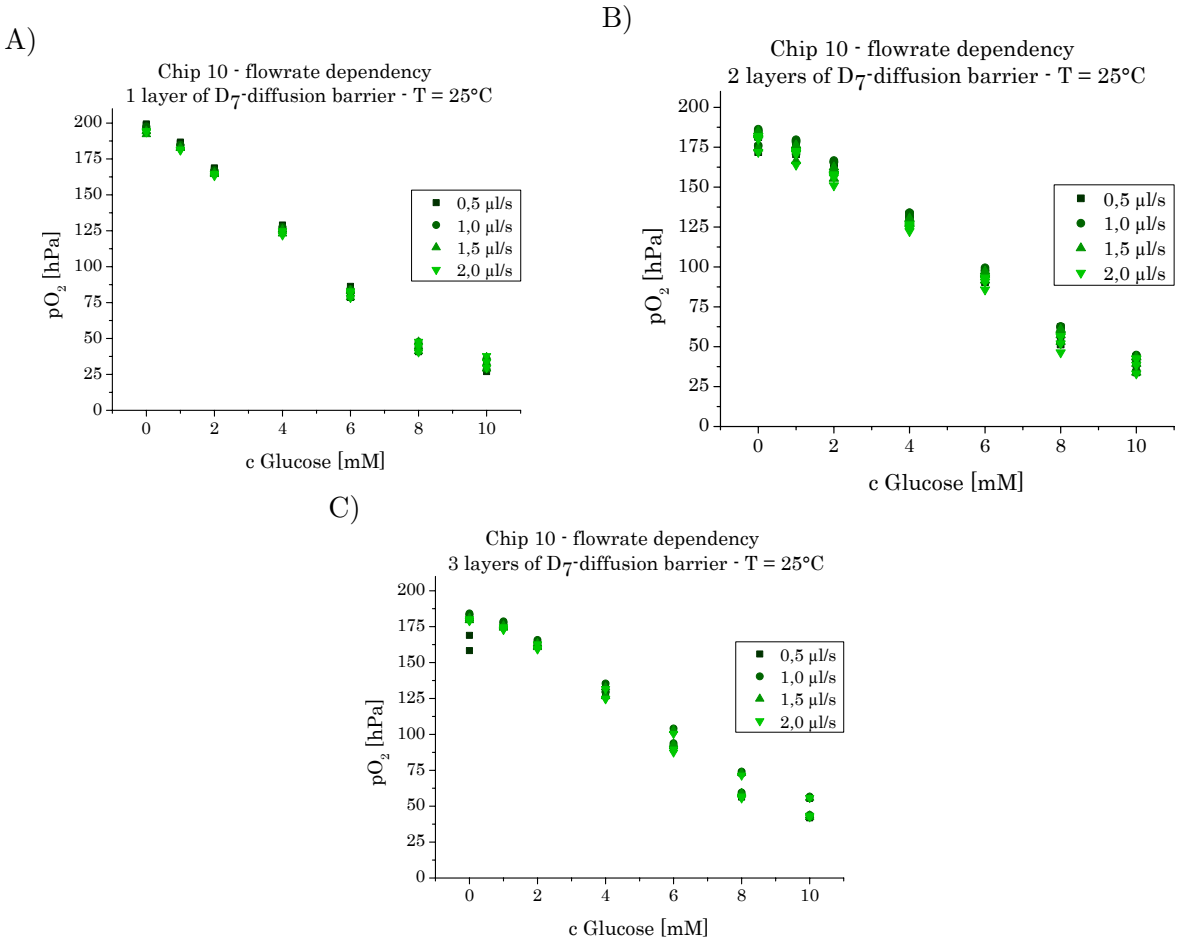

Figure 5.20: Measurements of 0; 1; 2; 4; 6; 8 and 10 mM glucose solutions in chip 10 (volume=100 µl) at flow rates of 0,5; 1,0; 1,5 and 2,0 µl/s and a temperature of 25°C. The glucose sensor spots were coated with A) 1 ; B): 2 and C): 3 layers of D_7 diffusion barrier

Figure 5.20 shows the measurements of 0; 1; 2; 4; 6; 8 and 10 mM glucose solutions at flow rates of 0,5; 1,0; 1,5 and 2,0 µl/s and a temperature of 25°C in Chip 10 (volume=100 µl), the glucose sensor spots were covered with a): 1 layer , b): 2 layers and c): 3 layers of D_7 diffusion barrier, each measurement was performed once with 4 different glucose sensors.
Unlike the flow rate dependency measurements of the sensors without a diffusion barrier(figure 5.13 on page 40) no trends related to the variation in flow rate could be observed.

5.3.4 Sensors coated with a polyHEMA Diffusion Barrier - 25°C

The glucose sensors were coated with a polyHEMA diffusion barrier using the microdispenser, in order to prevent the leaching of GOx. PolyHEMA was dissolved in a mixture of 80 vol% H_2O and 20 vol% EtOH. The high proportion of H_2O was to prevent the

D_7 host polymer of the sensitive layer from dissolving. The number of layers of glucose sensor cocktail and polyHEMA diffusion barrier cocktail were varied to achieve a satisfying signal splitting depending on the glucose concentration and to minimize the leaching of GOx.

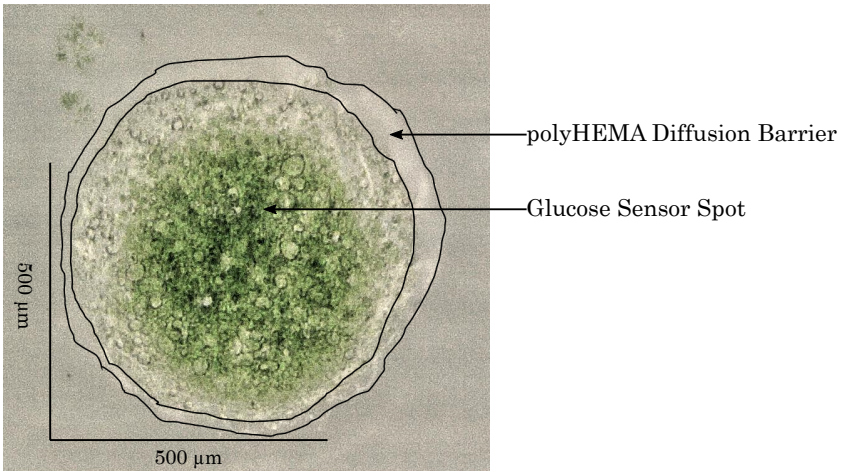

Figure 5.21: Glucose sensor spot covered with a polyHEMA diffusion barrier

Figure 5.21 depicts a sensor spot of chip 21, composed of 8 layers of glucose sensor and covered with 12 layers of polyHEMA. Comparing D_7 diffusion barrier to polyHEMA diffusion barrier (see figure 5.17 on page 44), a difference in merging with the glucose sensor underneath could be observed. D_7 diffusion barrier did show merging, whereas no similar effect could be detected with polyHEMA diffusion barrier. A possible reason for the differing characteristics are the different solvents used for the cocktails. a ratio of 9:1 of EtOH and H_2O in the D_7 diffusion barrier cocktail was used, whilst the ratio of the same components in the polyHEMA cocktail was 2:8. The high water and low EtOH content in the polyHEMA cocktail prevented the glucose sensor from solvation. However, the disadvantage of the high water content is the longer time needed for evaporation of the solvent and the higher pressure needed for the spotting progress leading to capturing air bubbles between the layers and subsequent formation of cavities.

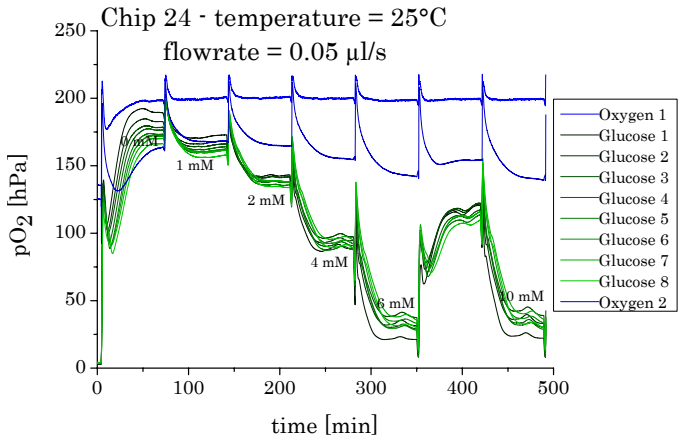

Figure 5.22: Measurement of 0; 1; 2; 4; 6 and 10 mM glucose solution in chip 24 at a flow rates of 0,05 µl/s and at a temperature of 25°C

Figure 5.22 shows course of two example measurements performed in chip 24 (single channel chip) at flow rates of 50 and 100 nl/s. The sensor spots were exposed to glucose concentrations of 0; 1; 2; 4; 6 and 10 mM.

Flow Rate Dependency

The flow rate dependency was investigated at flow rates of 0,05; 0,10; 0,19; 0,28; 0,37 and 0,93 µl/s of chip 24 at a temperature of 25°C.

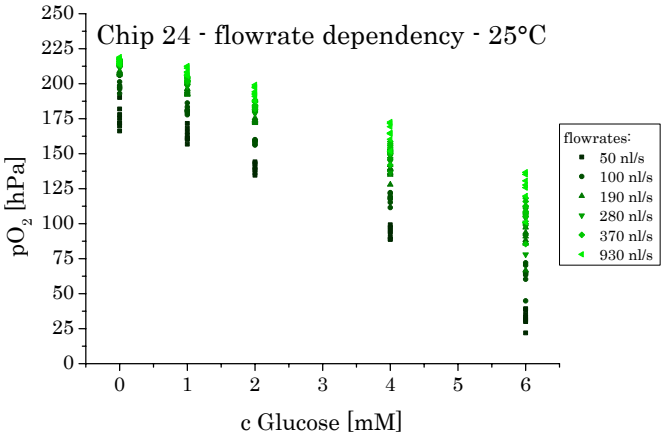

Figure 5.23: Flow rate dependency of glucose sensors in chip 24 (36 µl) exposed to glucose concentrations of 0; 1; 2; 4 and 6 mM glucose concentration and at 25°C

Figure 5.23 shows the flow rate dependency at glucose concentrations of 0; 1; 2; 4 and 6 mM and at flow rates of 0,05; 0,10; 0,19; 0,28; 0,37 and 0,93 µl/s in chip 24 (single

channel chip). Each measurement was performed once with 8 different sensor spots. As already described in figure 5.13 (page 40) a trend towards increased oxygen consumption at lower flow rates could be detected strengthening the results of a correlation between diffusion speed and flow rate.

5.3.5 Sensors coated with a polyHEMA Diffusion Barrier - 37°C

Chips with different numbers of glucose sensor layers and different numbers of polyHEMA diffusion barrier were prepared. The sensors were exposed to different glucose concentrations and different flow rates. Two different kinds of microfluidic chips were used, 100 µl rhombic chips (4,5 mm wide and 750 µm high) and a single channel chip (2,5 mm wide and 250 µm high, 36 µl).
Measurements were performed at 37°C, a heating block was used to keep the microfluidic chips at temperature.

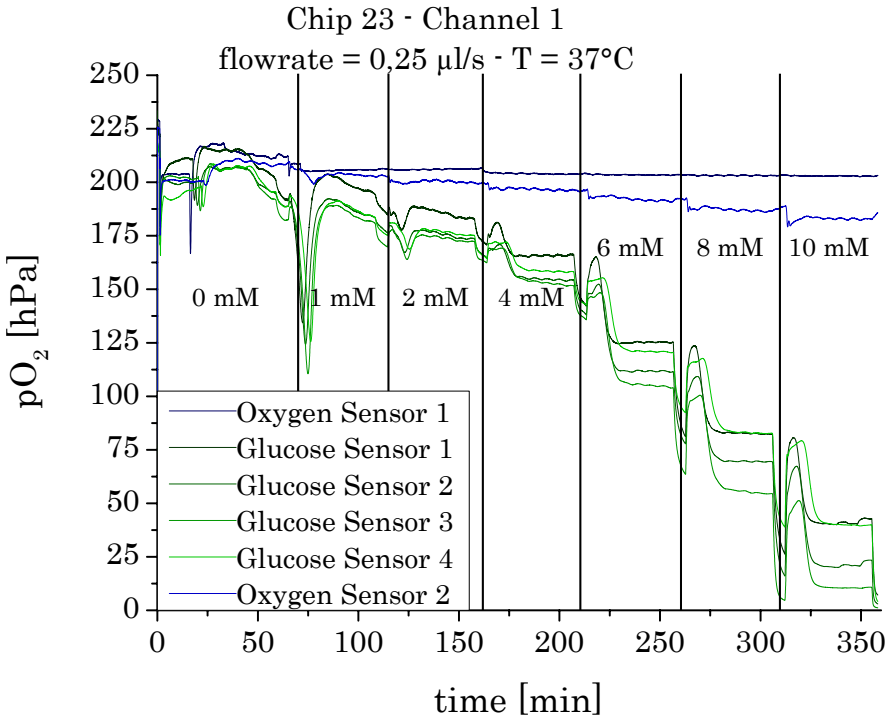

Figure 5.24: Example measurement at 37°C of chip 23 at glucose concentrations of 0; 1; 2; 4; 6; 8 and 10 mM and a flow rate of 0,25 µl/s

Figure 5.24 shows the glucose sensors in chip 23 exposed to glucose concentrations of 0; 1; 2; 4; 6; 8 and 10 mM, at a temperature of 37°C and a flow rate of 0,25 µl/s. Glucose sensor spots consisted of 12 layers of glucose sensor cocktail and 4 layers of polyHEMA cocktail.The high amount of layers did cause difficulties in the proper alignment during the spotting process.

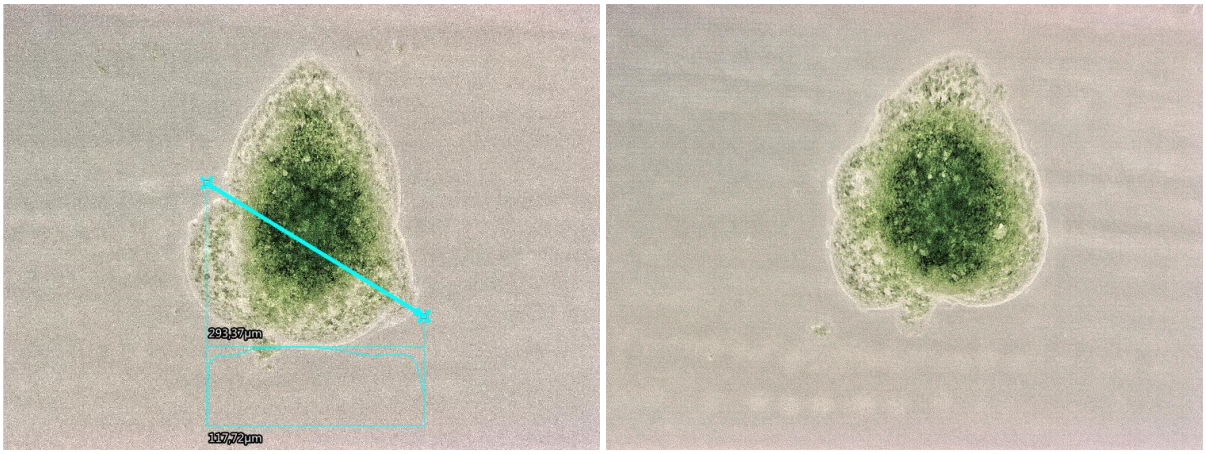

Figure 5.25: Two glucose sensor spots from chip 22, consising of 12 sensor layers and 12 polyHEMA diffusion barrier layers

Figure 5.25 shows 2 glucose sensor spots of chip 22. The sensors consisted of 12 layers of sensor cocktail and 12 layers of polyHEMA diffusion barrier cocktail. An inhomogeneous alignment of different layers could be observed resulting in different heights and surface area for each spot. This change in morphology further led to different outcomes during the glucose measurements.

Influence of Sensor Thickness

Glucose sensors consisting of different numbers of glucose sensor layers were prepared and measured at different glucose concentrations at 37°C. The goal was to detect possible influences of the sensor thickness.

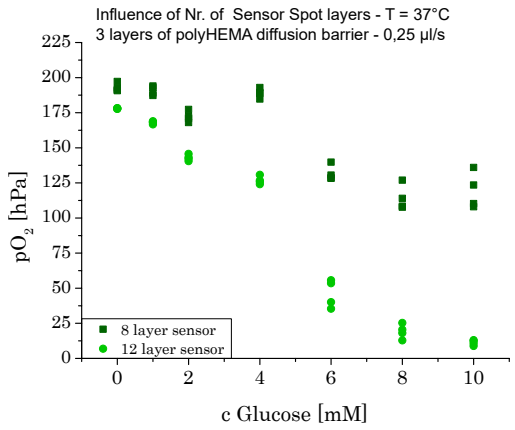

Figure 5.26: Influence of number of glucose sensor layers at glucose concentrations of 0; 1; 2; 4; 6; 8 and 10 mM, temperature of 37°C, flow rate of 0,25 µl/s and 3 layers of polyHEMA diffusion barrier

Figure 5.26 depicts the influence of the number of glucose sensor layers. Glucose concentrations of 0; 1; 2; 4; 6; 8 and 10 mM have been measured at a flow rate of 0,25 µl/s and a temperature of 37°C. The glucose sensors consisted of 8 or 12 layers of glucose cocktail coated with 3 layers of polyHEMA diffusion barrier.
As expected, sensors consisting of 12 layers of glucose sensor did consume more O_2 compared to sensors consisting of 8 layers of glucose sensor. Each measurement was done once with 4 different sensors.

Influence of polyHEMA Diffusion Barrier Thickness

Glucose sensors with different numbers of polyHEMA diffusion barrier layers were prepared and exposed to different glucose concentrations at 37°C to investigate possible influences.

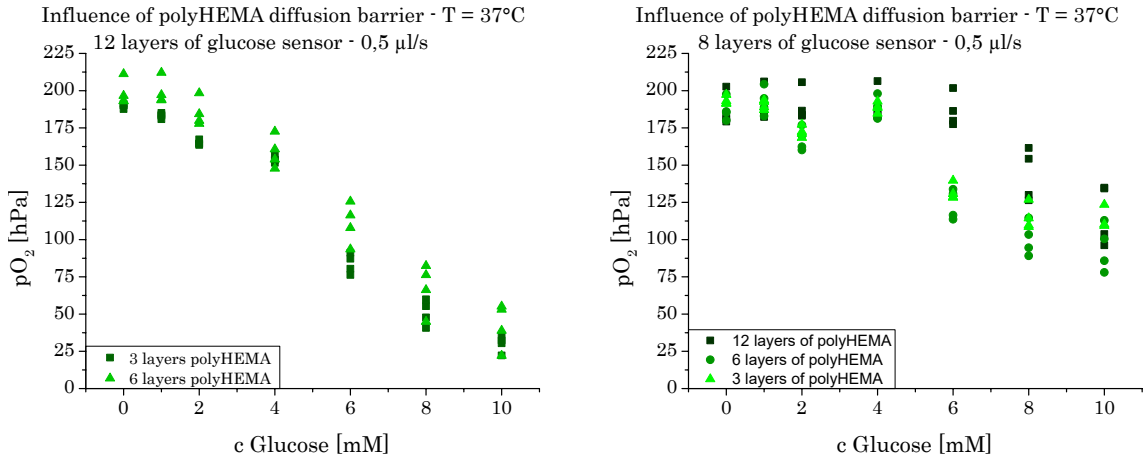

Figure 5.27: Influence of number of polyHEMA diffusion barrier layers at glucose concentrations of 0; 1; 2; 4; 6; 8 and 10 mM, temperature of 37°C, flow rate of 0,25 µl/s and 12 or 8 layers of glucose sensor

Figure 5.27 depicts the influence of the number of polyHEMA diffusion barrier layers. Glucose concentrations of 0; 1; 2; 4; 6; 8 and 10 mM were measured at a flow rate of 0,5 µl/s and a temperature of 37°C. The glucose sensors consisted of 12 layers (left side) or 8 layers (right side) of glucose cocktail and 3 or 6 layers (left side) or 12, 6 or 3 layers (right side) of polyHEMA diffusion barrier.
Again, this 2 graphs depict the importance of the number of glucose sensor layers. The first graph (12 layers of glucose sensor) shows a small trend related to the number of polyHEMA diffusion barrier (the glucose sensors with only 3 layers of polyHEMA diffusion barrier did consume slightly more oxygen). In the second graph (8 layers of polyHEMA) no change in O_2 consumption at 3 and 6 layers of diffusion barrier could be observed. Only 12 layers of diffusion barrier did show a noticeable change.

Flow Rate Dependency

To investigate the flow rate dependency, measurements at flow rates of 0,05; 0,10; 0,19; 0,28; 0,37 and 0,93 µl/s of chip 24 at a temperature of 37°C were plotted.

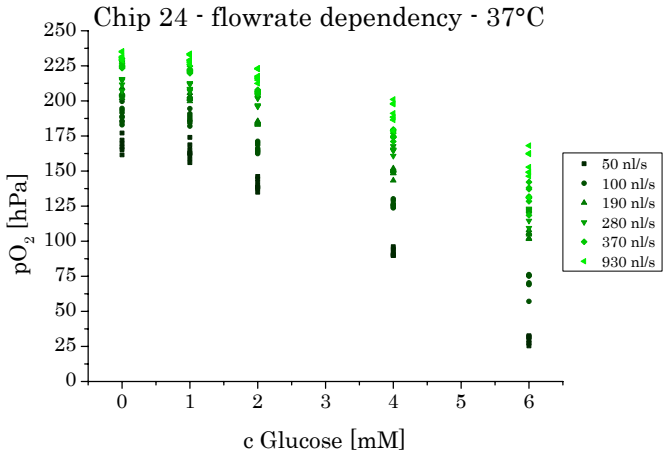

Figure 5.28: Flow rate dependency of the measurements at 0; 1; 2; 4 and 6 mM glucose concentration and at 37°C

Figure 5.28 shows the flow rate dependency of the measurements at glucose concentrations of 0; 1; 2; 4 and 6 mM. Again, an increased O_2-content at increased flow rates could be measured strengthening the results of a correlation between diffusion speed and flow rate.

Leaching of Enzyme

The leaching of the GOx at 37°C was tested at different numbers of polyHEMA diffusion barrier.

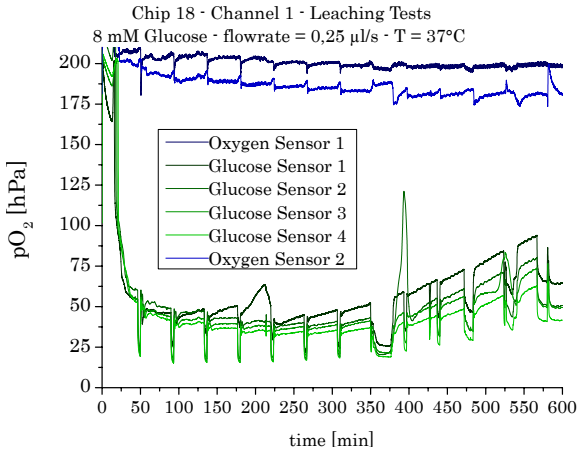

Figure 5.29: GOx-leaching test of glucose sensor spots with 1 layer of polyHEMA diffusion barrier with 8 mM glucose solution at a flow rate of 0,25 µl/s and a temperature of 37°C

Figure 5.29 shows the leaching results of the glucose sensors in chip 18. The glucose sensors were coated with 1 layer of polyHEMA diffusion barrier. These results did show the ineffectiveness of one single layer of polyHEMA diffusion barrier. Therefore further sensors with multiple layers were prepared.

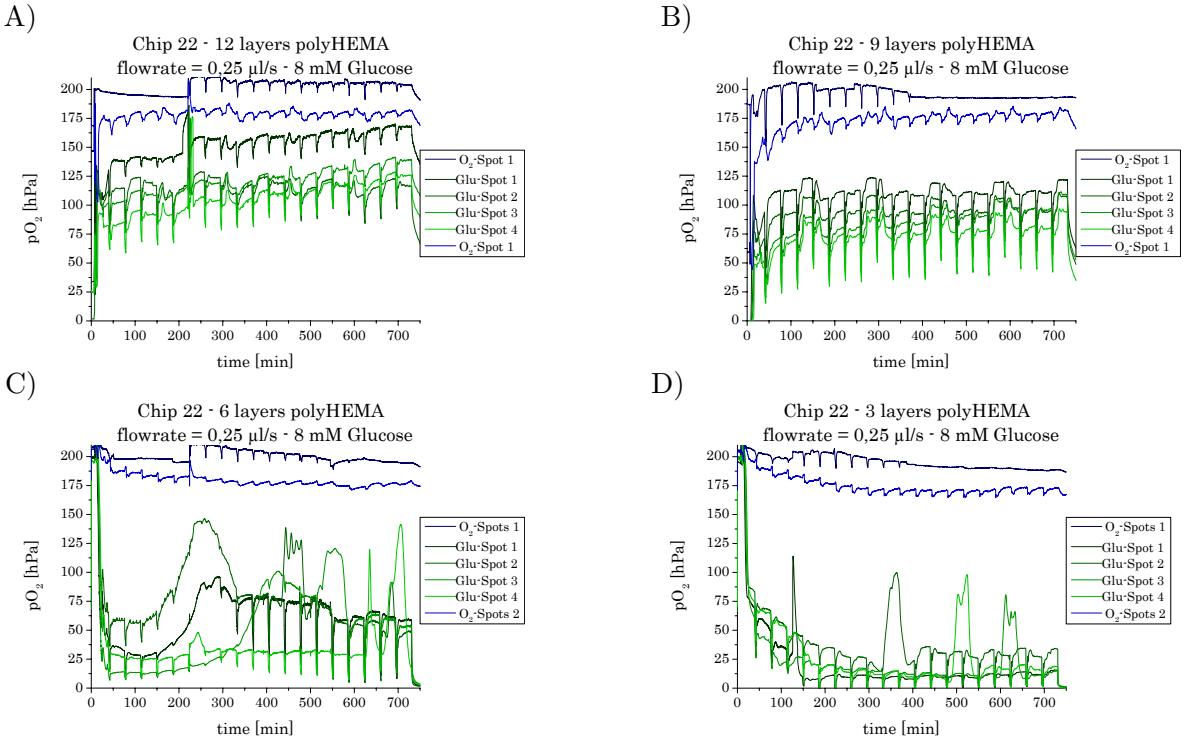

Figure 5.30: Glucose sensor spots in chip 22 exposed to 8 mM glucose solution at a flow rate of 0,25 µl/s and a temperature of 37°C. The glucose sensor spots were coated with A): 12; B): 9; C): 6 or D): 3 layers of polyHEMA diffusion barrier

Figure 5.3.5 shows the results of the leaching tests in chip 22. The sensors were exposed to a glucose concentration of 8 mM, at a temperature of 37°C and with a flow rate of 0,25 µl/s and were coated with 3; 6; 9 or 12 layers of polyHEMA diffusion barrier. The unstable signal can be explained by difficulties during the spotting process, which led to the formation of small cavities. These cavities result in a inhomogeneous thickness of the diffusion barrier leading to a vulnerability of the diffusion barrier of getting filled with air by passing air-bubbles. Despite these vulnerability GOx-leaching was not be observed.

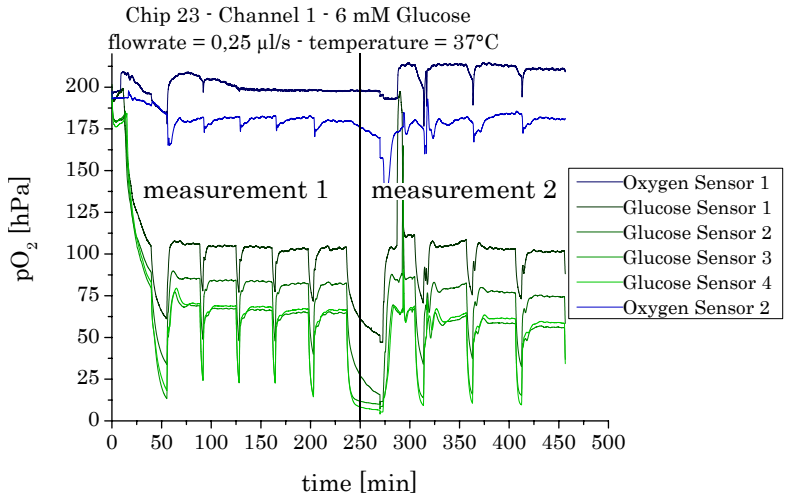

Figure 5.31: Leaching test with 6 mM glucose solution at a flow rate of 0,25 µl/s and at a temperature of 37°C. Measurement 2 was performed the one day after measurement 1 and the sensor spots were soaked in the glucose solution in the meantime

Figure 5.31 shows the leaching tests of the sensor spots in chip 23. The sensors were covered with 4 layers of polyHEMA diffusion barrier. The merged graph shows the first 6 cycles performed on day 1 and 4 subsequent cycles performed 1 day later. The sensor spots were soaked in glucose solution after ending of measurement 1 until the start of measurement 2. Neither a change in O_2 concentration, nor leaching of GOx out of the sensor spots could be observed.
The diverging results of O_2 concentrations obtained from different sensor spots is most likely related to difficulties during the spotting process. Since the spots consisted of several layers of glucose sensor and polyHEMA diffusion barrier, a consistent perfect alignment of all layers could not be assured. Due to this inconsistency in the alignment, different spot heights and surface area for each spot occurred.

Influence of the Channel Dimensions

The measurements of chips 23 and 24 were compared to each other. Both Chips were equipped with glucose sensor spots consisting of 12 layers of sensor cocktail covered with 4 layers of polyHEMA diffusion barrier. The flow rates were adjusted to the most similar flow velocity [mm/min] as possible (the difference at the 2 lowest flow rates was caused by 2 limitations: the lowest flow rate possible with the used syringe pumps was 0,05 µl/s and the option to only set 2 fractional digits.) The channels in chip 23 were 750 µm high (600 µm of the chip + 150 µm from the double sided adhesive tape) and 4,5 mm wide. The channel in chip 24 was 250 µm high (100 µm from the chip and 150 µm from the double-sided adhesive tape) and 2,5 µm wide.

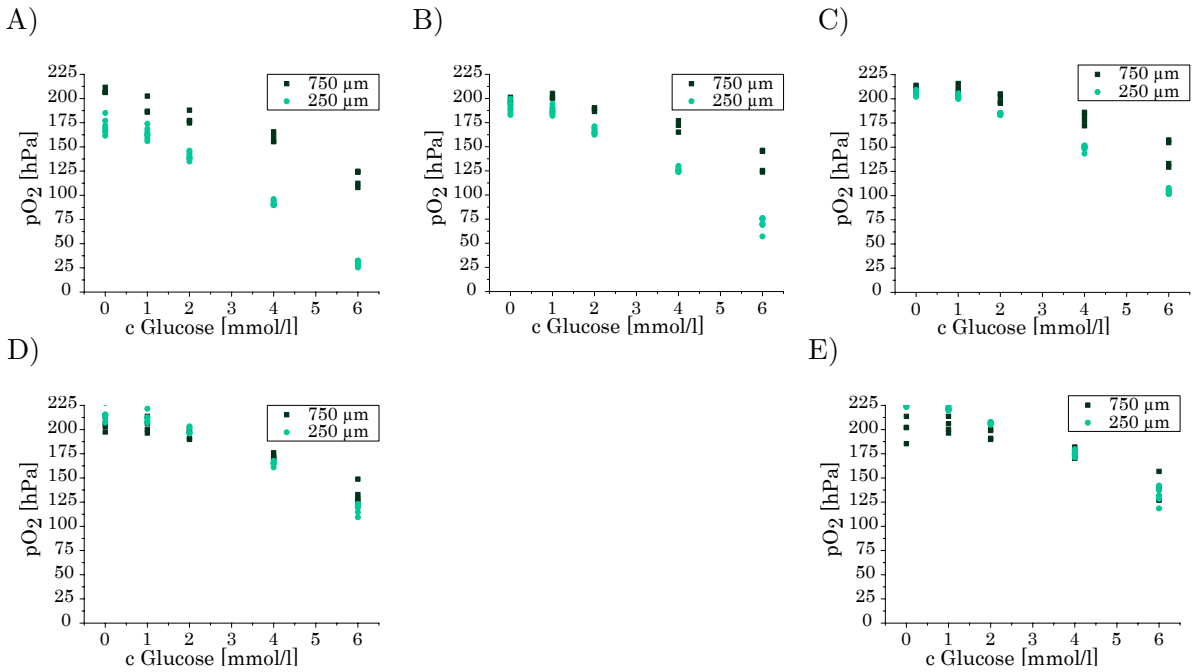

Figure 5.32: Influence of the channel depth at flow velocities of A) 4,44/4,8; B) 8,89/9,6; C) 17,78/18,24; D) 26,67/26,89 and E) 35,52/35,56 mm/min, glucose concentrations of 0-6 mM and 37°C. Chip 23 had a depth of 750 µm and width of 2,5 mm and 4 glucose sensor spots; chip 24 had a depth of 250 µm and width of 4,5 mm and 8 glucose sensor spots.

Figure 5.32 shows the graphical comparison of the glucose sensor spots in channel 1 of chip 23 and the glucose sensor spots in channel 24 at different flow velocities. An obviously large difference between the 2 chips at flow velocities of around 4.44 mm/min and 9,6 mm/min could be observed, however, this gap was reduced by increasing the flow velocity. At a flow velocity of 35,52 mm/min no difference between the 2 different chips could be detected.

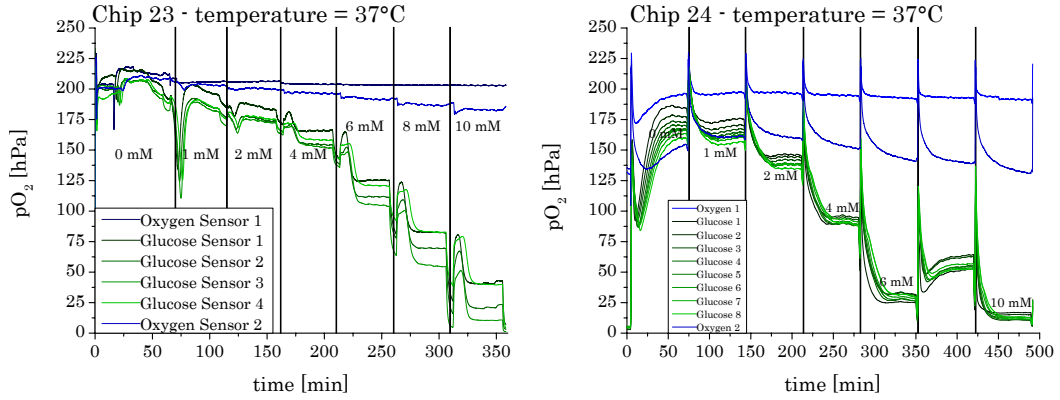

Figure 5.33: Example measurement of 0 - 10 mM glucose solution at a temperature of 37°C in the chips 23 and 24. The flow rates were 4,44 mm/min (chip 23) and 4,8 mm/min (chip 24). Chip 23 had a channel depth of 750 µm and chip 24 had a channel depth of 250 µm

Figure 5.33 displays the glucose sensors of the chips 23 (single channel chip) and 24 (100 µl chip) exposed to glucose concentrations from 0 to 10 mM at a flow velocity of 4,44 mm/min (chip 23) or 4,8 mm/min (chip 24). A big difference in oxygen consumption could be observed between chip 23 compared to chip 24, indicating the influence of the different structure of these chips (see experimental setup Chip 23 on page 30 and Chip 24 on page 30). Since chip 24 did have a different dimension of the channels and a higher number of glucose spots compared to chip 23, a big difference in oxygen concentration could be detected between the oxygen sensors located in front of the glucose sensors compared to that located at the end.

5.3.6 Sensors prepared with GOx-CLEA

Previously, GOx was dissolved in H_2O and precipitated to small aggregates using EtOH. The aggregates were added afterwards to the sensor cocktail. For the GOx-CLEA sensor cocktail (CLEA = cross linked enzyme aggregates) the GOx-CLEA was added to the sensor cocktail and dispersed using a supersonic sonifier.
Two chips (27 and 28) with glucose sensors consisting of GOx-CLEA were prepared. Chip 27 didn't have a diffusion barrier and consisted of 12, 9, 6 or 3 layers of glucose sensor. Chip 28 had 2/1/2/1 layers of polyHEMA diffusion barrier on top of 12/12/9/9 layers of glucose sensor.

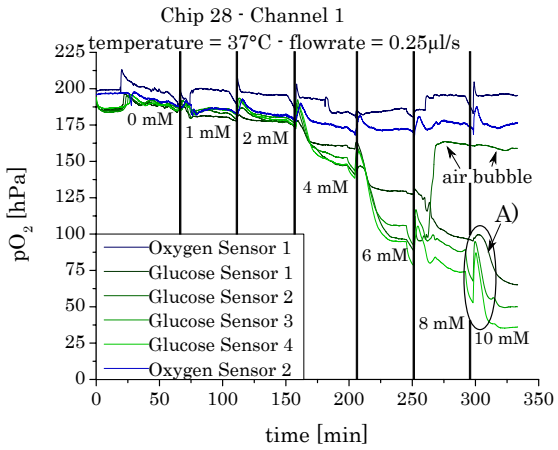

Figure 5.34: Example measurement at 37°C of chip 28 at glucose concentrations of 0; 1; 2; 4; 6; 8 and 10; mM and a flow rate of 0,25 µl/s. A) highlights the rather slow kinetics that can be observed.

Figure 5.34 shows the sensors in channel 1 of chip 28 exposed to glucose concentrations of 0; 1; 2; 4; 6; 8 and 10 mM, a flow rate of 0,25 µl/s and a temperature of 37°C. The glucose sensors consisted of 12 layers of glucose sensor cocktail and 2 layers of polyHEMA diffusion barrier. The capture of an air bubble on top of the sensor was could

be detected during measurement. Due to the partly inconsistent layer alignment, different O_2 contents at equal glucose concentrations were detected by different sensors. The note A) in the graph highlights the comparatively long time needed to achieve a steady state of the sensor. This effect is possibly evoked by the lower activity of GOx-CLEA due to deformation of the reactive site caused by cross-linking.

GOx-CLEA leaching

Sensors without a polyHEMA diffusion barrier were prepared and GOx-leaching tests were done with a 6 mM glucose solution at 37°C.

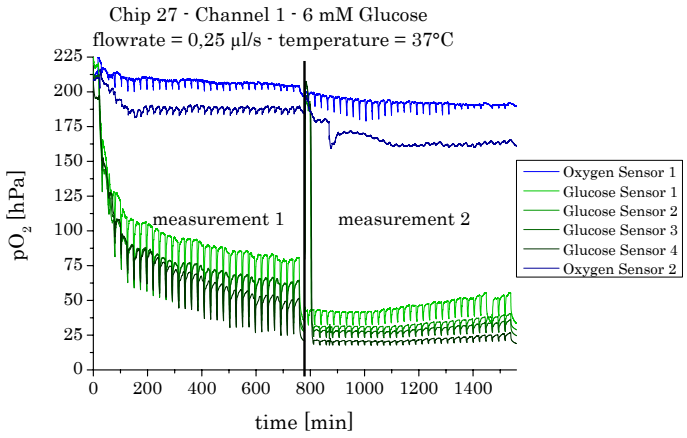

Figure 5.35: Leaching tests of the GOx-CLEA in the glucose sensor spots in channel 1 of chip 27 at a glucose concentration of 6 mM and at a temperature of 37°C. Measurement 2 was performed 1 day after measurement 1, the sensor spots remained soaked in the glucose solution between the measurements

Figure 5.35 shows the leaching tests of the glucose sensors without a diffusion barrier. The graph shows the result of 2 measurements. Measurement 2 was performed the day after measurement 1. During measurement 2, slight leaching of GOx-CLEA could be observed. Therefore, sensors containing a thin layer of polyHEMA diffusion barrier were prepared. Additionally, a relatively long time period for becoming "steady state" of the sensors as well as deviations in O_2-concentrations quantified during measurement 1 and 2 were detected. These findings were probably caused by a suboptimal temperature start of measurement 1 due to equipment fault as well as by the time period needed for swelling of the "dry" spots.

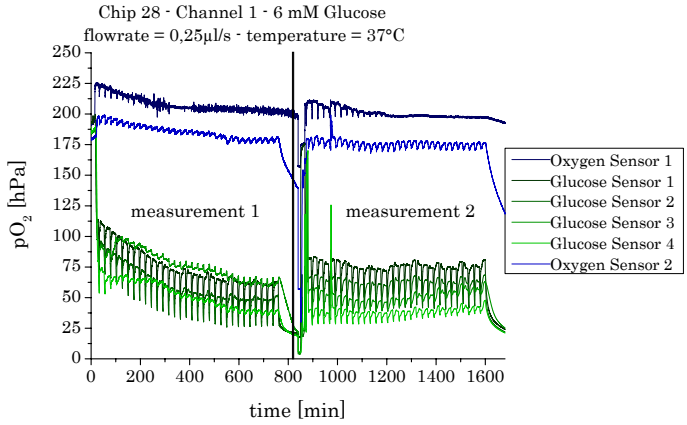

Figure 5.36: Leaching tests of the GOx-CLEA in the glucose sensor spots in channel 1 of chip 28 at a glucose concentration of 6 mM and at a temperature of 37°C. Measurement 2 was performed 1 day after measurement 1. The sensor spots remained soaked in the glucose solution between the measurements.

Figure 5.36 shows the results of the leaching tests of channel 1 (the leaching tests of channel 2 - 4 are shown in the appendix on page 96). The displayed results indicate a comparably long time period (almost the entire time period of measurement 1) to get a stable signal. Additionally, signal scattering of channels 1-3 could be observed. This effect obviously did not lead to a drift to higher oxygen concentrations, indicating the absence of leaching of GOx-CLEA in these channels. However, in channel 4 a drift of oxygen concentrations towards a higher level was detected.

Sensor thickness

Sensors with different numbers of glucose sensor layers were prepared in chip 28. The sensors were exposed to glucose concentrations of 0; 1; 2; 4; 6; 8 and 10 mM, a temperature of 37°C and flow rates of 0,25; 0,50; 1,00; 1,50; 2,00 and 5,00 µl/s.

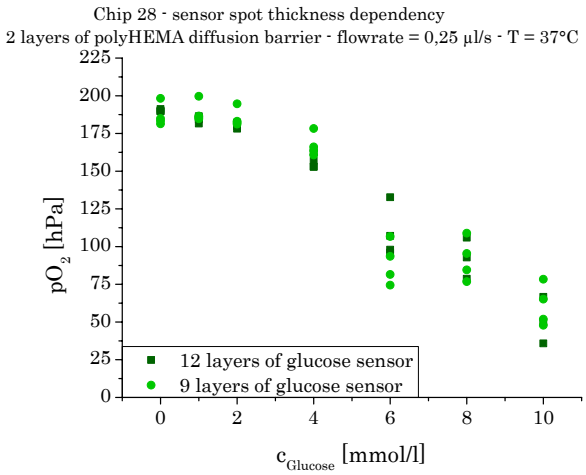

Figure 5.37: Comparison of the influence of the thickness of the glucose sensor spots, 4 glucose sensor spots were covered with 2 layers of polyHEMA diffusion barrier

Figure 5.37 shows the measurements at glucose concentrations of 0; 1; 2; 4; 6; 8 and 10 mM, at a flow rate of 0,25 µl/s and at a temperature of 37°C . The sensors consisted of 12 or 9 layers of glucose sensor, coated with 2 layers of polyHEMA. No effects related to the number of glucose sensor could be observed.

polyHEMA-Diffusion Barrier thickness

Sensors with different numbers of glucose sensor layers were prepared in chip 28. The sensors were measured at glucose concentrations of 0; 1; 2; 4; 6; 8 and 10 mM, at a temperature of 37°C and various flow rates.

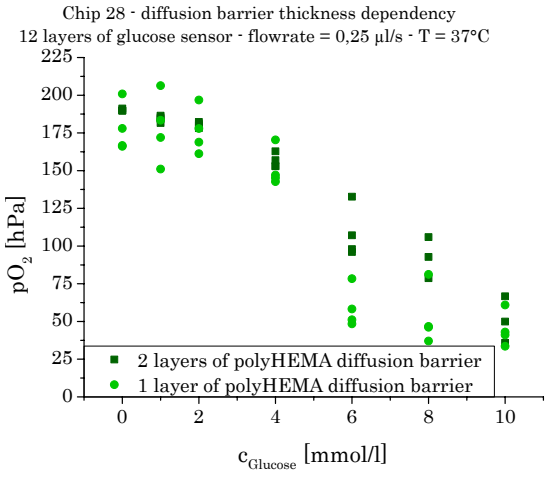

Figure 5.38: Comparison of the influence of the thickness of the polyHEMA diffusion barrier. Each 4 glucose sensor spots were 12 layers thick and coated with 1 or 2 layers of polyHEMA diffusion barrier. The sensors were exposed to glucose concentrations of 0-10 mM, a flow rate of 0,25 µl/s and 37°C

Figure 5.38 shows the measurements at glucose concentrations of 0; 1; 2; 4; 6; 8 and 10 mM, a flow rate of 0,25 µl/s and 37°C. The sensors consisted of 12 layers of glucose sensor and 1 or 2 layers of polyHEMA. A higher concentration of O_2 could be observed in sensor spots covered with 2 layers polyHEMA diffusion barrier compared to sensors covered with 1 layer. The number of layers of diffusion barrier did regulate the diffusion of glucose resulting in a reduced glucose concentration within the sensitive layer of the spot.

Flow Rate Dependency

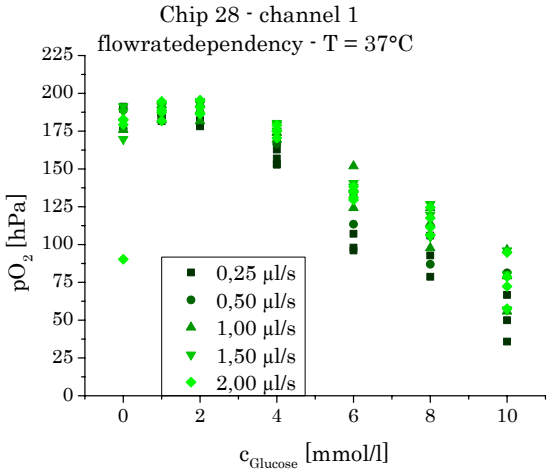

Figure 5.39: Flow rate dependency of 0; 1; 2; 4; 6; 8 and 10 mM glucose solution at flow rates of 0,25; 0,50; 1,00; 1,50 and 2,00 µl/s and at a temperature of 37°C

Figure 5.39 illustrates the flow rate dependency of the measurements at glucose concentrations of 0; 1; 2; 4; 6; 8 and 10 mM and 37°C. The sensors consisted of 12 layers of glucose sensor coated with 2 layers of polyHEMA diffusion barrier. A slight increase of oxygen concentration could be observed caused by accelerated diffusion rates at higher flow rates.

6 Conclusion and Outlook

At study start, knife-coated sensors were used. Satisfying performance of the sensors could be obtained at 25°C, however, exact positioning of the sensors was hardly to achieve. Additionally, due to an increasing demand on decreased sensor size, the printing technique was switched from knife-coating to microdispensing, allowing the fabrication of smaller and, due to being attached to a CNC-machine, more precise sensor spots.
The initially microdispened sensors were coated with a D_7 diffusion barrier. Satisfying results could be obtained at 25°C. However, at 37°C incoherent data resulting from increased water-uptake leading to leaching of GOx out of the glucose sensor spots were measured. These results demonstrated the importance of the sensor spot thickness. Therefore, the material of the diffusion barrier was changed from D_7 to polyHEMA.
After checking out various thicknesses of the sensor layer and diffusion barrier, stable glucose sensors could be generated. Thereafter, sensor spots did show any signs of GOx leaching and displayed a dynamic range within the desired glucose concentration range of 0 - 10 mM. Measurements were performed in 2 different types of microfluidic chips, a 100 µl rhombic chamber chip (width=4,5 mm; height=750 µm) and a single channel chip (width=2,5 mm; height=250 µm), as well as at different flow velocities (with adjusted flow rates to ensure a most possible equality of flow velocities). Diverging results of the two different chip types used were detected at lower flow velocities. Lower concentrations of oxygen were detected by sensors in the single channel chip due to smaller total amount of oxygen available. At higher flow velocities, the measured oxygen concentration within the different chip types converged.
To fix the issue of leaching, GOx-CLEA's was used instead of GOx. Despite of the need of a small polyHEMA diffusion barrier to fight the leaching and a slower response time, more suitable results especially regarding long term analysis could be obtained.

A short list containing the most important parameters to be considered by designing a corresponding sensor spot can be found below:

Spot thickness
: Increasing the amount of layers (and thus increasing in the thickness of the spot) led to a shift of sensitivity towards lower glucose concentrations.

Diffusion Barrier
: To prevent leaching of GOx out of the sensor spot a diffusion barrier was essential. Additionally the increasing thickness of this diffusion barrier shifted the range of optimal sensitivity of the sensor to higher glucose concentrations.

Flow Rate/Flow Velocity
: By increasing the flow rate/flow velocity the overall sensitivity of the sensor gets reduced.

Channel height
: The effect of the channel height was linked to the flow velocity. At a high flow velocity, no impact could be observed, however, at lower flow rates, sensors in smaller channels appeared to be more sensitive.

GOx / GOx-CLEA
: Leaching effects were minimized by using GOx-CLEA, however, due to crosslinking of GOx sensors do have a reduced enzyme activity.

By adjusting the above mentioned parameters, sensors being sensitive within the desired glucose range (for this study glucose concentrations from 1-10 mM) can be generated. A promising setup for further studies can be obtained by using GOx-CLEA due to decreased vulnerability towards leaching and can be therefore used for long-term experiments, particularly for the application in microfluidic cell cultivation systems.
Topics for prospective investigations could be the interaction of glucose sensors with an oxygen-permeable substrate. Due to the fact that GOx and O_2-particles are part of the same cocktail better results could possible achieved when compared to a 3 layer setup (oxygen sensor layer, separate GOx layer and diffusion layer on top). The benefit of an oxygen-permeable environment would be that the solution would be that the solution in the microfluidic device could easily be kept at air-saturated oxygen levels.
By exchanging the enzyme, the general design of these sensors could also probably be used for the measurement of other biological relevant substances (like lactate). However, since different enzymes do have different properties such as size, solubility, etc., which are relevant for the immobilization/entrapment of the enzyme in the sensor, adequate knowledge of the enzyme in use is essential.

7 References

1. Steiner, M.-S., Duerkop, A. & Wolfbeis, O. S. Optical methods for sensing glucose. en. *Chem Soc Rev* **40,** 4805 (2011).
2. Borisov, S. M. & Wolfbeis, O. S. Optical Biosensors. *Chem. Rev.* **108,** 423–461 (2008).
3. Fischer, E. Einfluss der Configuration auf die Wirkung der Enzyme. *Eur. J. Inorg. Chem.* **27,** 2985–2993 (Oct. 1894).
4. Pohanka, M. & Skládal, P. Electrochemical biosensors – principles and applications. *Journal of APPLIED BIOMEDICINE* **6,** 57–64 (Mar. 2008).
5. Chen, C., Xie, Q., Yang, D., Xiao, H., Fu, Y., Tan, Y. & Yao, S. Recent advances in electrochemical glucose biosensors. *RSC Advances* **3,** 4473–4491 (2013).
6. Jena, B. K. & Raj, C. R. Enzyme-Free Amperometric Sensing of Glucose by Using GoldNanoparticles. *Chem.-Eur. J.* **12,** 2702–2708 (Mar. 2006).
7. Emr, S. A. & Yacynych, A. M. Use of Polymer Films in Amperometric Biosensors. *Electroanalysis* **7,** 913–923 (Oct. 1995).
8. Sekretaryova, A. N., Vokhmyanina, D. V., Chulanova, T. O., Karyakina, E. E. & Karyakin, A. A. Reagentless Biosensor Based on Glucose Oxidase Wired by the Mediator Freely Diffusing in Enzyme Containing Membrane. *Anal. Chem.* **84,** 1220–1223 (2012).
9. Rajagopalan, R., Aoki, A. & Heller, A. Effect of Quaternization of the Glucose Oxidase "Wiring" Redox Polymer on the Maximum Current Densities of Glucose Electrodes. *J. Phys. Chem.* **100,** 3719–3727 (Feb. 1996).
10. Völkl, K.-P., Opitz, N. & Lübbers, D. W. in *Temperature Dependence of Enzyme Optodes as Exemplified by the Glucose Optode* 199–204 (Springer, Boston, MA, 1988).
11. Zach, P. W., Hofmann, O. T., Klimant, I. & Borisov, S. M. NIR Phosphorescent Intramolecularly Bridged Benzoporphyrins and Their Application in Oxygen-Compensated Glucose Optode. *Anal. Chem.* **90,** 2741–2748 (2018).
12. Moreno-Bondi, M. C., Wolfbeis, O. S., Leiner, M. J. P. & Schaffer, B. P. H. Oxygen Optrode for Use in a Fiber-Optic Glucose Biosensor. *Anal. Chem.* **62,** 2377–2380 (1990).
13. Rossi, L. M., Quach, A. D. & Rosenzweig, Z. Glucose oxidase–magnetite nanoparticle bioconjugate for glucose sensing. *Analytical and Bioanalytical Chemistry* **380,** 606–613 (Oct. 2004).

14. Whitesides, G. M. The origins and the future of microfluidics. *Nature* **442,** 368–373 (July 2006).

15. Chiu, D. T., deMello, A. J., Di Carlo, D., Doyle, P. S., Hansen, C., Maceicyk, R. M. & Wootton, R. C. R. Small but Perfectly Formed? Successes, Challenges, and Opportunities for Microfliudics in the Chemical and Biological Sciences. *Chem* **2,** 201–223 (Feb. 2017).

16. Wohlgemuth, R., Plazl, I., Žnidaršič-Plazl, P., Gernaey, K. V. & Woodley, J. M. Microscale technology and biocatalytic processes: opportunities and challenges for synthesis. *Trends Biotechnol.* **33,** 302–314 (May 2015).

17. Protasova, L. N., Bulut, M., Ornerod, D., Buekenhoudt, A., Berton, J. & Stevens, C. V. Latest Highlights in Liquid-Phase Reactions for Organic Synthesis in Microreactors. *Organic Process Research & Development* **17,** 760–791 (2013).

18. Kundu, S., Bhangale, A. S., Wallace, W. E., Flynn, K. M., Guttman, C. M., Gross, R. A. & Beers, K. L. Continuous Flow Enzyme-Catalyzed Polymerization in a Microreactor. *J. Am. Chem. Soc.* **133,** 6006–6011 (2011).

19. Yoshida, J.-I. Flash chemistry: flow microreactor synthesis based on high-resolution reaction time control. *The Chemical Record* **10,** 332–341 (Oct. 2010).

20. Bolivar, J. M., Wiesbauer, J. & Nidetzky, B. Biotransformations in microstructured reactors: more than flowing with the stream? *Trends Biotechnol.* **29,** 333–342 (July 2011).

21. Marques, M. P. C. & Fernandes, P. Microfluidic Devices: Useful Tools for Bioprocess Intensification. *Molecules* **16,** 8368–8401 (2011).

22. Matosevic, S., Szita, N. & Baganz, F. Fundamentals and applications of immobilizedmicrofluidic enzymatic reactors. *J. Chem. Technol. Biotechnol.* **86,** 325–334 (Mar. 2011).

23. Bolivar, J. M. & Nidetzky, B. Multiphase biotransformations in microstructured reactors: Opportunities for biocatalytic process intensification and smart flow processing. *Green Proc. Synth* **2,** 541–559 (Dec. 2013).

24. Tan, X. & Li, K. Membrane microreactors for catalytic reactions. *J. Chem. Technol. Biotechnol.* **88,** 1771–1779 (Oct. 2013).

25. Krull, R., Lladó-Maldonado, S., Lorenz, T., Demming, S. & Büttgenbach, S. en. in *Microsystems for Pharmatechnology: Manipulation of Fluids, Particles, Droplets, and Cells* 99–152 (Springer Berlin Heidelberg, New York, NY, 2016).

26. Edlich, A. *et al.* Microfluidic reactor for continuous cultivation of Saccharomyces cerevisiae. en. *Biotechnol. Prog.* **26,** 1259–1270 (Sept. 2010).

27. Ziółkowska, K., Kwapiszewski, R. & Brzózka, Z. Microfluidic devices as tools for mimicking the in vivo environment. en. *New J. Chem.* **35,** 979 (2011).

28. Krebs, F. C. Fabrication and processing of polymer solar cells: A review of printing and coating techniques. *Solar Energy Materials & Solar Cells* **93,** 394–412 (Apr. 2009).

29. Chang, Y.-H., Tseng, S.-R., Chen, C.-Y., Meng, H.-F., Chen, E.-C., Horng, S.-F. & Hsu, C.-S. Polymer solar cell by blade coating. *Org. Electron.* **10,** 741–746 (Aug. 2009).

30. Tahirbegi, I. B., Ehgartner, J., Sulzer, P., Zieger, S., Kasjanow, A., Paradiso, M., Strobl, M., Bouwes, D. & Mayr, T. Fast pesticide detection inside microfluidic device with integrated optical pH, oxygen sensors and algal fluorescence. *Biosens. Bioelectron.* **88,** 188–195 (Feb. 2017).

8 List of Figures

9 List of Tables

10 Appendix

10.1 List of Abbreviations

Table 10.1: List of Abbreviations

Abbreviation	**Name**
GOx	Glucose oxidase
O_2	Oxygen
H_2O_2	Hydrogen peroxide
PS	Polystyrene
polyHEMA	Polyhydroxyethylmethacrylate
ConA	Concanavalin A
IC	Internal conversion
ISC	Intersystem crossing
QL	Quencher-luminophore complex
EC	Enzyme Comission
ISE	Ion-selective electrodes
ISFET	Ion-sensitive field effect transistor
Pt	Platinum
Au	Gold
Pt-TTTBPtBu	Pt(II) tetraphenyltetra(t-butyl)tetrabenzoporphyrin
PS-DVB	1,2-Dichlorobenzene, poly- (styrene-co-divinylbenzene)-microspheres
Ru	Ruthenium
bpy	2,2'-Bipyridine
THF	Tetrahydrofuran
Na_2HPO_4	Disodiumhydrogenphosphate
NaH_2PO_4	Sodiumdihydrogenphosphate
NaCl	Sodiumchloride
PtTPTBPF	platinum(II)- meso-tetra(4-fluorophenyl)tetrabenzoporphyrin
EtOH	Ethanol
H_2O	Water
GOx-CLEA	Glucose oxidase-crosslinked enzyme aggregate
DCM	Dichlormethane
wt%	Weight percent
CNC	Computerized Numerical Control

10.2 Microdispenser Settings

Chips 3-5

Table 10.2: Microdispenser Settings for Chips 3-5

	Sensor Cocktail	**D_7 Diffusion Barrier**		
parameters	**Chips 3-5**	**Chip 3**	**Chip 4**	**Chip 5**
tapped lift	40	50	60	60
rising time	0,2	0,2	0,2	0,2
open time	0,05	0,1	0,1	0,15
falling time	0,1	0,1	0,1	0,15
delay	0,1	0,1	0,1	0,1
number of pulses	1	1	1	2
pressure [mbar]	200	200	200	200
no. of layers	1	1	1	1

Chips 6-7

Table 10.3: Microdispenser Settings for Chips 6 and 7

	Sensor Cocktail	**D_7 Diffusion Barrier**
parameters	**Chips 6-7**	**Chips 6-7**
tapped lift	55	60
rising time	0,3	0,2
open time	0,1	0,15
falling time	0,15	0,1
delay	0,3	0,1
number of pulses	3	1
pressure [mbar]	200	200
no. of layers	1	2/2/2/1/1/0/0

Chips 8-10

Table 10.4: Microdispenser settings for chips 8 - 10

parameters	Glucose Sensor Cocktail Chips 8-10	O_2 Sensor Cocktail Chips 8-10	D_7 Diffusion Barrier Chips 8-10
tapped lift	28	28	50
rising time	0,2	0,2	0,2
open time	0	0	0,1
falling time	0,1	0,1	0,1
delay	0,3	0,3	0,2
number of pulses	10	10	10
pressure [mbar]	200	200	200
no. of layers	1	10	3/2/1/0

Chips 11-12

Table 10.5: Microdispenser settings for chips 11 and 12

parameters	Glucose Sensor Cocktail Chips 11-12	O_2 Sensor Cocktail Chips 11-12
tapped lift	45	45
rising time	0,2	0,2
open time	0	0
falling time	0,07	0,07
delay	0,1	0,1
number of pulses	1	1
pressure [mbar]	200	200
no. of layers	1	1

Chips 13-14

Table 10.6: Microdispenser settings for chips 13 and 14

parameters	Glucose Sensor Cocktail Chip 13	Glucose Sensor Cocktail Chip 14	O_2 Sensor Cocktail Chips 13-14
tapped lift	45	30	35
rising time	0,2	0,2	0,2
open time	0,1	0,2	0,1
falling time	0,07	0,07	0,07
delay	0,1	0,1	0,1
number of pulses	1	1	1
pressure [mbar]	200	200	200
no. of layers	1	1	1

Chip15

Table 10.7: Microdispenser settings for chip 15

parameters	**Glucose Sensor Cocktail Chip 15**	**O_2 Sensor Cocktail Chip 15**
tapped lift	40	40
rising time	0,2	0,2
open time	0,1	0,1
falling time	0,07	0,07
delay	0,1	0,1
number of pulses	2	2
pressure [mbar]	200	200
no. of layers	4/3/2/1	1

Chips 16-17

Table 10.8: Microdispenser settings for chips 16 and 17

parameters	**Glucose Sensor Cocktail Chips 16-17**	**O_2 Sensor Cocktail Chips 16-17**
tapped lift	45	37
rising time	0,2	0,2
open time	0,1	0,1
falling time	0,07	0,07
delay	0,1	0,1
number of pulses	2	2
pressure [mbar]	200	200
no. of layers	4/3/2/1	1

Chips 18-19

Table 10.9: Microdispenser settings for chips 18 and 19

parameters	Glucose Sensor Cocktail Chip 18	Glucose Sensor Cocktail Chip 19	O_2 Sensor Cocktail Chips 18-19	polyHEMA Cocktail Chips 18-19
tapped lift	37	37	37	55
rising time	0,2	0,2	0,2	0,2
open time	0,1	0,1	0,1	0,2
falling time	0,07	0,07	0,07	0,07
delay	0,1	0,1	0,1	0,1
no. of pulses	2	5	2	5
pressure [mbar]	200	200	200	300
no. of layers	4/3/2/1	4/3/2/1	1	1

Chips 20-22

Table 10.10: Microdispenser settings for chips 20 - 22

parameters	Glucose Sensor Cocktail Chip 20	Glucose Sensor Cocktail Chip 21	Glucose Sensor Cocktail Chip 22	O_2 Sensor Cocktail Chips 20-22	polyHEMA Cocktail Chips 20-22
tapped lift	35	35	35	37	55
rising time	0,2	0,2	0,2	0,2	0,2
open time	0,1	0,1	0,1	0,1	0,2
falling time	0,06	0,06	0,06	0,07	0,07
delay	0,1	0,1	0,1	0,1	0,1
no. of pulses	3	3		3	5
pressure [mbar]	200	200		200	300
no. of layers	4	8	12	2	12/9/6/3

Chip 23

Table 10.11: Microdispenser settings for chip 23

parameters	Glucose Sensor Cocktail Chip 23	O_2 Sensor Cocktail Chip 23	polyHEMA Cocktail Chip 23
tapped lift	35	37	50
rising time	0,2	0,2	0,2
open time	0,1	0,1	0,2
falling time	0,06	0,07	0,07
delay	0,1	0,1	0,1
no. of pulses	5	5	5
pressure [mbar]	200	200	300
no. of layers	12/12/8/8	2	4

Chip 24

Table 10.12: Microdispenser settings for chip 24

parameters	Glucose Sensor Cocktail Chip 24	O_2 Sensor Cocktail Chip 24	polyHEMA Cocktail Chip 24
tapped lift	40	37	50
rising time	0,2	0,2	0,2
open time	0,1	0,1	0,2
falling time	0,06	0,07	0,07
delay	0,1	0,1	0,1
no. of pulses	5	5	3
pressure [mbar]	200	200	300
no. of layers	12	2	4

Chip 27

Table 10.13: Microdispenser settings for chip 27

parameters	Glucose Sensor Cocktail Chip 27	O_2 Sensor Cocktail Chip 27
tapped lift	40	37
rising time	0,2	0,2
open time	0,1	0,1
falling time	0,07	0,07
delay	0,1	0,1
number of pulses	4	4
pressure [mbar]	200	200
no. of layers	12/9/6/3	3

Chip 28

Table 10.14: Microdispenser settings for chip 28

parameters	**Glucose Sensor Cocktail Chip 28**	**O_2 Sensor Cocktail Chip 28**	**polyHEMA Cocktail Chip 28**
tapped lift	40	37	50
rising time	0,2	0,2	0,2
open time	0,1	0,1	0,2
falling time	0,08	0,08	0,07
delay	0,1	0,1	0,1
no. of pulses	4	4	3
pressure [mbar]	200	200	300
no. of layers	12/12/9/9	3	2/1/2/1

10.3 Experimental Set-Up

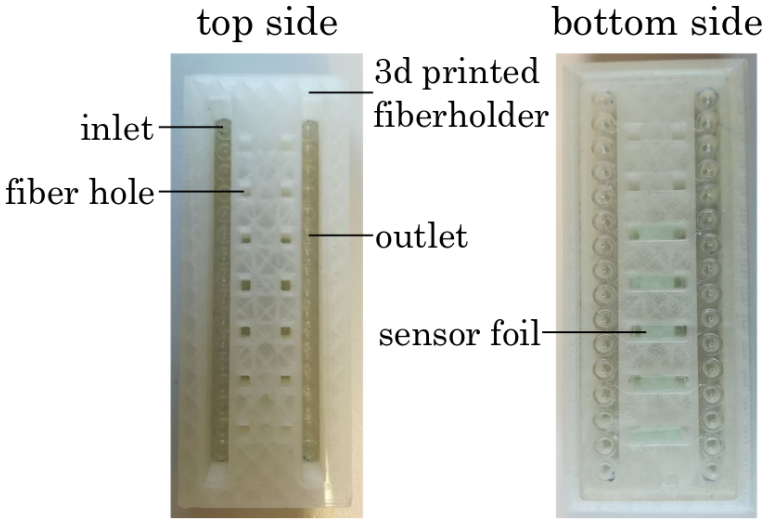

Figure 10.1: Chip 1

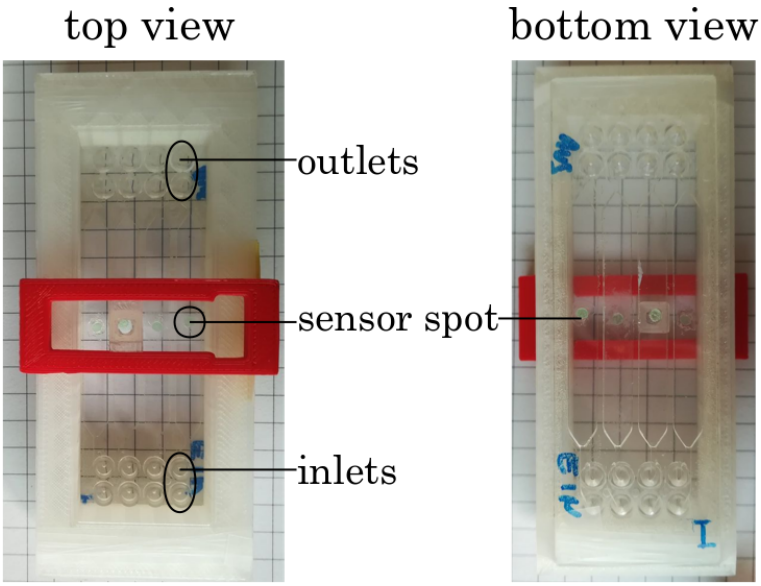

Figure 10.2: Chip 2

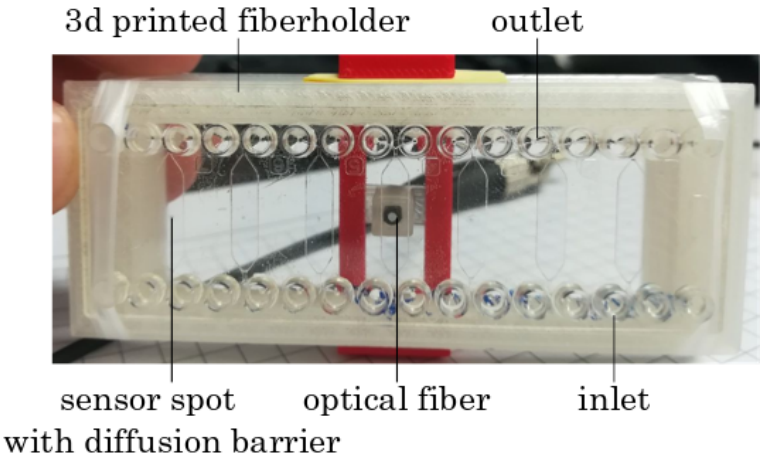

Figure 10.3: Chip 3-5

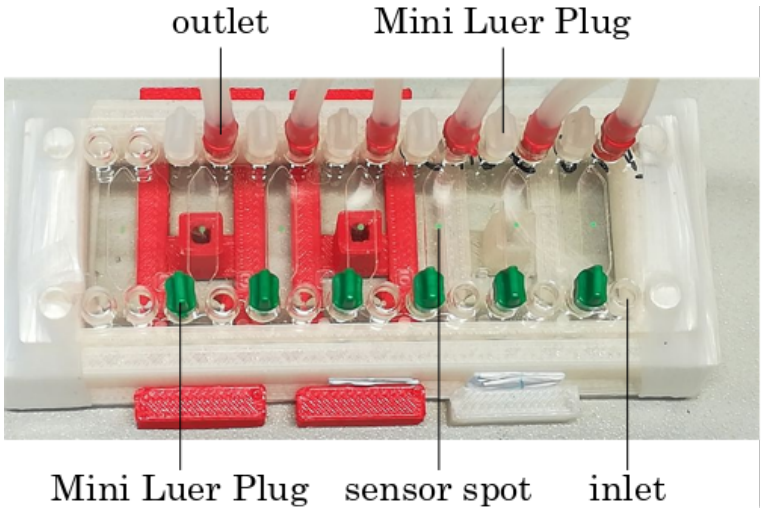

Figure 10.4: Chip 6-7

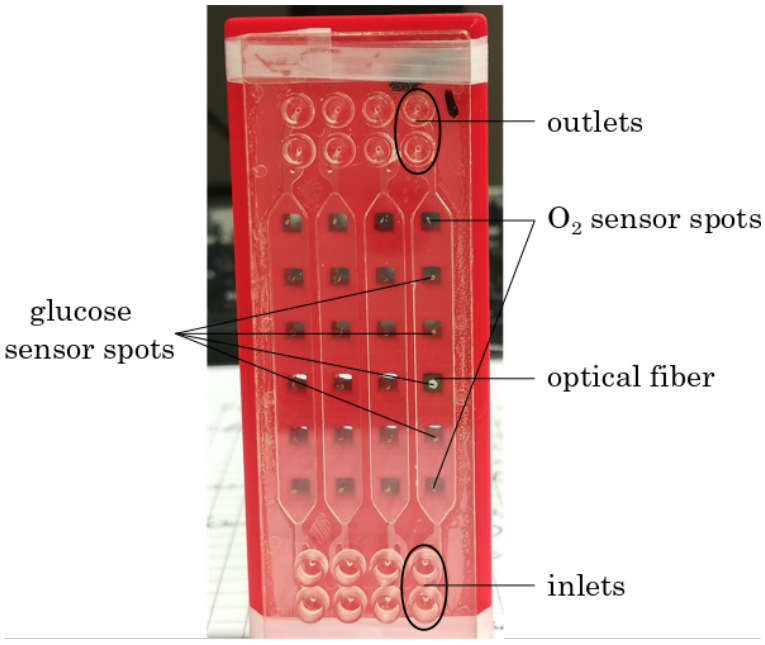

Figure 10.5: Chip 8-10

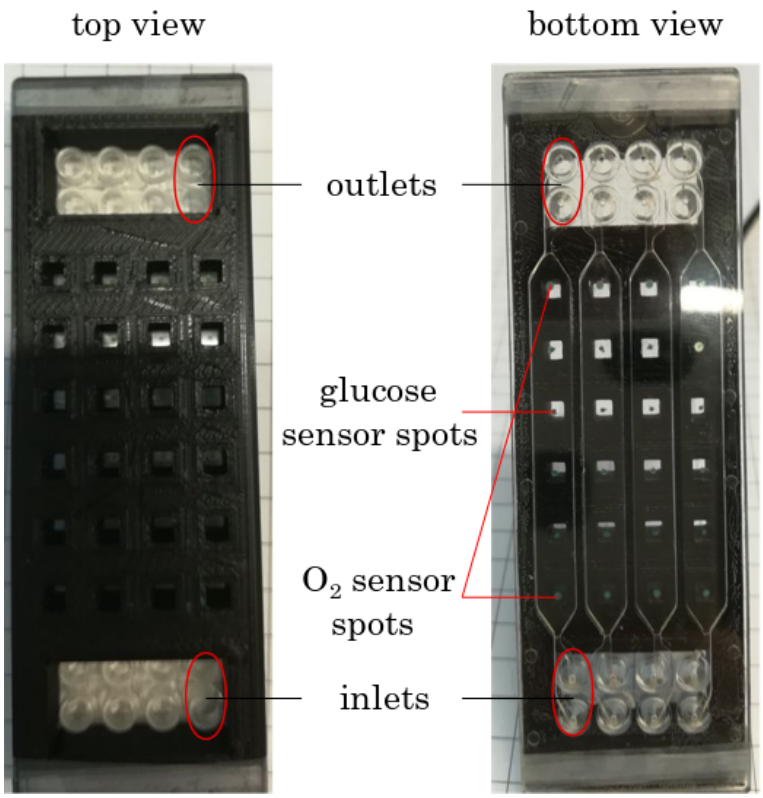

Figure 10.6: Chip 15

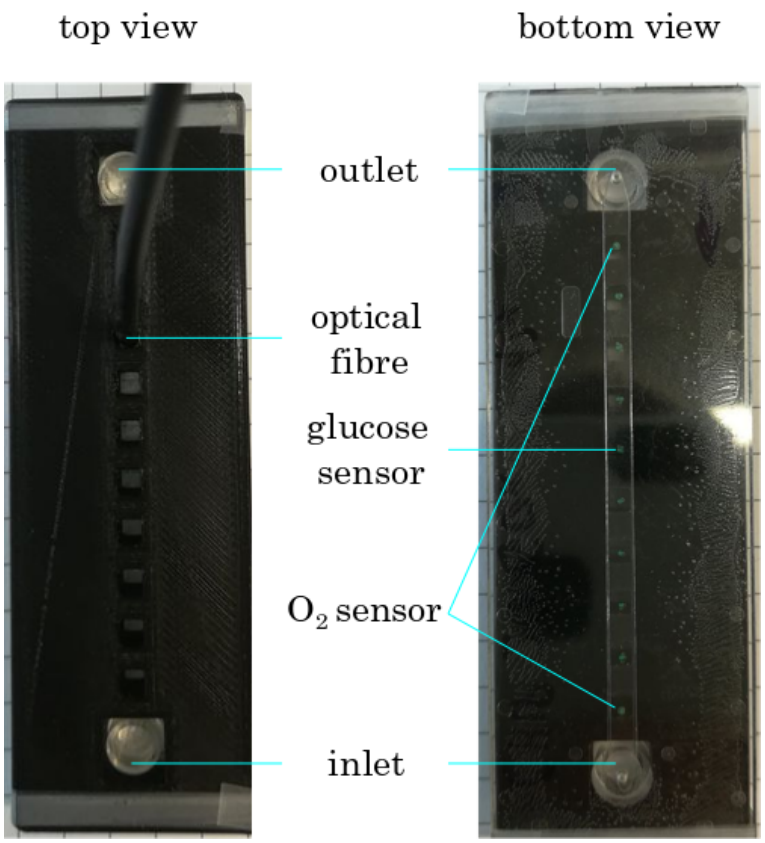

Figure 10.7: Chip 24

10.4 Spot sizes measured with the microscope

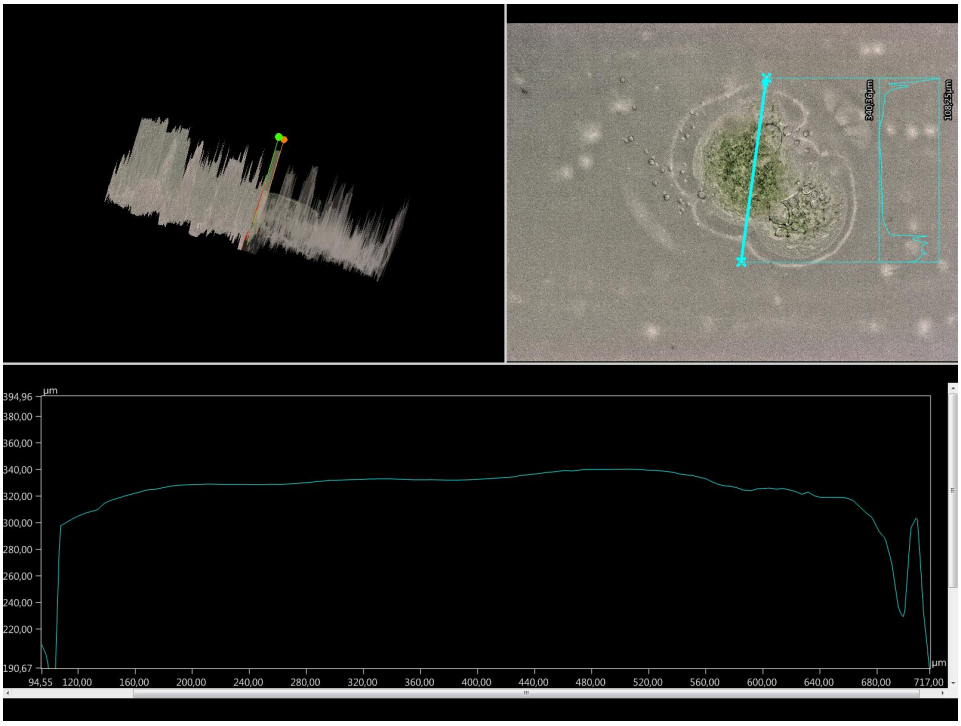

Figure 10.8: Sensor spots in channel 1 of chip 20

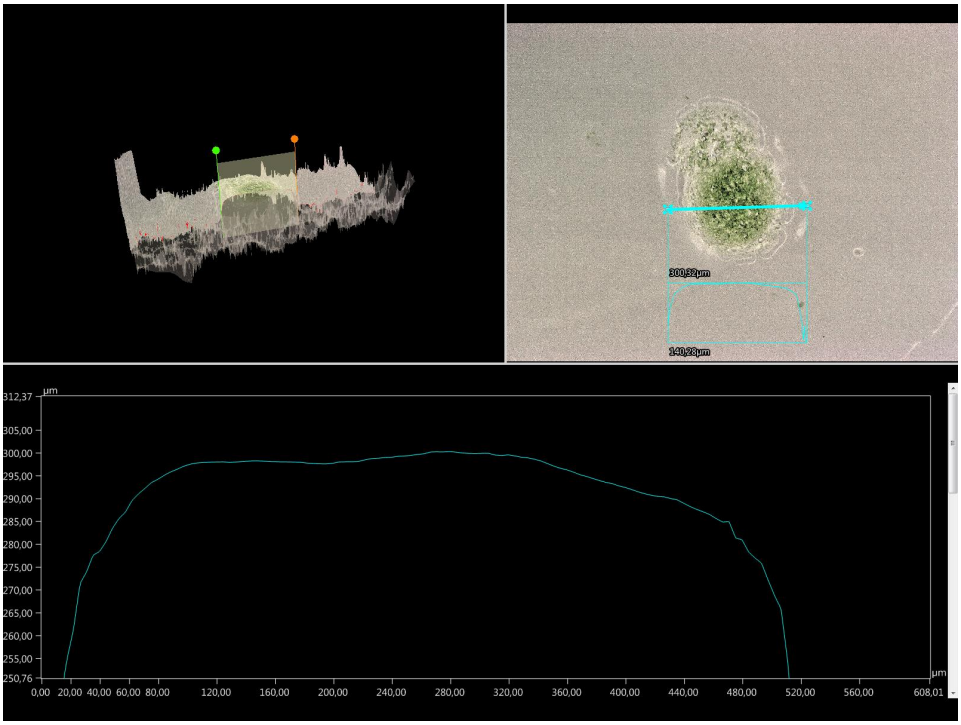

Figure 10.9: Sensor spots in channel 4 of chip 20

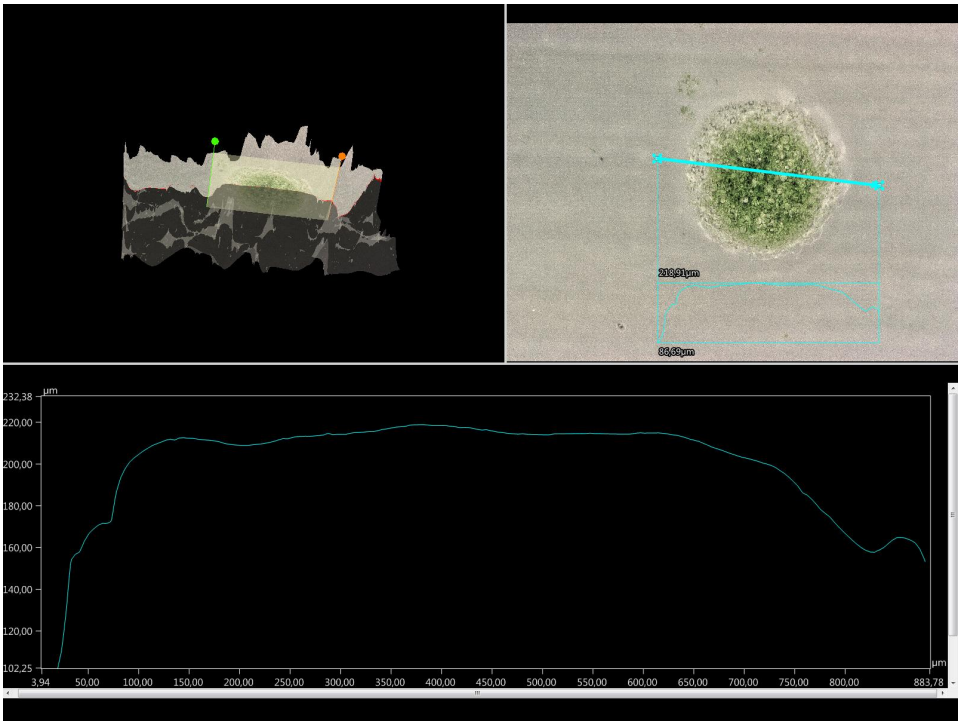

Figure 10.10: Sensor spots in channel 1 of chip 21

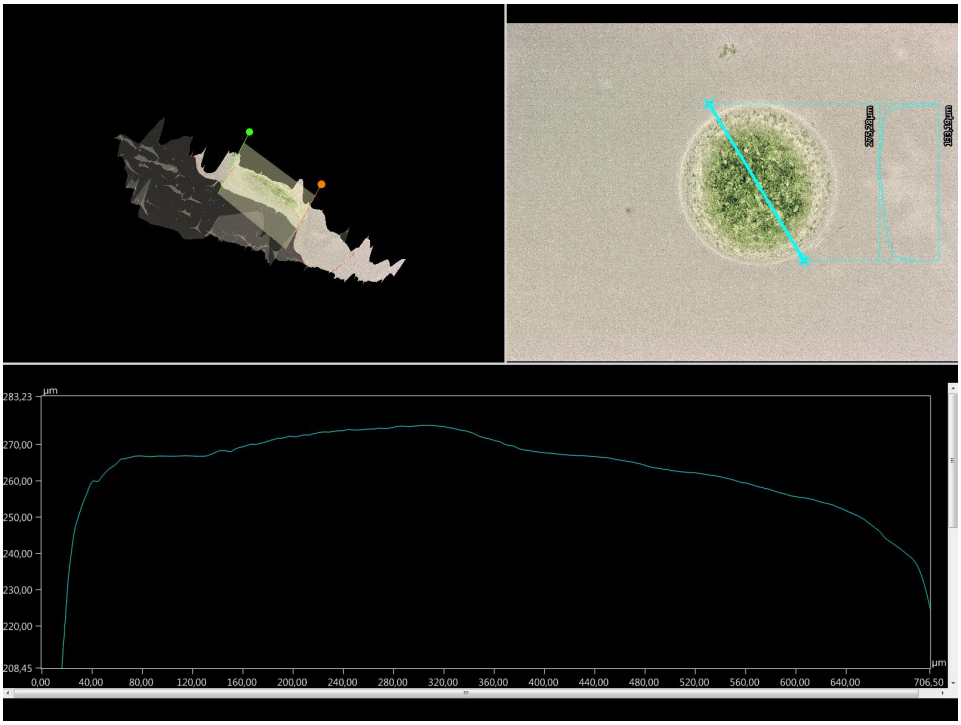

Figure 10.11: Sensor spots in channel 4 of chip 21

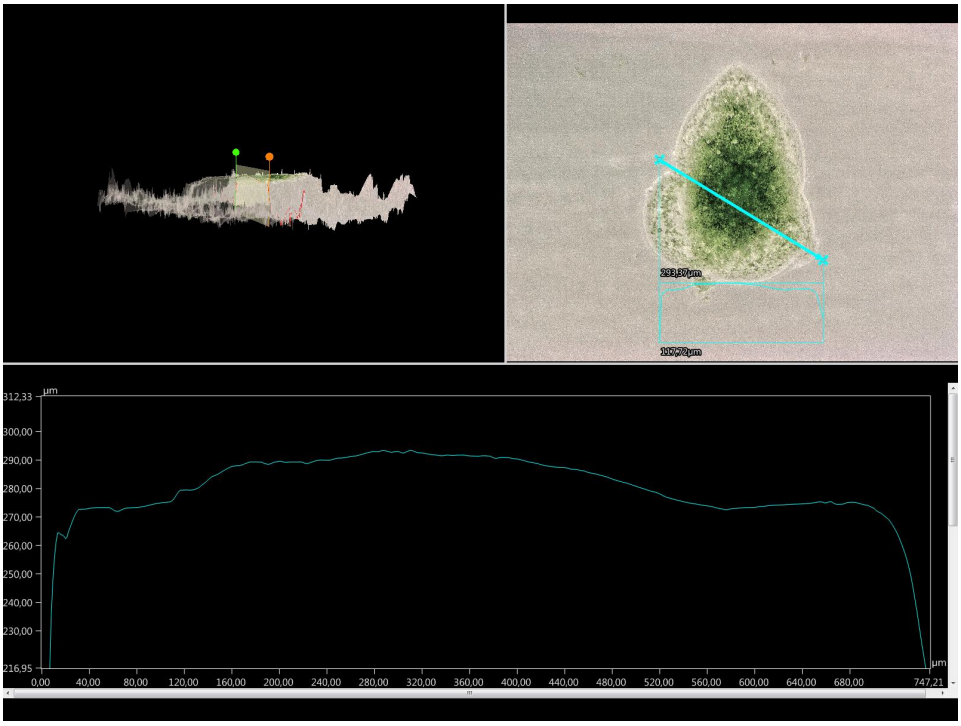

Figure 10.12: Sensor spots in channel 1 of chip 22

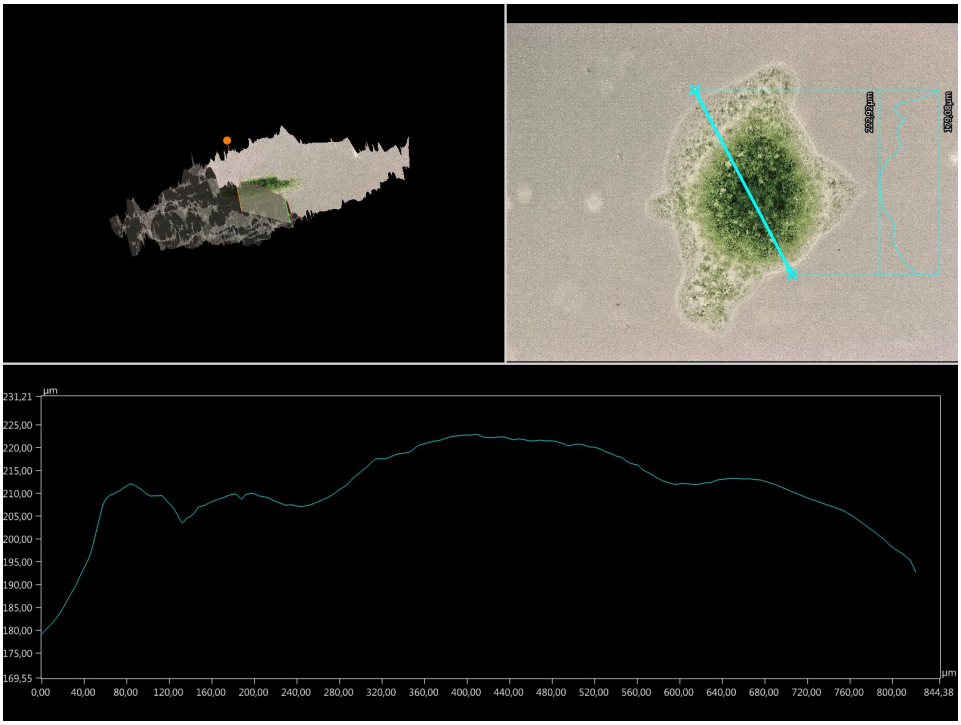

Figure 10.13: Sensor spots in channel 4 of chip 22

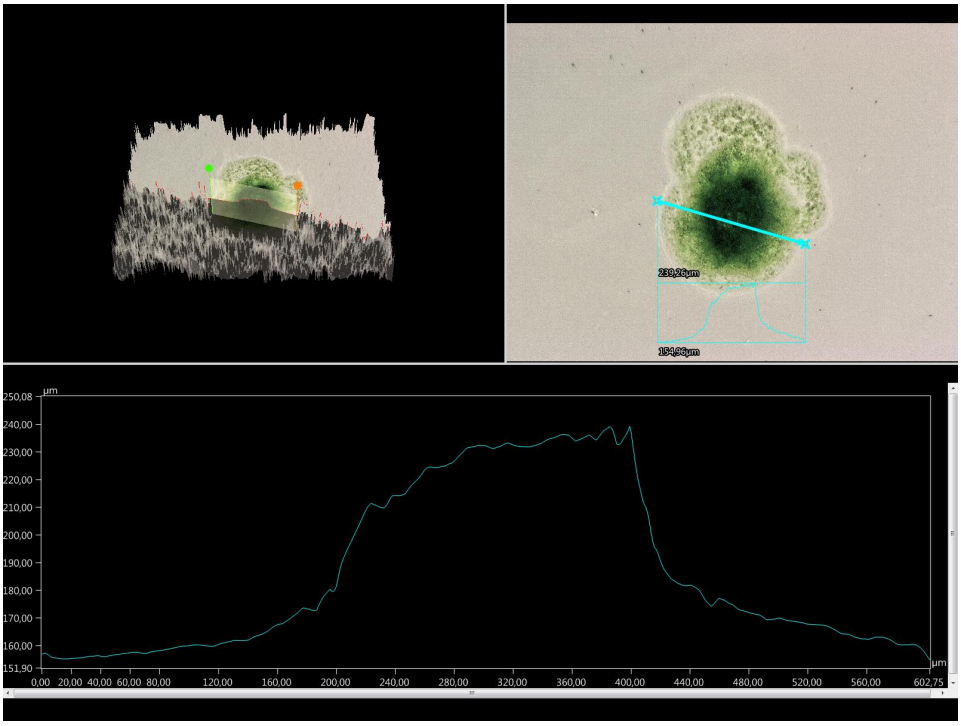

Figure 10.14: Sensor spot in chip 24

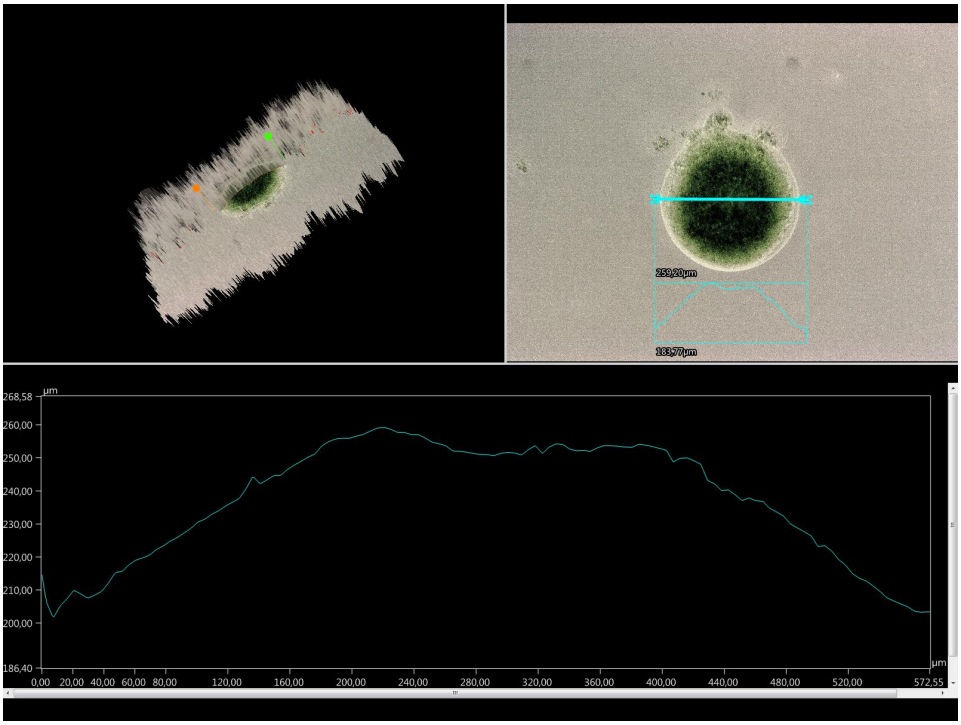

Figure 10.15: Sensor spots in channel 1 of chip 27

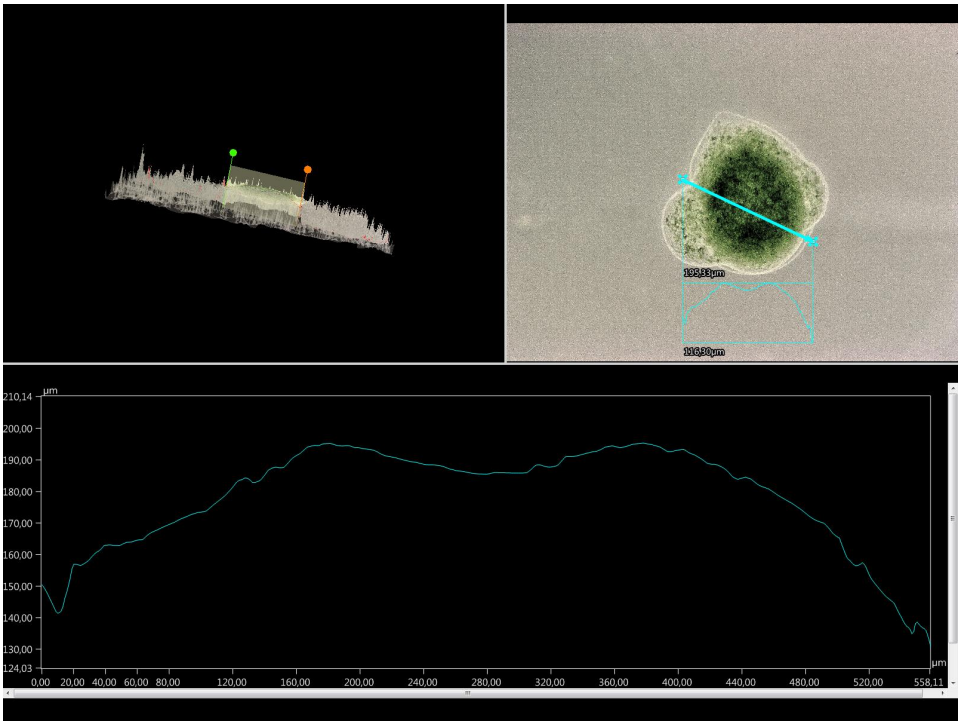

Figure 10.16: Sensor spots in channel 2 of chip 27

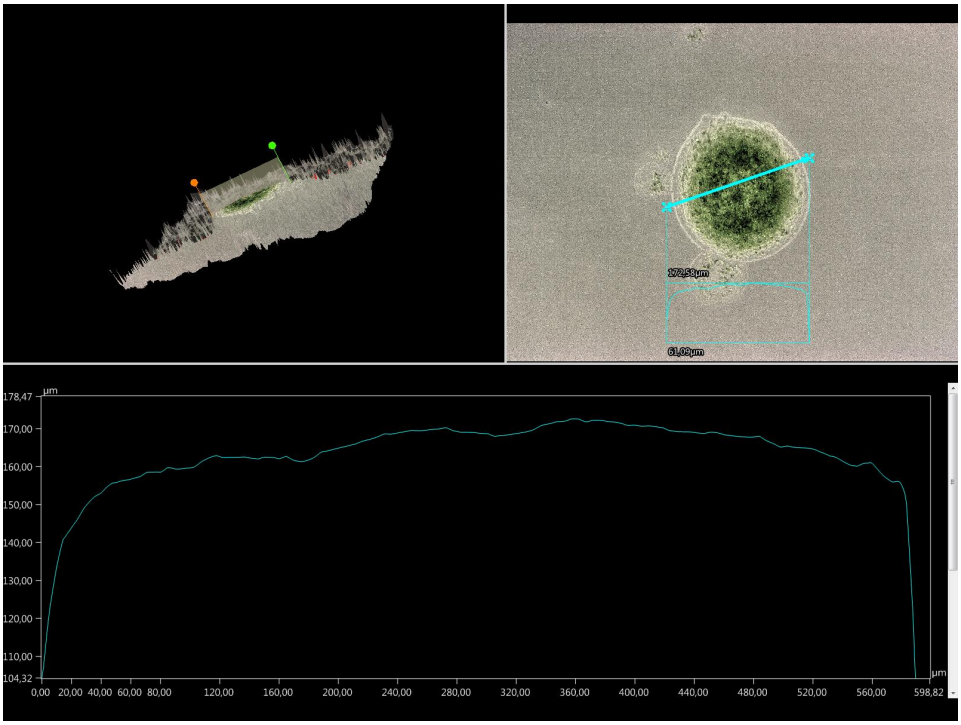

Figure 10.17: Sensor spots in channel 3 of chip 27

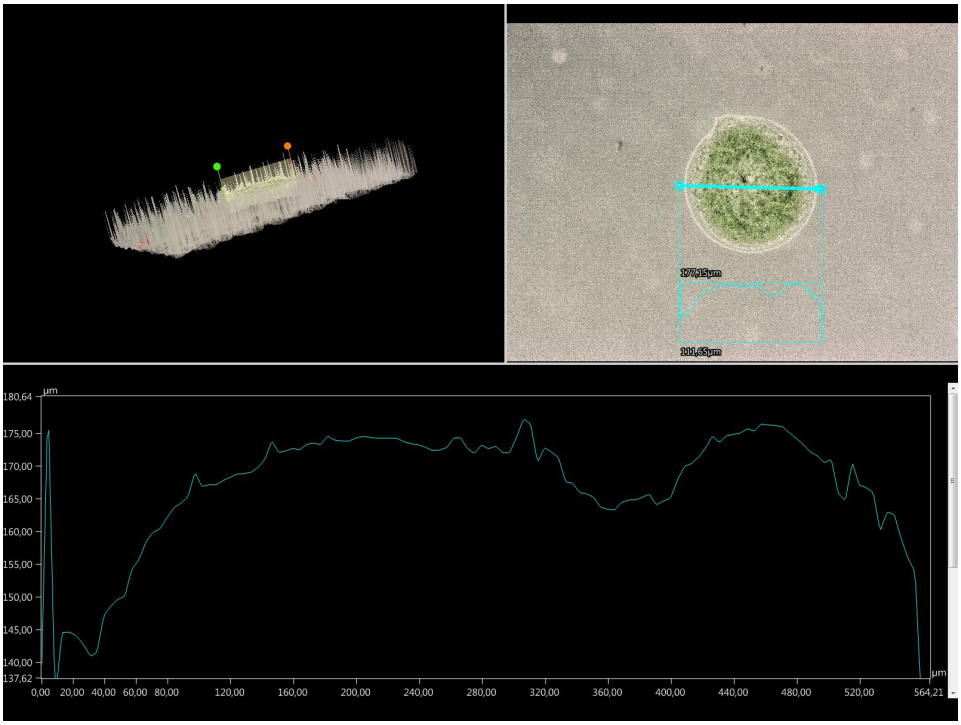

Figure 10.18: Sensor spots in channel 4 of chip 27

10.5 Interesting measurement graphics

10.5.1 Chip 5

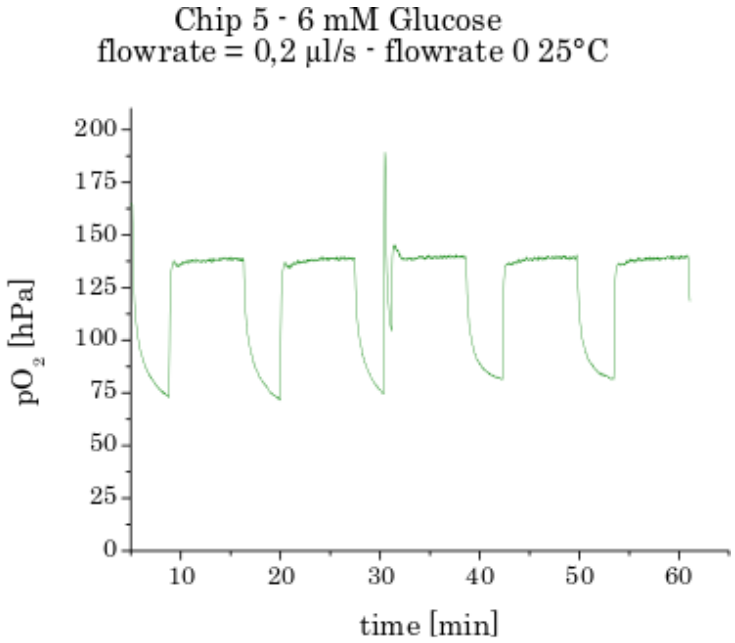

Figure 10.19: Example measurement of 6 mM glucose at flow rates of 0,2 µl/s at 25°C

The figure 10.19 shows an example measurement of 6 mM glucose being pumped through at flow rate of 0,2 µl/s.

10.5.2 Chip 6 and 7

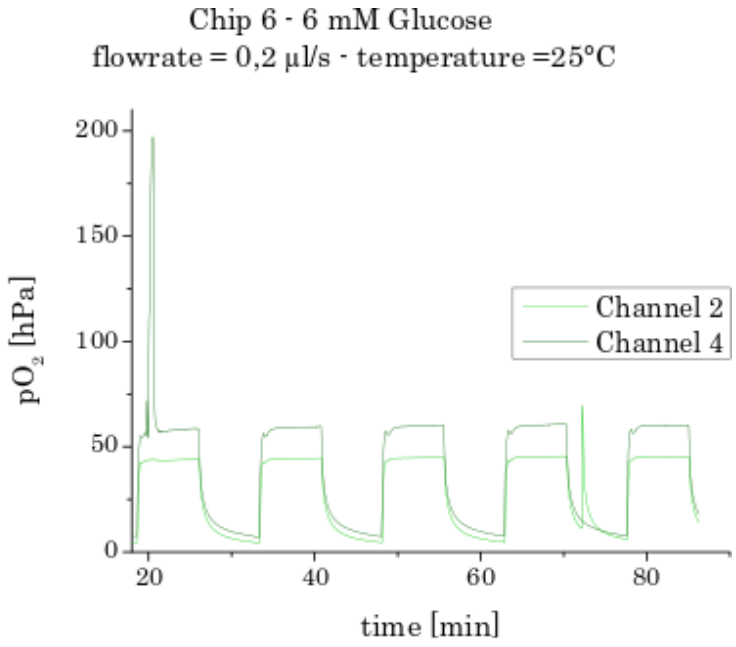

Figure 10.20: Example measurement of 6 mM glucose at flow rates of 0,2 µl/s at 25°C

The figure 10.20 shows an example measurement of 6 mM glucose being pumped through the channel 2 and 4 at a flow rate of 0,2 µl/s.

10.5.3 Chip 15

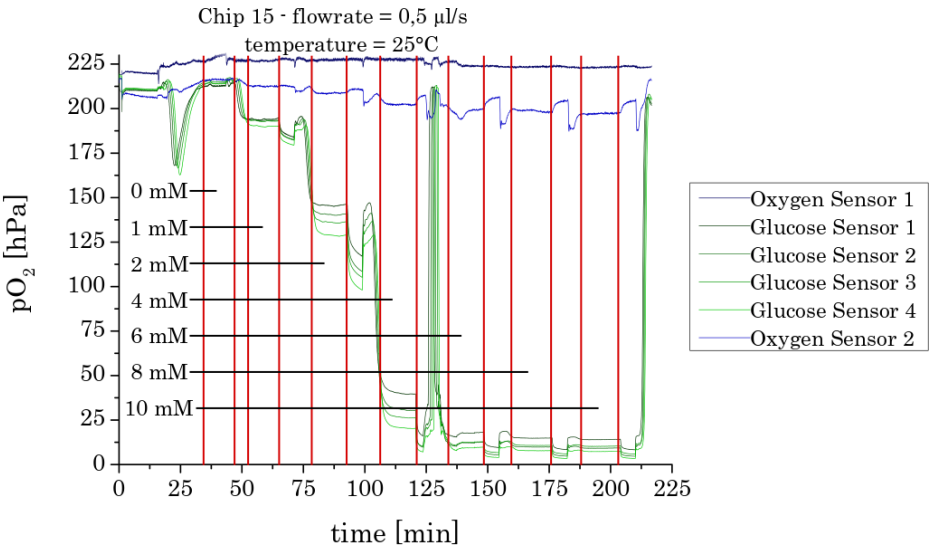

Figure 10.21: Example measurement of the glucose- and oxygen sensor spots of channel 1 with 0; 1; 2; 4, 6; 8 and 10 mM glucose solution at a flow rate of 0,5 µl/s and at a temperature of 25°C

The figure 10.21 shows the measurement of the sensor spots in channel 1. It can be seen that the sensitivity of these glucose sensor spots is better than the sensitivity of the glucose sensor spots in the chip 15.

10.5.4 Chip 20-22

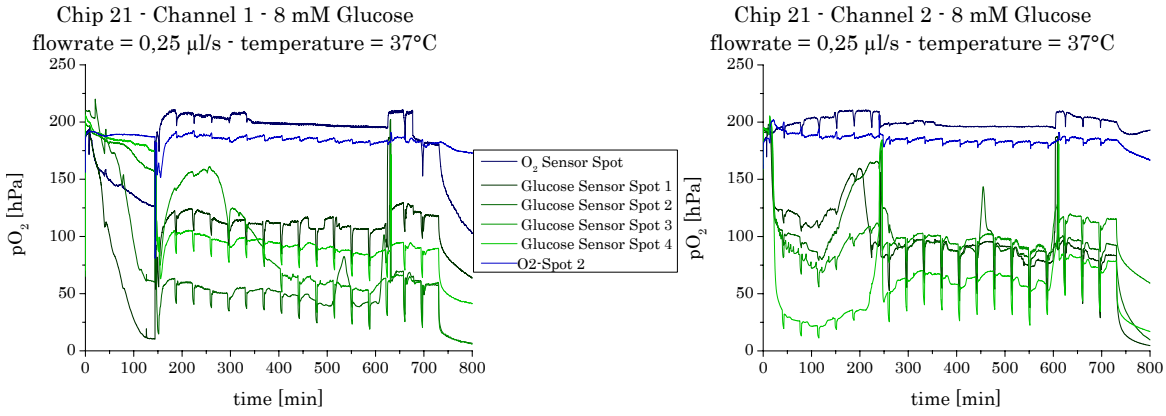

Figure 10.22: Leaching tests of the sensor spots in the channels 1 and 2 in chip 21 with 8 mM glucose solution at a flow rate of 0,25 µl/s and at a temperature of 37°C

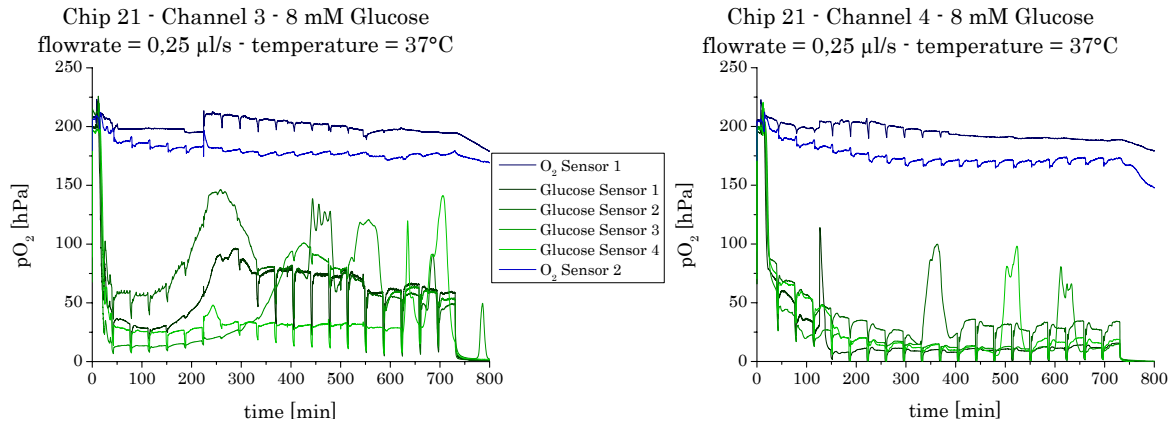

Figure 10.23: Leaching tests of the sensor spots in the channels 3 and 4 in chip 21 with 8 mM glucose solution at a flow rate of 0,25 µl/s and at a temperature of 37°C

The figures 10.22 and 10.23 show the results of the leaching tests of the chip 21. The glucose sensor spots were 8 layers thick, channel 1 had 12; channel 2 had 9; channel 3 had 6 and channel 4 had 3 layers of polyHEMA diffusion barrier on top of the sensor spots. The signal is again not very stable, which is most likely the cause of cavities between the layers of polyHEMA diffusion barrier (which are caused by air bubbles in the spotting process) and because of this air can get trapped in these cavities which disturb the measurements.

10.5.5 Chip 23

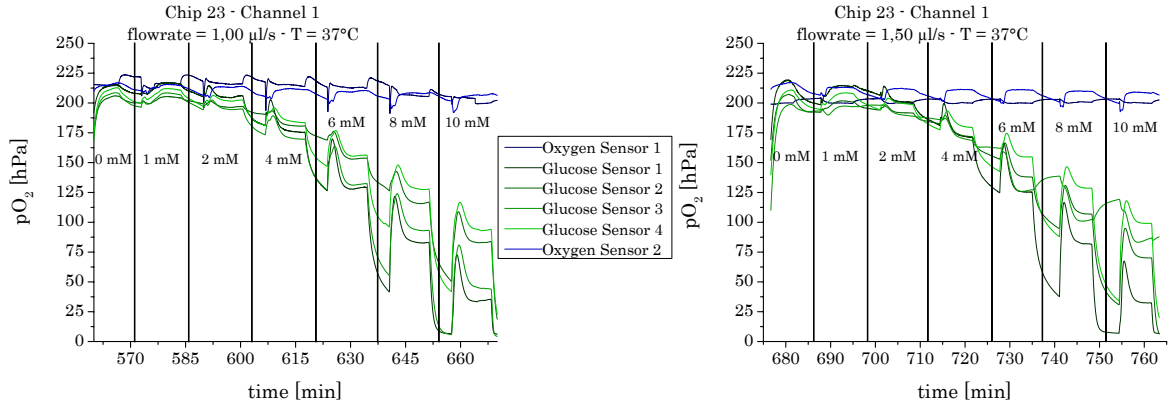

Figure 10.24: Measurement of 0; 1; 2; 4; 6; 8 and 10 mM glucose solution in channel 1 of chip 23 at flow rates of 1,00 and 1,50 µl/s and at a temperature of 37°C

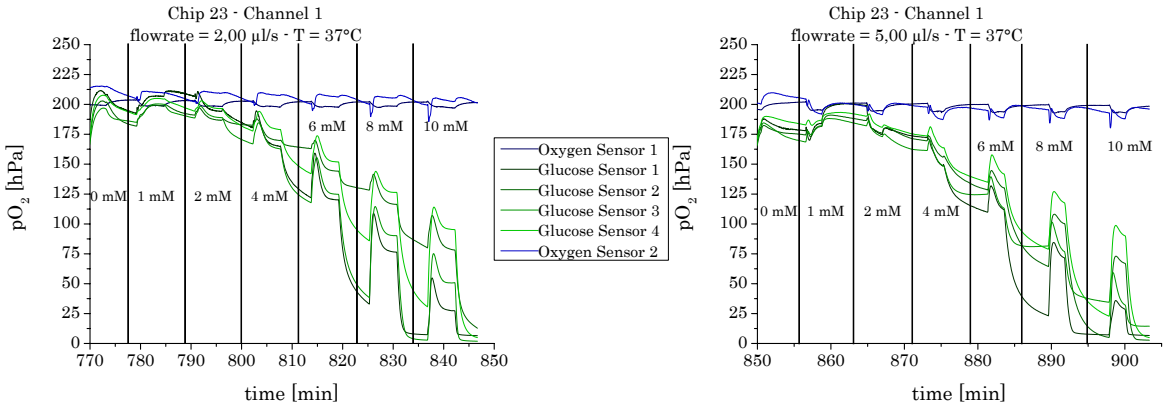

Figure 10.25: Measurement of 0; 1; 2; 4; 6; 8 and 10 mM glucose solution in channel 1 of chip 23 at flow rates of 2,00 and 5,00 µl/s and at a temperature of 37°C

10.5.6 Chip 24

Measurements at 25°C

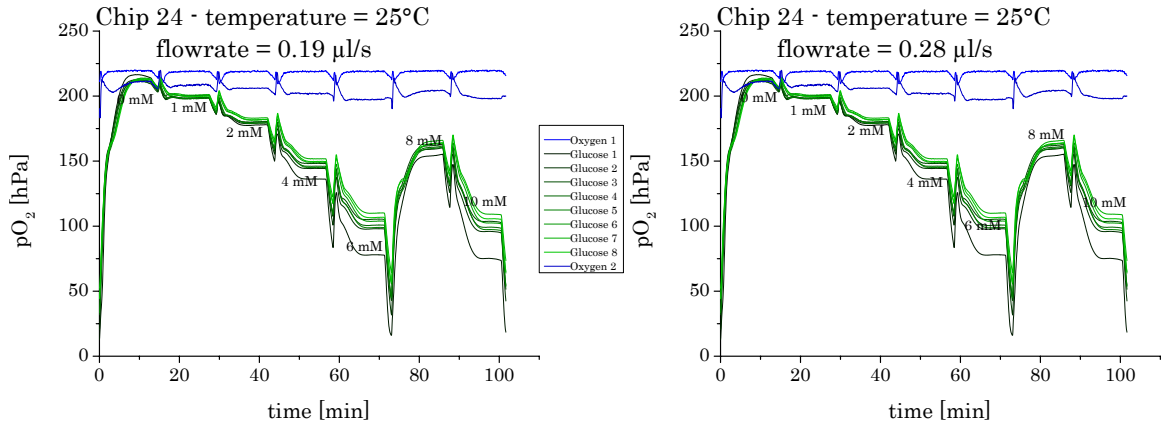

Figure 10.26: Measurement of 0; 1; 2; 4; 6; 8 and 10 mM glucose solution in chip 24 at flow rates of 0,19 and 0,28 µl/s and at a temperature of 25°C

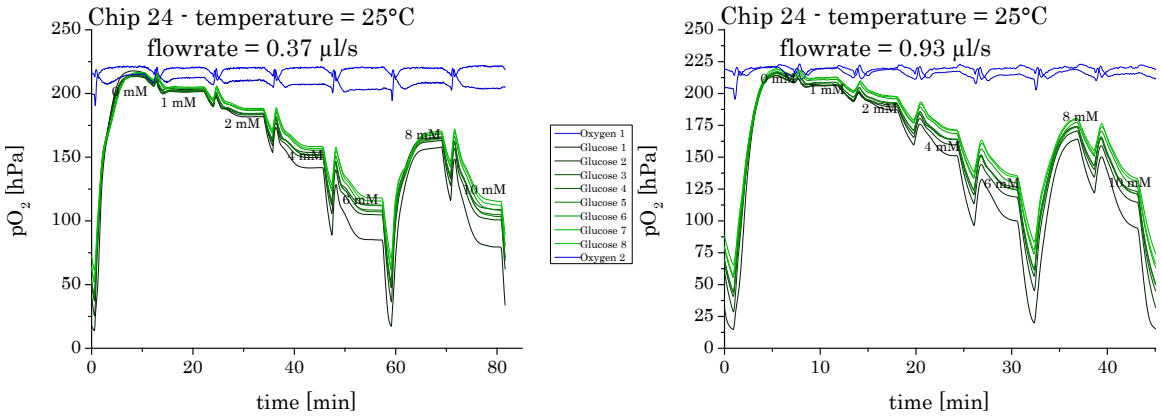

Figure 10.27: Measurement of 0; 1; 2; 4; 6; 8 and 10 mM glucose solution in chip 24 at flow rates of 0,37 and 0,93 µl/s and at a temperature of 25°C

Measurement at 37°C

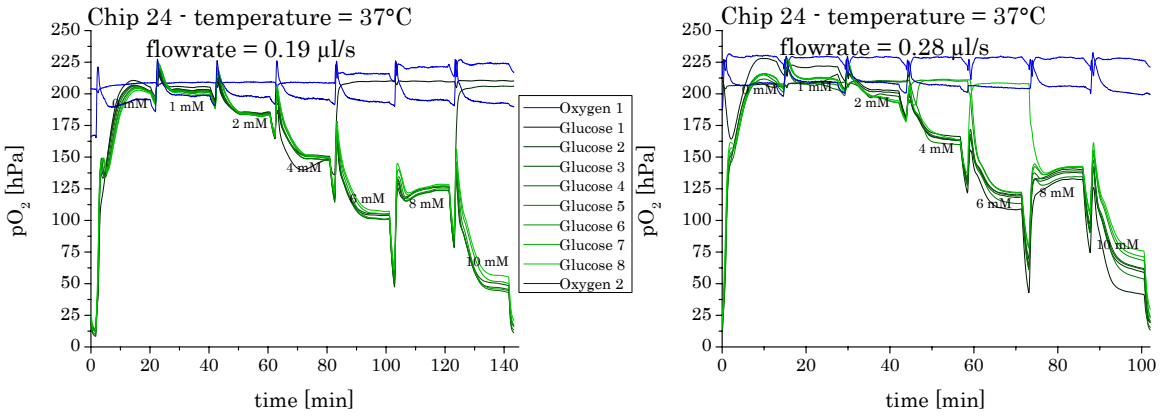

Figure 10.28: Measurement of 0; 1; 2; 4; 6; 8 and 10 mM glucose solution in chip 24 at flow rates of 0,19 and 0,28 µl/s and at a temperature of 37 °C

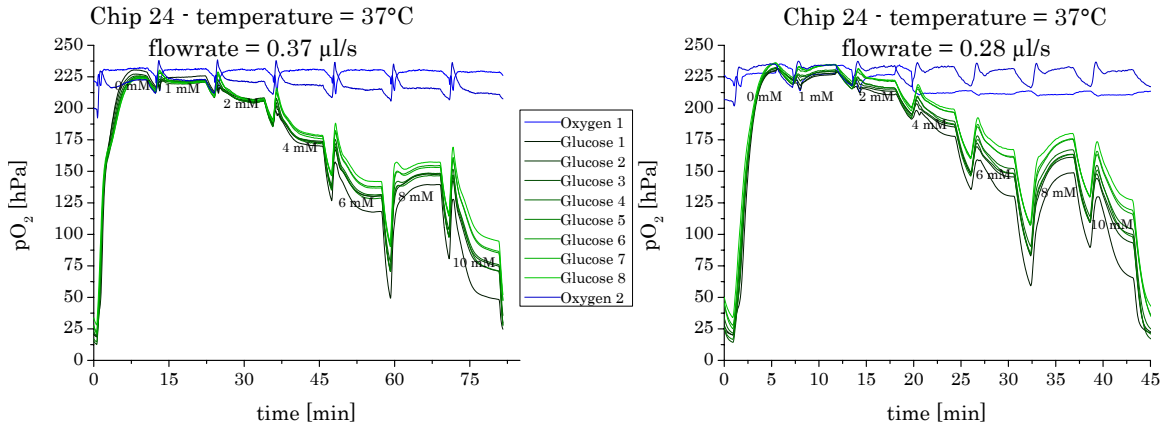

Figure 10.29: Measurement of 0; 1; 2; 4; 6; 8 and 10 mM glucose solution in chip 24 at flow rates of 0,37 and 0,93 µl/s and at a temperature of 37 °C

10.5.7 Chip 28

Leaching Tests

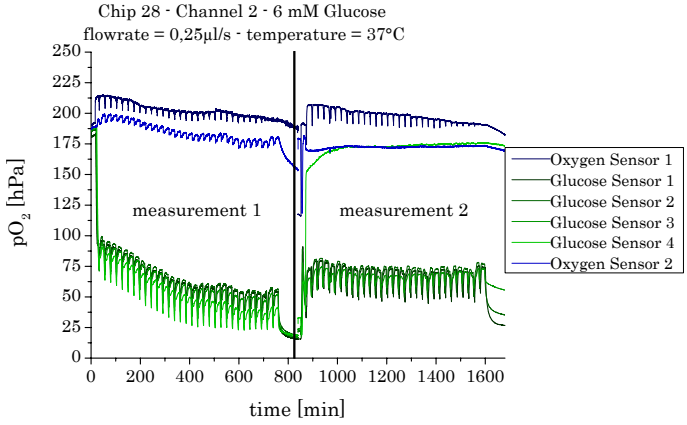

Figure 10.30: Leaching tests of the GOx-CLEA in the glucose sensor spots in channel 2 of chip 28 at a glucose concentration of 6 mM and at a temperature of 37°C

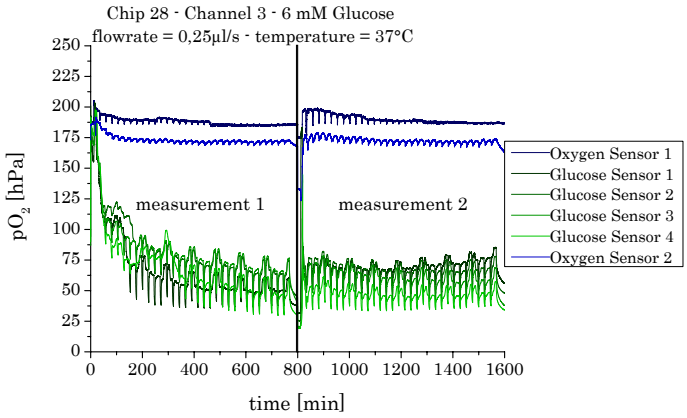

Figure 10.31: Leaching tests of the GOx-CLEA in the glucose sensor spots in channel 3 of chip 28 at a glucose concentration of 6 mM and at a temperature of 37°C

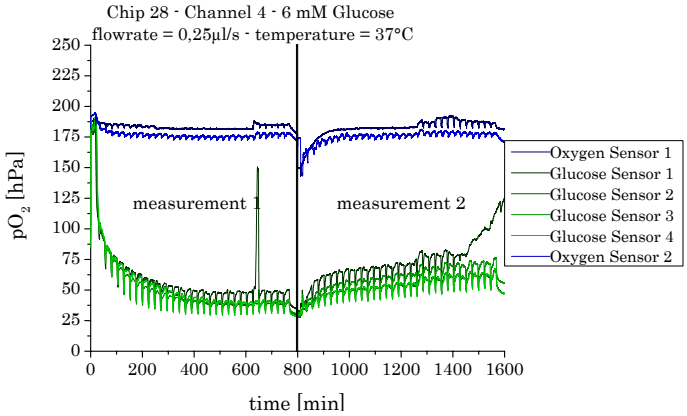

Figure 10.32: Leaching tests of the GOx-CLEA in the glucose sensor spots in channel 4 of chip 28 at a glucose concentration of 6 mM and at a temperature of 37°C

10.6 g-code of the CNC-machine

10.6.1 g-code of the CNC-machine for the glucose sensors in 10 µl-chips

```
%

(for you to change)

#<correction_y>= 9 (correction in x axis in mm)
#<correction_x>=    13 (correction in y axis in mm)
#<correction_z>= 0 (correction in z axis in mm)
#<squares_per_line>= 3 (number of squares in y direction)
```

```
#<lines>= 1 (number of lines)
#<square_length_y>= 1 (number of spots per square edge)
#<square_length_x>= 1 (number of spots per square edge)
#<dist_squares_y>= 9 (distance of squares in line)
#<dist_squares_x>= 1 (distance between lines)
#<spot_distance>= 1 (distance between spots in square)
#<repeat_all>  =  1  (repeat all including cleaning process)
#<wait_all>  =  0  (waiting time between repetitions)


(try not to change those. if you do, be careful! If you have questions ask Fipsotro

#<repeat_count>=1
#<move_speed>=2000
#<wait_pass> = 0.1 (wait between passes)
#<wait_trigger> = 0.02 (wait trigger)
#<repeat_clean> = 6 (cleaning steps)
#<wait_clean> = 0.06
#<repeat_all> = 1
#<wait_all> = 0

(program starts here)

O109 if [#<correction_y> GE 0]
O108 if [#<correction_x> GE 0]
O107 if [#<correction_z> GE 0]
O106 repeat [#<repeat_all>]
#<counter>=0
#<counter_x>=0
g4 p#<wait_all>
G90 (absolute mode)
G40 (toolradius correction off)
G21
g54 g0 z30
g54 g0 x-20 y[#<correction_y>]
g54 g0 z5
O105 repeat [#<repeat_clean>]
g54 g0 y[[#<correction_y>]+30]
```

```
g54 g0 y[#<correction_y>]
O105 endrepeat
g54 g0 x[#<correction_x>] y[#<correction_y>] z[#<correction_z>]
O100 repeat [#<lines>]
O101 repeat [#<squares_per_line>]
g90 x[#<counter_x>*#<dist_squares_x>+#<correction_x>]
g90 z[#<correction_z>]
O102 repeat [#<repeat_count>]
#<line_counter>=1
O103 repeat [#<square_length_x>]
g90 y[#<counter>*#<dist_squares_y>+#<correction_y>]
O110 if [#<line_counter> EQ 2]
g91 G1 y[#<spot_distance>/-2] f#<move_speed>
O110 endif
O104 repeat [#<square_length_y>]
g4 p#<wait_pass>
s1m3
g4 p#<wait_trigger>
s1m5
g4 p#<wait_pass>
g91 G1 y#<spot_distance> f#<move_speed>
O104 endrepeat
O111 if [#<line_counter> EQ 1]
#<line_counter> = 2
O111 else
#<line_counter> = 1
O111 endif
g91 x#<spot_distance>
O103 endrepeat
O102 endrepeat
#<counter>=[#<counter>+1]
O101 endrepeat
#<counter>=0
#<counter_x>=[#<counter_x>+1]
O100 endrepeat
(g28)
(g91 z-22)
(g91 g1 x6 f100)
```

```
(f#<move_speed>)
g90 x0 y0 z35
O106 endrepeat
g54 g0 z30
g54 g0 x-20 y[#<correction_y>]
g54 g0 z5
O121 repeat [#<repeat_clean>]
g54 g0 y[[#<correction_y>]+30]
g54 g0 y[#<correction_y>]
O121 endrepeat
g90 x0 y0 z35
O107 else
(MSG, You would have crashed! Do not set correction z lower than 0!)
O107 endif
O108 else
(MSG, You would have crashed! Do not set correction x lower than 0!)
O108 endif
O109 else
(MSG, You would have crashed! Do not set correction y lower than 0!)
O109 endif
%
```

10.6.2 g-code of the CNC-machine for the glucose sensors in 100 µl-chips

```
%

(for you to change)

#<correction_y>= 24.9 (correction in x axis in mm)
#<correction_x>=       4.23 (correction in y axis in mm)
#<correction_z>= 3.5 (correction in z axis in mm)
#<squares_per_line>= 4 (number of squares in y direction)
#<lines>= 4 (number of lines)
#<square_length_y>= 1  (number of spots per square edge)
#<square_length_x>= 1 (number of spots per square edge)
#<dist_squares_y>= 6.5 (distance of squares in line)
#<dist_squares_x>= 5.45 (distance between lines)
```

```
#<spot_distance>= 0 (distance between spots in square)
#<repeat_all>  =  1  (repeat all including cleaning process)
#<wait_all>  =  0  (waiting time between repetitions)


(try not to change those. if you do, be careful! If you have questions ask Fipsotron)

#<repeat_count>=1
#<move_speed>=4000
#<wait_pass> = 0.01 (wait between passes)
#<wait_trigger> = 0.05 (wait trigger)
#<repeat_clean> = 0 (cleaning steps)
#<wait_clean> = 0.06
#<repeat_all> = 1
#<wait_all> = 0

(program starts here)

O106 repeat [#<repeat_all>]
#<counter>=0
#<counter_x>=0
g4 p#<wait_all>
G90 (absolute mode)
G40 (toolradius correction off)
G21
g54 g0 z20
g54 g0 x-27 y0
g54 g0 z2

O105 repeat [#<repeat_clean>]
s1m3
g4 p#<wait_trigger>
s1m5
g4 p#<wait_clean>
O105 endrepeat


O107 repeat [6]
```

```
g0 z9
g54 g0 y25
g54 g0 y0
O107 endrepeat

g54 g0 x[#<correction_x>] y[#<correction_y>] z[#<correction_z>]
O100 repeat [#<lines>]
g90 y[-15] x[#<counter_x>*#<dist_squares_x>+#<correction_x>] z[#<correction_z>]

O117 repeat [10]
s1m3
g4 p#<wait_trigger>
s1m5
g4 p0.2
O117 endrepeat

O101 repeat [#<squares_per_line>]
O102 repeat [#<repeat_count>]
#<line_counter>=1
O103 repeat [#<square_length_x>]
g90 y[#<counter>*#<dist_squares_y>+#<correction_y>] x[#<counter_x>*#<dist_squares_x
O110 if [#<line_counter> EQ 2]
g91 G1 y[#<spot_distance>/-2] f#<move_speed>
O110 endif

O104 repeat [#<square_length_y>]
s1m3
g4 p#<wait_trigger>
s1m5
g4 p#<wait_pass>
g91 G1 y#<spot_distance> f#<move_speed>
O104 endrepeat

O111 if [#<line_counter> EQ 1]
#<line_counter> = 2
O111 else
#<line_counter> = 1
O111 endif
```

```
g91 x#<spot_distance>
O103 endrepeat
O102 endrepeat
#<counter>=[#<counter>+1]
O101 endrepeat

#<counter>=0
#<counter_x>=[#<counter_x>+1]
g90 g0 z20
g90 g0 x-27 y0
g90 g0 z2
O116 repeat [6]
g0 z9
g90 g0 y25
g90 g0 y0
O116 endrepeat
O100 endrepeat
(g28)
(g91 z-22)
(g91 g1 x6 f100)
(f#<move_speed>)
g90 x0 y0 z35
O106 endrepeat
%
```

10.6.3 g-code of the CNC-machine for the oxygen sensors in 100 µl-chips

```
%

(for you to change)

#<correction_y>= 18.5 (correction in x axis in mm)
#<correction_x>=       4.18 (correction in y axis in mm)
#<correction_z>= 3.5 (correction in z axis in mm)
#<squares_per_line>= 2 (number of squares in y direction)
#<lines>= 4 (number of lines)
#<square_length_y>= 1  (number of spots per square edge)
#<square_length_x>= 1 (number of spots per square edge)
```

```
#<dist_squares_y>= 32.5 (distance of squares in line)
#<dist_squares_x>= 5.5 (distance between lines)
#<spot_distance>= 0 (distance between spots in square)
#<repeat_all>  =  1  (repeat all including cleaning process)
#<wait_all>  =  0  (waiting time between repetitions)


(try not to change those. if you do, be careful! If you have questions ask Fipsotro

#<repeat_count>=1
#<move_speed>=4000
#<wait_pass> = 0.01 (wait between passes)
#<wait_trigger> = 0.05 (wait trigger)
#<repeat_clean> = 0 (cleaning steps)
#<wait_clean> = 0.06
#<repeat_all> = 1
#<wait_all> = 0

(program starts here)

O106 repeat [#<repeat_all>]
#<counter>=0
#<counter_x>=0
g4 p#<wait_all>
G90 (absolute mode)
G40 (toolradius correction off)
G21
g54 g0 z20
g54 g0 x-27 y0
g54 g0 z2

O105 repeat [#<repeat_clean>]
s1m3
g4 p#<wait_trigger>
s1m5
g4 p#<wait_clean>
O105 endrepeat
```

```
O107 repeat [6]
g0 z9
g54 g0 y25
g54 g0 y0
O107 endrepeat

g54 g0 x[#<correction_x>] y[#<correction_y>] z[#<correction_z>]
O100 repeat [#<lines>]
g90 y[-15] x[#<counter_x>*#<dist_squares_x>+#<correction_x>] z[#<correction_z>]

O117 repeat [10]
s1m3
g4 p#<wait_trigger>
s1m5
g4 p0.2
O117 endrepeat

O101 repeat [#<squares_per_line>]
O102 repeat [#<repeat_count>]
#<line_counter>=1
O103 repeat [#<square_length_x>]
g90 y[#<counter>*#<dist_squares_y>+#<correction_y>] x[#<counter_x>*#<dist_squares_x>+#<c
O110 if [#<line_counter> EQ 2]
g91 G1 y[#<spot_distance>/-2] f#<move_speed>
O110 endif

O104 repeat [#<square_length_y>]
s1m3
g4 p#<wait_trigger>
s1m5
g4 p#<wait_pass>
g91 G1 y#<spot_distance> f#<move_speed>
O104 endrepeat

O111 if [#<line_counter> EQ 1]
#<line_counter> = 2
O111 else
#<line_counter> = 1
```

```
O111 endif

g91 x#<spot_distance>
O103 endrepeat
O102 endrepeat
#<counter>=[#<counter>+1]
O101 endrepeat

#<counter>=0
#<counter_x>=[#<counter_x>+1]
g90 g0 z20
g90 g0 x-27 y0
g90 g0 z2
O116 repeat [6]
g90 g0 y25
g90 g0 y0
O116 endrepeat
O100 endrepeat
(g28)
(g91 z-22)
(g91 g1 x6 f100)
(f#<move_speed>)
g90 x0 y0 z35
O106 endrepeat
%
```

10.6.4 g-code of the CNC-machine for the glucose sensors in the single channel chips

```
%

(for you to change)

#<correction_y>= 17.1 (correction in x axis in mm)
#<correction_x>=       12.5 (correction in y axis in mm)
#<correction_z>= 2.5 (correction in z axis in mm)
#<squares_per_line>= 8 (number of squares in y direction)
#<lines>= 1 (number of lines)
#<square_length_y>= 1  (number of spots per square edge)
```

```
#<square_length_x>= 1 (number of spots per square edge)
#<dist_squares_y>= 5 (distance of squares in line)
#<dist_squares_x>= 5.45 (distance between lines)
#<spot_distance>= 0 (distance between spots in square)
#<repeat_all>  =  1  (repeat all including cleaning process)
#<wait_all>  =  0  (waiting time between repetitions)


(try not to change those. if you do, be careful! If you have questions ask Fipsotron)

#<repeat_count>=1
#<move_speed>=4000
#<wait_pass> = 0.01 (wait between passes)
#<wait_trigger> = 0.05 (wait trigger)
#<repeat_clean> = 0 (cleaning steps)
#<wait_clean> = 0.06
#<repeat_all> = 1
#<wait_all> = 0

(program starts here)

O106 repeat [#<repeat_all>]
#<counter>=0
#<counter_x>=0
g4 p#<wait_all>
G90 (absolute mode)
G40 (toolradius correction off)
G21
g54 g0 z20
g54 g0 x-27 y0
g54 g0 z2

O105 repeat [#<repeat_clean>]
s1m3
g4 p#<wait_trigger>
s1m5
g4 p#<wait_clean>
O105 endrepeat
```

```
O107 repeat [6]
g0 z9
g54 g0 y25
g54 g0 y0
O107 endrepeat

g54 g0 x[#<correction_x>] y[#<correction_y>] z[#<correction_z>]
O100 repeat [#<lines>]
g90 y[-15] x[#<counter_x>*#<dist_squares_x>+#<correction_x>] z[#<correction_z>]

O117 repeat [10]
s1m3
g4 p#<wait_trigger>
s1m5
g4 p0.2
O117 endrepeat

O101 repeat [#<squares_per_line>]
O102 repeat [#<repeat_count>]
#<line_counter>=1
O103 repeat [#<square_length_x>]
g90 y[#<counter>*#<dist_squares_y>+#<correction_y>] x[#<counter_x>*#<dist_squares_x
O110 if [#<line_counter> EQ 2]
g91 G1 y[#<spot_distance>/-2] f#<move_speed>
O110 endif

O104 repeat [#<square_length_y>]
s1m3
g4 p#<wait_trigger>
s1m5
g4 p#<wait_pass>
g91 G1 y#<spot_distance> f#<move_speed>
O104 endrepeat

O111 if [#<line_counter> EQ 1]
#<line_counter> = 2
```

```
O111 else
#<line_counter> = 1
O111 endif

g91 x#<spot_distance>
O103 endrepeat
O102 endrepeat
#<counter>=[#<counter>+1]
O101 endrepeat

#<counter>=0
#<counter_x>=[#<counter_x>+1]
g90 g0 z20
g90 g0 x-27 y0
g90 g0 z2
O116 repeat [6]
g0 z9
g90 g0 y25
g90 g0 y0
O116 endrepeat
O100 endrepeat
(g28)
(g91 z-22)
(g91 g1 x6 f100)
(f#<move_speed>)
g90 x0 y0 z35
O106 endrepeat
%
```

10.6.5 g-code of the CNC-machine for the oxygen sensors in the single channel chips

```
%

(for you to change)

#<correction_y>= 12.2 (correction in x axis in mm)
#<correction_x>=       12.5 (correction in y axis in mm)
#<correction_z>= 2.5 (correction in z axis in mm)
```

```
#<squares_per_line>= 2 (number of squares in y direction)
#<lines>= 1 (number of lines)
#<square_length_y>= 1  (number of spots per square edge)
#<square_length_x>= 1 (number of spots per square edge)
#<dist_squares_y>= 45 (distance of squares in line)
#<dist_squares_x>= 5.5 (distance between lines)
#<spot_distance>= 0 (distance between spots in square)
#<repeat_all>  =  1  (repeat all including cleaning process)
#<wait_all>  =  0  (waiting time between repetitions)


(try not to change those. if you do, be careful! If you have questions ask Fipsotro

#<repeat_count>=1
#<move_speed>=4000
#<wait_pass> = 0.01 (wait between passes)
#<wait_trigger> = 0.05 (wait trigger)
#<repeat_clean> = 0 (cleaning steps)
#<wait_clean> = 0.06
#<repeat_all> = 1
#<wait_all> = 0

(program starts here)

O106 repeat [#<repeat_all>]
#<counter>=0
#<counter_x>=0
g4 p#<wait_all>
G90 (absolute mode)
G40 (toolradius correction off)
G21
g54 g0 z20
g54 g0 x-27 y0
g54 g0 z2

O105 repeat [#<repeat_clean>]
s1m3
g4 p#<wait_trigger>
```

```
s1m5
g4 p#<wait_clean>
O105 endrepeat

O107 repeat [6]
g0 z9
g54 g0 y25
g54 g0 y0
O107 endrepeat

g54 g0 x[#<correction_x>] y[#<correction_y>] z[#<correction_z>]
O100 repeat [#<lines>]
g90 y[-15] x[#<counter_x>*#<dist_squares_x>+#<correction_x>] z[#<correction_z>]

O117 repeat [5]
s1m3
g4 p#<wait_trigger>
s1m5
g4 p0.2
O117 endrepeat

O101 repeat [#<squares_per_line>]
O102 repeat [#<repeat_count>]
#<line_counter>=1
O103 repeat [#<square_length_x>]
g90 y[#<counter>*#<dist_squares_y>+#<correction_y>] x[#<counter_x>*#<dist_squares_x>+#<
O110 if [#<line_counter> EQ 2]
g91 G1 y[#<spot_distance>/-2] f#<move_speed>
O110 endif

O104 repeat [#<square_length_y>]
s1m3
g4 p#<wait_trigger>
s1m5
g4 p#<wait_pass>
g91 G1 y#<spot_distance> f#<move_speed>
O104 endrepeat
```

```
O111 if [#<line_counter> EQ 1]
#<line_counter> = 2
O111 else
#<line_counter> = 1
O111 endif

g91 x#<spot_distance>
O103 endrepeat
O102 endrepeat
#<counter>=[#<counter>+1]
O101 endrepeat

#<counter>=0
#<counter_x>=[#<counter_x>+1]
g90 g0 z20
g90 g0 x-27 y0
g90 g0 z2
O116 repeat [6]
g90 g0 y25
g90 g0 y0
O116 endrepeat
O100 endrepeat
(g28)
(g91 z-22)
(g91 g1 x6 f100)
(f#<move_speed>)
g90 x0 y0 z35
O106 endrepeat
%
```